SHAKE TABLE TESTS OF A ¼ SCALED MASS CONCENTRIC THREE STOREY STEEL STRUCTURE ISOLATED BY A HYBRID PASSIVE CONTROL SYSTEM

by

H.Cem Yenidoğan

B.S., Civil Engineering, Yıldız Technical University, 2003

M.Sc., Geotechnical Engineering, Yıldız Technical University, 2006

Submitted to Kandilli Observatory and Earthquake Research Institute

in partial fulfillment of the requirements for the degree of

Master of Science

Graduate Program in Earthquake Engineering

Boğaziçi University

2007

SHAKE TABLE TESTS OF A ¼ SCALED MASS CONCENTRIC THREE STOREY STEEL STRUCTURE ISOLATED BY A HYBRID

PASSIVE CONTROL SYSTEM

APPROVED BY:

Assistant Prof. Dr. Eren Uçkan …….

(Thesis Supervisor)

Prof. Dr. Mustafa Erdik …….

Assistant Prof. Dr. Bülent Akbaş …….

DATE OF APPROVAL**:**

This study is dedicated to Füsun Yenidoğan, Cabbar Yenidoğan and all of my family members. Without their endless support, patience and faith on me, this achievement could not be possible.

ACKNOWLEDGEMENTS

I would like to express my deepest gratitude to Assistant Prof. Dr. Eren Uckan for his guidance and support throughout this research academically. His outstanding leadership and personality are the most valuable drive and source in my experience in KOERI. I appreciate his instructions and encouragement in difficult situations in the past and future.

I would like to thank to Professor Mustafa ERDİK for his contributions to my study with his outstanding experience and engineering judgement and for his precious time. I would also like to thank deeply to Assistant Prof. Gülüm Birgören Tanırcan and all the academicians and staff of Earthquake Engineering Department of KOERI.

My acknowledgement also goes to FIP Industrial for their support and providing the isolators on this project and Miss Castellano and Mircan Kaya who are members of FIP Industriale.

Also I would like to thank to KOERI shake table team, Dr. Waiel Mowrtage, Oktay Cırag and technician Ahmet for their help during the instrumentation of the isolated structure and performing the test.

I wish to express my special thanks to my dear friend Ph.D candidate Yavuz Kaya for his solid knowledge in structural engineer and guidance during the prepration of this study. In addition, I would like to thank to my dear friend Ali Cem Öztürk for his support and reviews during those stressful nites.

Also I would like to address my thanks to Ph. D candidates Goktürk Önem and

Cüneyt Tüzün for their sharing of experience in KOERI laboratory and modeling, and last but not the least my grateful thanks to my parents and my aunt Sakine Renklibulut who is encouraged me to be a civil engineer.

ABSTRACT

SHAKE TABLE TESTS OF A ¼ SCALED MASS CONCENTRIC THREE STOREY STEEL STRUCTURE ISOLATED BY A HYBRID PASSIVE CONTROL SYSTEM

Objective of this study is to investigate the effectiveness of a hybrid isolation system for a three-storey mass concentric steel structure. The isolation system consists of 2 elastomeric bearings and 4 flat sliding bearings, which are located below the central and corner columns, respectively. A ¼ scaled isolated model of the structure has been tested on a shake table under real earthquakes and sinusoidal base motions. Measurements were taken at structural points and at base slab level. Two types of high damping elastomeric bearings, one with low shear modulus and the other with high shear modulus, were tested to see the effects of different target isolation periods. A numerical model for the structure was developed and calibrated by the data from the experimental studies. In this dissertation effectiveness of the hybrid isolation system is verified by comparing the results obtained from isolated and fixed base models.

ÖZET

PASİF HİBRİT CONTROL SİSTEMLERİ TARAFINDAN İZOLE EDİLMİŞ ¼ ÖLÇEKLİ 3 KATLI ÇELİK YAPININ SARSMA MASASI DENEYLERİ

Yapılan bu çalışmanın amacı, pasif hibrit yalıtım sisteminin etkinliğinin ¼ ölçekli 3 katlı çelik yapı için araştırılmasıdır. Yalıtım sistemi 2 elastomer mesnet ve 4 düz kayıcı mesnetten oluşmakta ve sırasıyla elastomer mesnetler uzun doğrultu boyunca orta kolonların altında, kayıcı mesnetler is köşe kolonlar altında yer almaktadır. Yalıtımış ¼ ölçekli çelik yapı modeli sarsma masasında gerçek deprem kayıtları ve sinus dalgaları altında davranışı incelenmiştir. Deney sırasında ölçüm kayıtları üst yapıdan ve taban döşemesinden alınmıştır. İki çeşit yüksek sönümlemeli elastomer mesnetlerden birisi düşük kayma modülüne diğeri ise yüksek kayma modülüne sahip olmak şartıyla farklı hedef yalıtım periyotlarında deneyler yürütülmüştür. Hazırlanan numerik model, yapılmış olan deneylerin sonuçlarına bakılarak ayarlanmıştır. Bu tez çalısmasında, hibrit yalıtım sistemlerinin etkinliği, yalıtılmış yapı ve yalıtılmamış yapının numerik ve deneysel olarak çıkan değerlerine bakarak doğrulaması yapılmıştır.

TABLE OF CONTENTS

ACKNOWLEDGEMENTS iv

ABSTRACT vi

ÖZET vii

TABLE OF CONTENTS viii

LIST OF FIGURES xi

LIST OF TABLES xviii

LIST OF SYMBOLS / ABBREVIATIONS xix

1. INTRODUCTION 1

1.1. General Description 1

2. SEISMIC ISOLATION DEVICES 6

2.1. General Information 6

2.2. Elastomeric Bearings 7

2.2.1. Low Damping Rubber Bearing 9

2.2.2. Lead Rubber Bearing (LRB) 9

2.2.3. High Damping Rubber Bearing (HDR) 11

2.3. Sliding Bearings 15

2.3.1. PTFE Sliding Bearings 16

2.3.2. Friction Pendulum System 16

2.3.3. Resilient Friction Base Isolator(R-FBI) 19

2.4. Spring Type Systems 20

2.4.1. Gerb System 20

2.5. Dampers 20

2.5.1. Steel Hysteretic Dampers 21

2.5.2. Viscous Dampers 22

2.5.3. Friction Dampers 23

3. DESIGN CONSIDERATIONS OF ISOLATORS 24

3.1. General Definitions 24

3.2. Design Criteria for Isolators 25

3.2.1. Design of High Damping Rubber Bearing 26

3.2.2. Shear Strain and Stability Conditions for HRD Bearings 32

3.2.3. Design of Lead Rubber Bearings 34

3.2.4. Design Procedure for LRB 34

3.2.5. Shear strain and Stability Checks for LRB 38

3.2.6. Design of Friction Pendulum Systems (FPS) 39

4. LINEAR THEORY 42

5. CODE PROVISIONS 55

5.1. SEISMIC HAZARD LEVEL 55
5.2. Design Methods 56
5.3. Static Analysis 57
5.3.1. Seismic Zone Factor Z 59
5.3.2. Site Soil Profile Type 59
5.3.3. Seismic Source Types 60
5.3.4. Near Source Factors :Na and Nv 60
5.3.5. MCE Response Coefficient M_M 60
5.3.6. Spectral Seismic Coefficients: CVD,CVM and CAD, CAM 61
5.3.7. Damping Coefficients : BD and BM 62
5.3.8. Effective Vibration Periods: TD and TM 64
5.3.9. Total Design Displacements: DTD and DTM 65
5.3.10. Design Forces 66
5.3.11. Vertical Distribution of Force 68
5.3.12. Drift Limits 69
5.3.13. Dynamic Analysis 69
5.3.14. Time History Analyis 70
5.3.15. Scaling 70
5.3.16. Design and Testing Requirements for Isolaters 71
6. APPLICATIONS OF SEISMIC ISOLATION 73
6.1. Seismic Isolation in the United States 74
6.1.1. The Salt Lake City and County Building, Utah 74
6.1.2. The University Hospital of the University of Southern California 76
6.1.3. San Francisco City Hall 78
6.1.4. Los Angeles City Hall 79
6.2. Seismic Isolation in Japan 80
6.2.1. The High-Tech R&D Centre, Obayashi Corporation, Tokyo 81
6.2.2. The C-1 Building, Tokyo 81
6.2.3. The Computer Center of the Tohoku Electric Power Company, Sendai 82
6.3. Seismic Isolation in New Zealand 82
6.3.1. New Zealand Parliament Buildings 82
6.3.2. The William Clayton Building 84
6.3.3. Wellington Central Police Station 84
6.4. Seismic Isolation in Italy 85
6.4.1. The SIP Complex, Ancona 85
6.4.2. The Mortaiolo Bridge 86
6.5. Seismic Isolation in Turkey 86
6.5.1. Kocaeli University Hospital 87
6.5.2. EGEGAZ, LNG Tanks 88
6.5.3. Tarabya Hotel 90
6.5.4. TEB General Directorate Building 93
6.5.5. Atatürk Airport 95
6.5.6. Bolu Viaducts 97
7. TEST SETUP AND INSTALLATION 100
7.1. Shake Table Test 100
7.2. Test Setup and Instrumentation 101
7.3. The Isolation System 102
7.4. The Data Acquisition and Control System 104

7.5. Tests Conducted 106
8. TEST RESULTS 108
8.1. General Description 108
8.2. Input data for Shake Table Tests 108
8.3. Tests of Normal Compound HDR Bearings at Different PGA Scaled Earthquakes (SI-N 150/136) 109
8.4. Tests of Soft Compound HDR Bearings at Different PGA Scaled Earthquakes (SI-N 150/136) 114
8.5. Sinusoidal Harmonic Tests 117
8.6. Comparison of Numerical and Experimental Results 119
8.7. Determination of Characteristic of Two Isolated Structure and Fixed Supported Structure 121
9. CONCLUSION 124

APPENDIX A 126

REFERENCES 139

LIST OF FIGURES

Figure 1.1. Comparison of fixed supported system with an isolated system..... 2

Figure 1.2. Effect of lenghtening period by seismic isolation (Skinner, 1993)..... 2

Figure 1.3. Effect of damping on deformation (Skinner, 1993) 3

Figure 2.1. Cross-section of an elastomeric bearing..... 8

Figure 2.2. (a) Vertical behavior of laminated rubber bearing under service loads (b) Horizontal behavior under lateral loads..... 8

Figure 2.3. Cross-section of a lead rubber bearing and the location of a lead core..... 10

Figure 2.4. Idealized force-displacement loops of LRB(FEMA 356, 2000) 11

Figure 2.5. Rectangular HDR bearing for bridge applications 12

Figure 2.6. Application of HDR bearing which is mounted below steel columns 12

Figure 2.7. Analytical Force Displacement Loops of HDR bearing (FEMA 356, 2000)... 13

Figure 2.8. Force-Displacement graphs of a stiffening bilinear spring (Tsopelas and Constantinou, 1994) 14

Figure 2.9. Stiffness-displacement graphs of stiffening bilinear spring (Tsopelas and Constantinou, 1994) 14

Figure 2.10. Idealized behavior of flat sliding bearings (FEMA 356, 2000) 16

Figure 2.11. Parts of a FPS bearing 17

Figure 2.12. Characteristics of a pendulum motion 17

Figure 2.13. Prototype of FPS bearing (Uçkan, 2005) 18

Figure 2.14. Size of a FPS isolator that was used in Benecia Martinez Bridge 18

Figure 2.15. Section of a viscous damper 23

Figure 3.1. Different types of damper devices 25

Figure 3.2. Reduced cross-sectional area 30

Figure 4.1. Two-Degree-of freedom system for isolated structures 43

Figure 5.1. Design spectra in IBC 2000 55

Figure 6.1. Salt Lake City Hall 75

Figure 6.2. Plan view of Salt Lake City 76

Figure 6.3. Wall connections of Salt Lake City Hall 76

Figure 6.4. Acceleration records of USC University Hospital during 1994 Northridge earthquake 77

Figure 6.5. Test had done in for USC University and rolling effect of rubber 78

Figure 6.6. View of San Francisco City Hall 79

Figure 6.7. New Zealand Parliamant Building (Skinner,1993) 83

Figure 6.8. Kocaeli Hospital 87

Figure 6.9. Construction stages of Kocaeli Hospital 88

Figure 6.10. Egegaz LNG storage tanks 89

Figure 6.11. Locations of isolation devices for LNG tanks 89

Figure 6.12. Cross-section of a LNG tank and location of isolators 90

Figure 6.13. Tarabya Hotel 90

Figure 6.14. Locations of FPS bearings and plan view of Tarabya Hotel 91

Figure 6.15. Cross-section of columns at Tarabya Hotel 91

Figure 6.16. Implemantation process of FPS 92

Figure 6.17. Implementation of FPS devices 92

Figure 6.18. Replacement of FPS isolators to colums for retrofit project 93

Figure.6.19. Mounted FPS isolator in Tarabya Hotel 93

Figure 6.20. TEB Building 94

Figure 6.21. SAP2000 model of TEB building 94

Figure 6.22. Plan view and isolator locations of TEB building 95

Figure 6.23. Location of FPS at airport 96

Figure 6.24. Locations of FPS isolators in Atatürk Airport 96

Figure 6.25. Location of a FPS isolator in Atatürk Airport 97

Figure 6.26. Bolu Viaducts 97

Figure 6.27. Locations of FPS isolators at bolu Viaducts 98

Figure 6.28. Plan view of Bolu Viaducts 98

Figure 6.29. Mounted FPS isolator at Bolu Viaducts 99

Figure 6.30. Size of FPS bearings that have used in Bolu Viaduct project 99

Figure 7.1. Plan view of the base slab and floor levels 101

Figure 7.2. Passive Hybrid Isolation System 102

Figure 7.3. Configuration of isolators 104

Figure 7.4. Locations of LVDTs to measure translational displacements 105

Figure 7.5. Locations of Accelerometers 106

Figure 8.1. Acceleration records at three different levels of the isolated structure under 110

Figure 8.2.Displacement records from three different locations under El Centro Earthquake (Pga=0.293) 111

Figure 8.3. Base shear under El Centro Earthquake (Pga=0.293g) 111

Figure 8.4. Base Shear-Displacement loops under El Centro earthquake (PGA=0.293g) 112

Figure 8.5. Acceleration records under scaled El Centro earthquake (PGA=0.556g) 112

Figure 8.6. Displacement records under Scaled El Centro Earthquake (Pga=0.556g) 113

Figure 8.7. Base Shear at slab level under Scaled El Centro Earthquake(Pga=0.556g)... 113

Figure 8.8. Base Shear-Displacement loops for PGA scaled El Centro (Pga=0.556g) 114

Figure 8.9.Acceleration records for the second isolation system under El Centro Earthquake(Pga=0.293) 115

Figure 8.10.Displacement records for the second isolation system under El Centro Earthquake (Pga=0.293g) 115

Figure 8.11.Base shear of second isolation system under El Centro Earthquake (Pga=0.293g) 116

Figure 8.12. Base Shear Displacement loops for the second isolation system under El Centro Earthquake (Pga=0.293g) Periods of hybrid isolation system 116

Figure 8.13. Acceleration records under Sinewave3 118

Figure 8.14. Comparison of harmonic excitations to determine the effective damping of SI-N 150/136 118

Figure 8.15. Comparison of Base Shear-time graphs 119

Figure 8.16. Comparison of numerical and measured relative displacements under El Centro Earthquake which has PGA value equal to 0.293g 120

Figure 8.17. Comparison of base shear of fixed supported system with isolated system1 (SI-N 150/136) and isolated system2 under El Centro Earthquake 120

Figure 8.18. Comparison of effective damping of combined system under real earthquakes 121

Figure 8.19. Transfer function of first isolated system that has normal compound high damping rubbers 121

Figure 8.20. Evaluation of transfer function of fixed supported system for the first test setup 122

Figure 8.21. Transfer function of second isolated system which has soft compound high damping rubbers 122

Figure 8.22. Transfer function of fixe supported system which has determined from second test setup 123

Figure A.1. Scaled El Centro record for test 1 126

Figure A. 2. Acceleration records at different levels of isolated structure during test1 ... 127

Figure A.3. Displacement records at different levels of the isolated structure during test1 127

Figure A.4. Base Shear- Time graph of test1 128

Figure A.5. Base Shear-Diplacement graph of the isolated structure during test1 128

Figure A.6. Scaled El Centro record for test 2 129

Figure A.7. Acceleration records at different levels of isolated structure during test2 129

Figure A.8. Displacement records at different levels of the isolated structure during test2 130

Figure A.9. Base Shear- Time graph of test2 130

Figure A.10. Base Shear-Diplacement graph of the isolated structure during test2..... 131

Figure A.11. Scaled El Centro record for test 3..... 131

Figure A.12. Acceleration records at different levels of isolated structure during test3 .. 132

Figure A.13. Displacement records at different levels of the isolated structure during test3..... 132

Figure A.14. Base Shear- Time graph of test3 133

Figure A.15. Base Shear-Diplacement graph of the isolated structure during test3..... 133

Figure A.16. Scaled El Centro record for test 4..... 134

Figure A.17. Acceleration records at different levels of isolated structure during test4 .. 134

Figure A. 18. Displacement records at different levels of the isolated structure during test4 135

Figure A. 19. Base Shear- Time graph of test4 135

Figure A. 20. Base Shear-Diplacement graph of the isolated structure during test1..... 136

Figure A. 21. Sap2000 Model of the isolated building..... 137

Figure A. 22. Base Shear–displacement loops of HDR bearings inSAP2000..... 138

Figure A. 23. Base Shear–Displacement loops of flat sliding bearings 138

LIST OF TABLES

Table 3.1. Design values for rubber (Bridgestone, 1990) 28

Table 5.1. Response Coefficient due to IBC 2000 61

Table 5.2. Damping Coefficient values in IBC 2000 63

Table 5.3. Reduction factors for fixed-base and isolated structure 67

Table 7.1. Properties of 2 HDR bearings 103

Table 8.1. Properties of HDR isolators 109

Table 8.2. Properties of harmonic motions that were applied during tests 117

LIST OF SYMBOLS / ABBREVIATIONS

k_h	Horizontal stiffness of isolators
k_v	Vertical Stiffness of isolators
k_{eff}	Effective stiffness of isolators
k_p	Post Yield Stiffness of isolators
k_I	Initial Stiffness of isolators
G	Shear modulus of isolators
A_r	Bonded rubber area
ϕ	Shape factor of rubber isolators
R	Radius of curvature of FPS
E	Compressive strength of concrete
K	Yield strength of reinforcement
Q	Characteristic Strength
N	Axial load
$fmax$	Maximum dynamic coefficient of friction
$fmin$	Minimum dynamic coefficient of friction
a	Rate parameter
μ_s	Dynamic coefficient of friction
γ	Shear strain
Δ	Displacement
f_{py}	Yield strength of the lead plug in shear
Q_d	Yield force of the lead plug
W_D	Energy dissipated per cycle
D	Design displacement of the bearing

LRB	Lead Rubber Bearing
LB	Low Damping Rubber Bearing
HDR	High Damping Rubber Bearing
PTFE	Polytetraflouroethylene
FPS	Friction Pendulum Systems
DBE	Design Base Earthquake

MCE	Maximum Credible Earthquake
KOERI	Kandilli Observatory and Earthquake Reseach Institute
ASSHTO	American Association of State Highway and Transportation Officials
EC	Eurocode
IBC	International Building Code
FEMA	Federal Emergency
MCEER	Multidiciplinary Center For Earthquake Engineering Research
ABYYHY	Afet Bölgelerinde Yapılacak Yapılar Hakkında Yönetmelik
ARS	Acceleration Response Spectra
DRS	Displacement Response Spectra
RC	Reinforced concrete

1. INTRODUCTION

1.1. General Description

Earthquakes are natural disasters which can cause serious threats for human lives and economies. During an earthquake significant damages can occur in the superstructure and the contents of the infrastructure. Earthquake resistant design of structures are based on conventional design philosophy which is a demand and capacity relation. Capacity of the superstructure has to exceed the demand to avoid structural damage and collapse. Due to increase of demand it is necessary to increase the strength of the building but it is not practical and economic to increase the capacity infinitely. Because of this reason, most codes that has a conventional design philosophy that allows to use ductility to achieve the required capacity. .Ductility is a concept of allowing the structural elements to deform beyond their elastic limits in a controllable manner. Main problems about the conventional design are interstory drifts for flexible structures or high floor accelerations for stiff buildings. In order to minimize the interstory drifts, the structure must be stiffned which leads to amplification of the eartquake excitation with high floor accelerations. This can be a problem for the contents of the superstructure. In contrast, floor accelerations can be reduced by the flexibility but at that point interstory drifts are increased. Thus, contents of the structure and nonstructural components may suffer significant damages during strong ground motions even if the structure do not collapse. Best way to avoid those two problem are achieved by isolation systems. Figure 1.1. shows the comparison of fixed supported system with an isolated system.

Objective of seismic isolation is to mitigate earthquake effects and to make superstructure remain essentially elastic during earthquakes by shifting the fundamental frequency of the structure from the dangerous resonance range. In other words, seismically isolated structures has a fundamental frequency that is much lower than the corresponding fixed-supported structure and the usual predominant frequencies of a typical earthquake. Seismic isolation concept is very simple and based on the decoupling of the superstructure

from the ground.

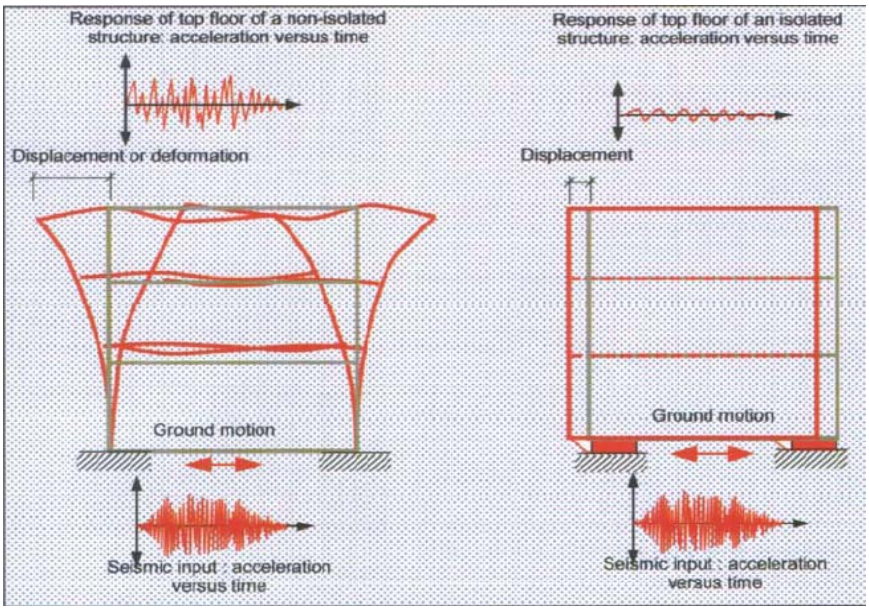

Figure 1.1. Comparison of fixed supported system with an isolated system

Even though it is not a new concept for earthquake-resistant design it has received a great attention during recent two decades. Rather than increasing the capacity of structure, demand of the superstructure is reduced at the isolation level. Various isolation systems are used to decouple the superstructure and with the help of isolation layer. Structures are not normally isolated with vertical motion because vetical motions are relatively smaller than the horzontal motions by means of magnitude.

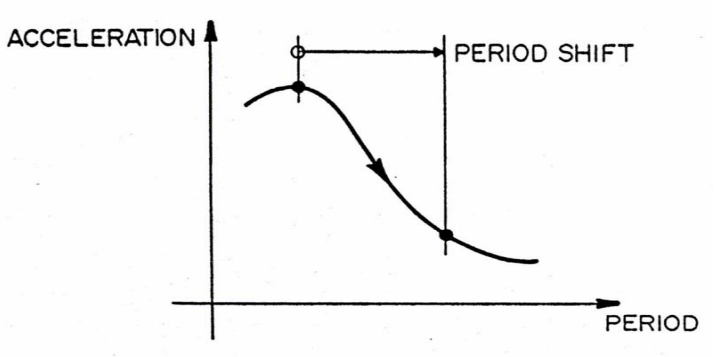

Figure 1.2. Effect of lenghtening period by seismic isolation (Skinner, 1993)

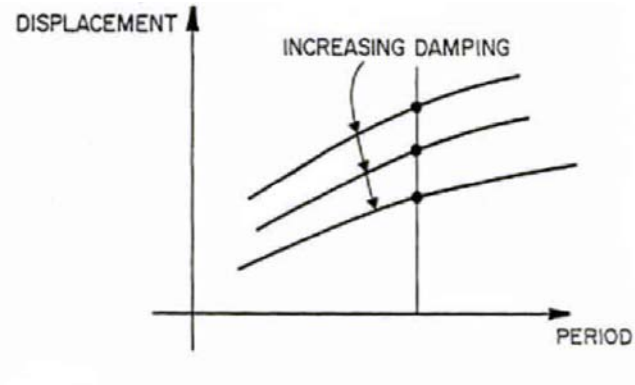

Figure 1.3. Effect of damping on deformation (Skinner, 1993)

Majority of buildings in seismic regions are low-to-medium rise buildings where the seismic isolation is applicable to these type of buildings. In contrast, high rise buildings even in high seimic regions are dominated by wind loads rather than earthquake induced external loads. Thus, passive seismic isolation devices are not prefered to use in high rise buildings to lengthen the period of a high rise building.

Furthermore, the increasing acceptance of seimic isolation as a technique is shown with the retrofitting projects all over the world. Seismic isolation is started to consider as a solution in such cases. The effectiveness of isolation system depends upon the characteristics of the earthquake ground motion and the superstructure. In addition, site characteristics are very important to determine the design method with respect to code provisions.

There are generally two basic approaches for passive seismic isolation systems. First approach is to install a flexible layer between the ground and the superstructure. This flexible layer is provided by elastomeric bearing which has a high vertical stiffness and relatively low horizontal stiffness to achieve the desired flexibility. With the help of such isolation devices, natural period of the structure will be significantly lengthened. Elastomeric bearing is also known as laminated rubber bearing because of the steel layers between the rubbers. Main principle of using steel layer is to sustain the vertical load acting on the bearings. In addition, rubber provides the flexibility to the isolation layer.

Major function of elastomeric bearing is to reduce the transmission of shear forces to the superstructure through lengthening of vibration period of the entire system. Transmission of reduced shear force is achieved by large displacements occured at the isolation layer. To avoid large displacements inherent damping or additional devices can be used. Inherent damping properties of high damping rubber is provided by the special compound that has used in the manufacturing process or lead plug is used to at the center of LRB to achieve the damping required to minimize the displacements. Also, elastomeric bearings have to provide sufficient rigidity under the service load levels for winds and minor earthquakes.

The other approach is to provide a sliding layer or friction surface between the foundation and ground. The shear force transmitted to the superstructure is limited by the static friction force which is equal to the product of axial load and the friction coefficient. Effectiveness of sliding isolation system depends on the friction coefficient. Manufacturers try to keep that value as low as possible. Nonetheless, sliding system has to sustain minor earthquakes and wind loads. Sliding bearings can be divided into two main categories, one of them is flat sliding bearings and the other one is FPS which has a concave surface. Flat sliding bearings do not have a restoring force where residual displacements can occur after each earthquake.Thus, restoring force component is provided by only elastomeric bearings or by only linear spring elements. In contrast, restoring force is achieved by geometry of FPS type of bearings.

Extensive researches about passive isolation systems have been carried out during recent two decades. One of the advantage of base isolation system is that the applicability of system is not restricted to the civil structures. It is also applicable to the sensitive equipments, too. In this wide range of use seismic isolation can be used for in many projects as an alternative of conventional design.

Passive isolation systems are sometimes used as a combined system to take advantage of both of the systems. However, there are some uncertainties about the effectiveness of this kind of systems. Main objective of this study is to evaluate the

performance of a ¼ scaled mass concentric symmetric system with a passive hybrid isolation system. In this research study, hybrid isolation system consists of 2 HDR bearing and 4 flat bearings. Semi active and active control systems are beyond the scope of this study.

2. SEISMIC ISOLATION DEVICES

2.1. General Information

Seismic isolation is started to use in seismic regions with an increasing attention, especially from the beginning of the previous century. One of the most important features of a convenient seismic isolation of structures is that determining proper isolator devices - or systems, we shall say- in order to achieve enough horizontal flexibility and also effective damping, too.

Seismic isolators are used as buffer zones for limiting the isolators' displacement at a possible, destructive earthquake. The fundamental purpose of an isolation system is backing up a structure. At the mean time, it shall resist a high capacity of a horizontal flexibility. The most remarkable function of a structure which has an isolation system is to survive about 30 to 80 or a few more years. During this period, the isolation system is expected to remain operational.

There are so many seismic isolation devices that have been used throughout the world. Most of them are mainly developed for practical purposes. Some of these devices have widespread acceptance and especially by the improvement of technology on isolation systems, they are patented each year with an increasing tendency. Although these great sparkling of development, some of these devices are impractical and furthermore they have high prices which make them impossible to use in the applications except big and important projects.

Nowadays, it is known that elastomeric bearings and sliding systems are the most common types of isolator devices which have been used in the applications all over the

world. These devices are preferred mostly because they provide economy, reliability and simplicity. Moreover, there are some other systems that combine elastomeric bearings and sliding bearings which have proposed as passive hybrid isolation systems. Among many isolation systems, these two seem the most successfully used ones. Further information about all of these systems have been explained in details as follows:

2.2. Elastomeric Bearings

Elastomeric bearings have been used in most of the projects until now. Generally, elastomeric bearings are classified as low-damping natural rubber bearing, lead rubber bearing and as high damping rubber bearing. The first application of natural rubber bearing is used for the protection of Pestalozzi School in Skopje, Macedonia. Large blocks without steel reinforcing plates had used in that project. Experiences showed that vertical load on the natural bearings had caused reduction of height. Because the vertical stiffness of the bearings are just only a few times the horizontal stiffness and the rubber is relatively undamped. The natural bearing that have used at Skopje was tested on the shake table at the EERC in 1982 (Staudacher, 1982). Tests were showed that horizontal motion is strongly coupled to a rocking motion. The system is still in Skopje and the isolation system is monitored from time to time.

In order to reduce the lateral bulging of natural rubber bearing, steel plates are installed between rubber blocks to increase the vertical stiffness with only small deformations. By the help of steel shims vertical stiffness is increased to approximately several hundreds times of horizontal stiffness and do not effect the laminated bearing in horizontal direction. Main function of steel shims are shown in the figure below

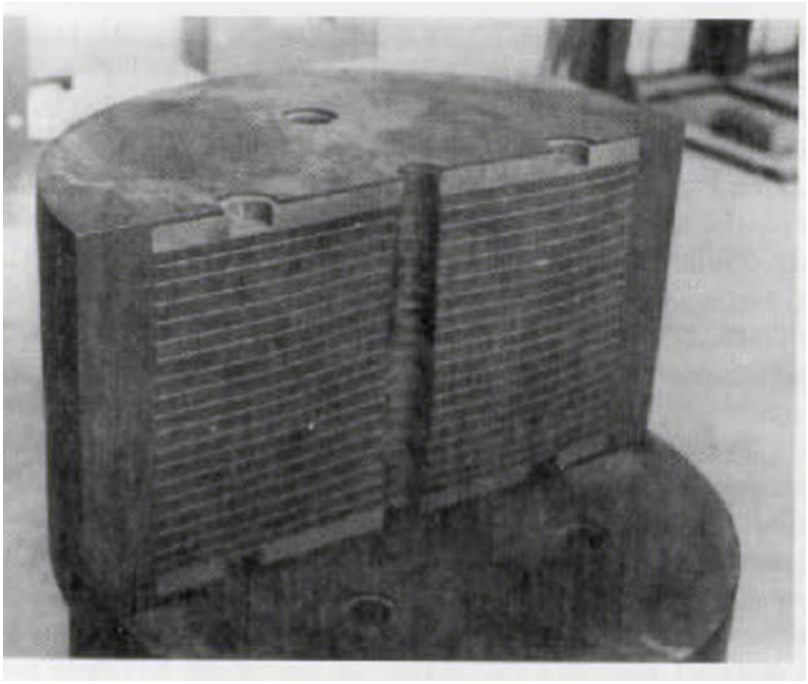

Figure 2.1. Cross-section of an elastomeric bearing

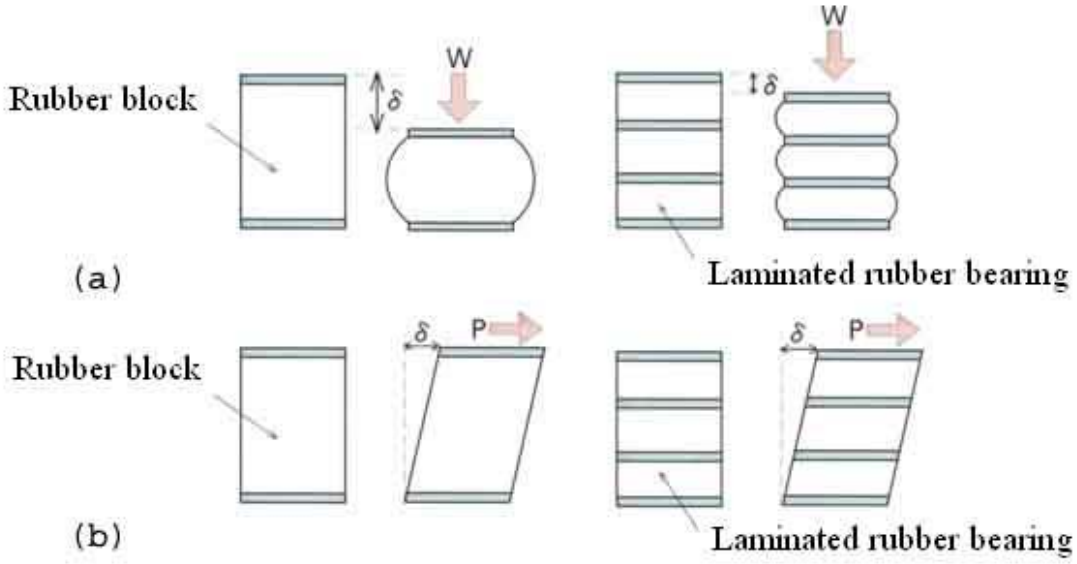

Figure 2.2. (a) Vertical behavior of laminated rubber bearing under service loads
(b) Horizontal behavior under lateral loads

The essential function of elastomeric bearings is decreasing the transition of shear forces to the superstructure by lengthening the structure's period. Also, they should meet

the sufficient rigidity requirement for the isolated structure against wind or earthquake loads.

2.2.1. Low Damping Rubber Bearing

Low damping rubber bearing is manufactured from natural rubbers and it has steel shims between the rubber layers to avoid the lateral bulging as mentioned above. Steel shims are vulcanized and bonded to rubber blocks in a single process with pressure and heat. Steel shims do not have any effects on horizontal stiffness of the low damping rubber bearing. Horizontal stiffness is only controlled by the low shear modulus. Because of the material have used in the manufacturing process LR bearings exhibits linear up to shear strains. Low damping rubber bearing is widely used with supplemental devices such as viscous dampers, steel bars, frictional devices and etc.

2.2.2. Lead Rubber Bearing (LRB)

Lead rubber bearing is a single compact component that combines a lead plug and natural rubber bearing. Lead plug provides the hysteretic damping and laminated natural rubber is able to supply the required displacements for seismic isolation. Lead rubber bearings consist of the combination of elastomeric bearings and dampers, that is also called as single or separate combination. In this type of combination, which lead rubber is an example for, isolator has two functions. These functions are energy dissipation and horizontal flexibility.

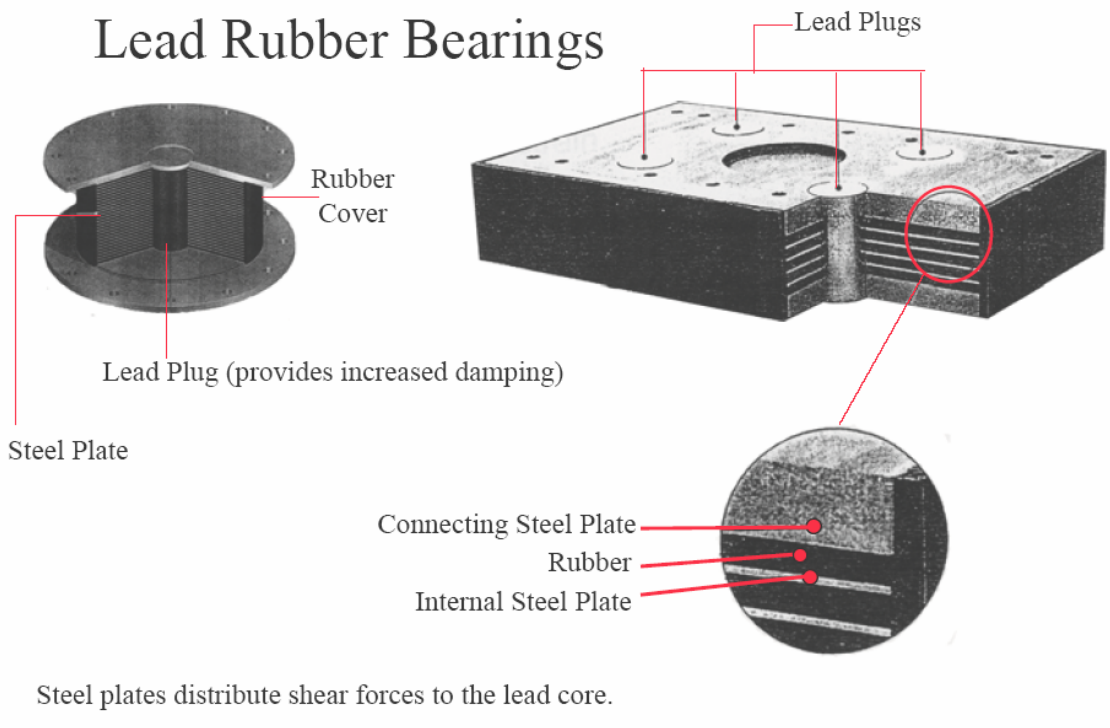

Figure 2.3. Cross-section of a lead rubber bearing and the location of a lead core

Lead rubber bearing consists of natural rubber with thin steel plates and a lead core that has plugged at the center location. Lead plug is confined with the natural rubber and thin steel plates. Horizontal flexibility of lead rubber bearing is achieved by very low shear modulus of the rubber. Moreover, lead rubber bearing exhibits linear behavior for strains up to 100-250%. The research studies have shown that its mechanical properties are not influenced by temperature, aging, and rate or history of loading (Komodromos, 2000).

One of the important properties of LRB is the crystallization of lead core. In other words, lead can change its structural property temporarily under deformations beyond its yield point and then relatively behaves like linear. Main objective of using lead is that the lead yields in pure shear at the relatively at low level of stress (~ 10MPa). Idealized hysteretic force-displacement loop of LRB is shown in Figure 2.4.

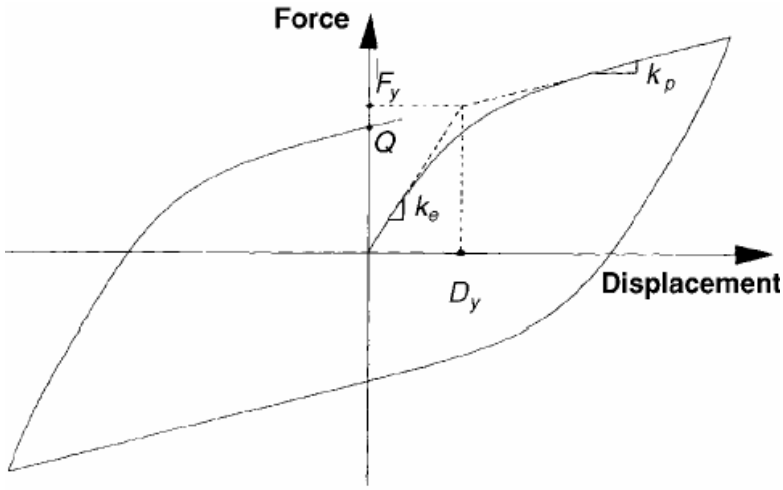

Figure 2.4. Idealized force-displacement loops of LRB(FEMA 356, 2000)

2.2.3. High Damping Rubber Bearing (HDR)

In the last couple of decades, the technology of seismic isolation concept has rapidly improved so that many innovations in terms of isolation devices occurred one after the other. High damping rubber (HDR) bearings are one of the significant of those that are composed of thin steel plates and special rubber compound which has an inherent damping property. The rubber sheets are vulcanized and bonded to thin steel plates under pressure and heat. Thin steel plates provide the vertical stiffness to avoid the bulging of the rubber under axial loads. Due to the addition of special fillers, such as carbon and resins. The addition of fillers increases the damping properties without affecting its mechanical properties (Komodromos, 2000). Shape of elastomeric bearings can be cylindrical or rectangular.

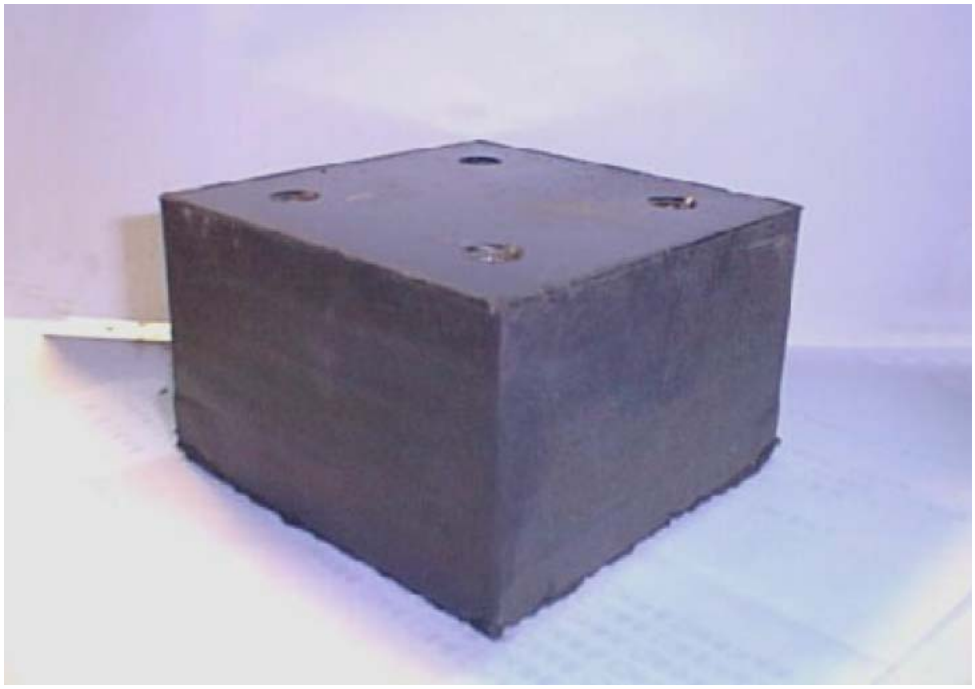

Figure 2.5. Rectangular HDR bearing for bridge applications

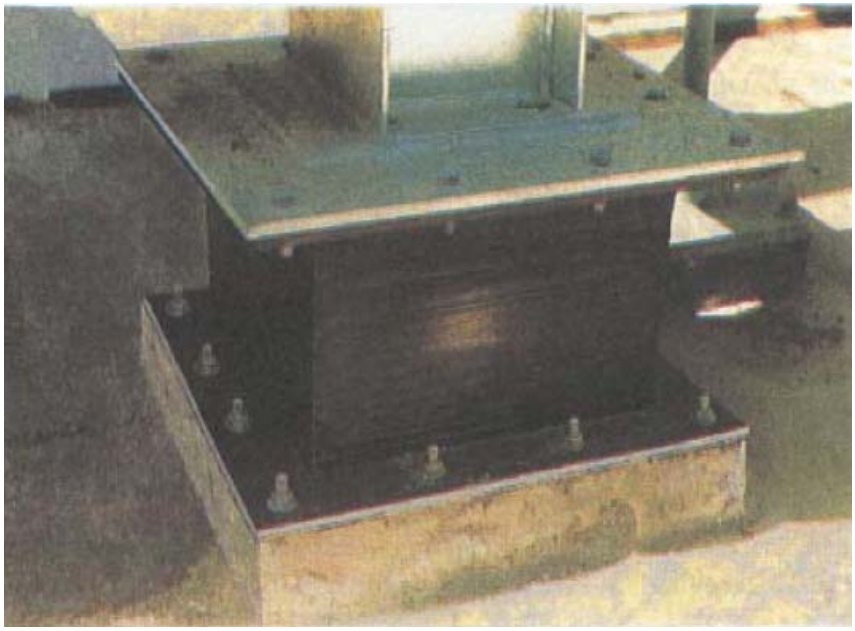

Figure 2.6. Application of HDR bearing which is mounted below steel columns

HDR bearing performs effective damping in the range of 0.10-0.20 and it is achieved by addition of special chemical compounds. Stiffness and damping properties of the HDR

are required to resist wind and minor earthquakes. In practice, the stiffness and damping properties of the HDR remain quite stable under one or more design earthquakes. Analytical hysteresis loops of HDR is given in Figure 2.7.

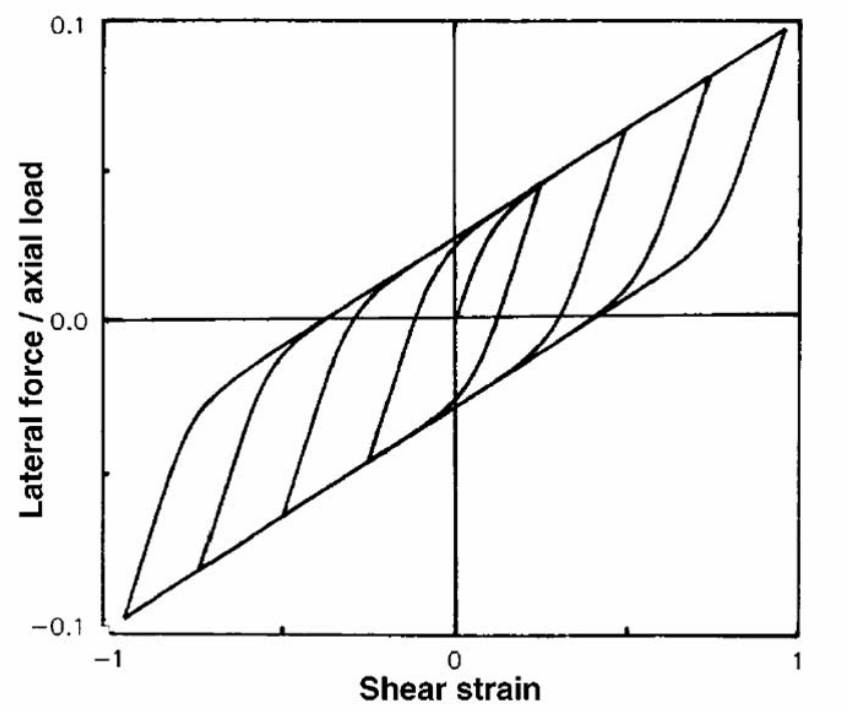

Figure 2.7. Analytical Force Displacement Loops of HDR bearing (FEMA 356, 2000)

High damping rubber bearings exhibit higher stiffness at large strains and element is formed by combining the elastoplastic version ($\alpha = 0$) of the biaxial hysteretic element and a stiffening bilinear spring. K_1 is the tangent stiffness which is mobilized for displacements less than the limit D_1 and K_2 is the higher tangent stiffness which is mobilized for displacements larger than the limit D_2.

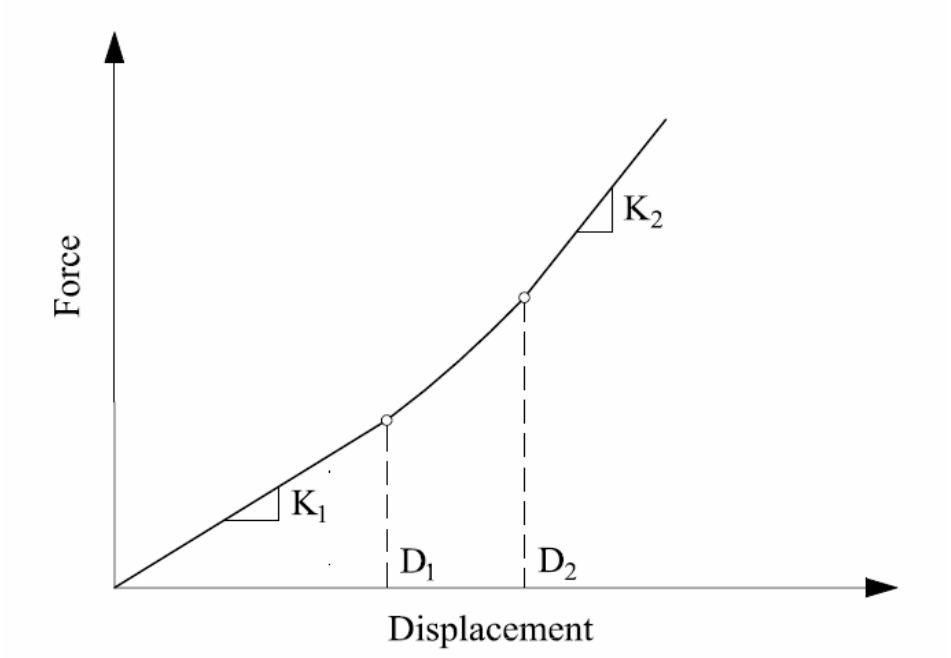

Figure 2.8. Force-Displacement graphs of a stiffening bilinear spring (Tsopelas and Constantinou, 1994)

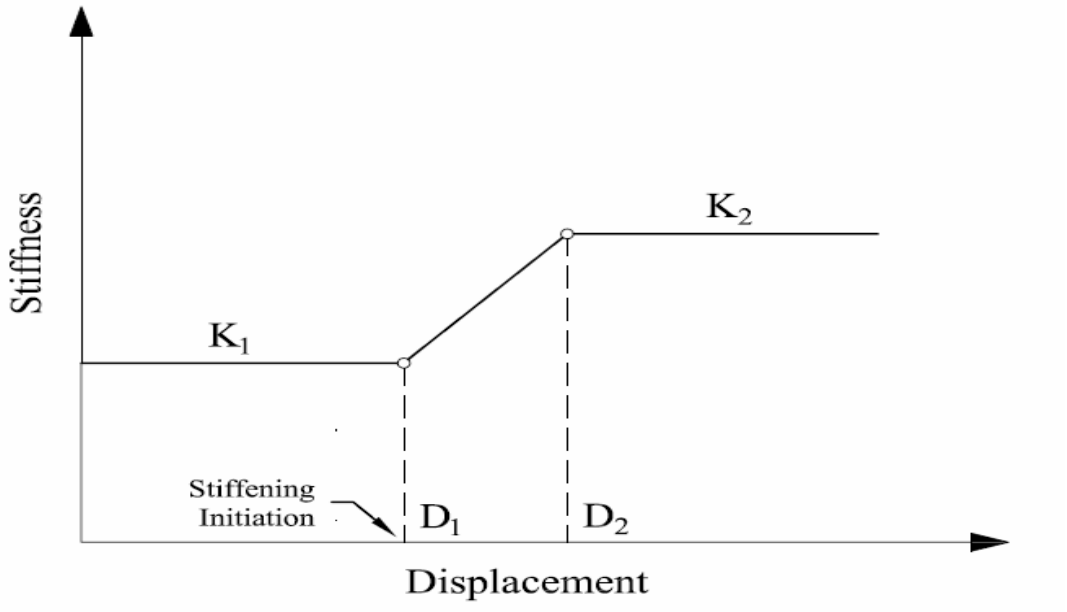

Figure 2.9. Stiffness-displacement graphs of stiffening bilinear spring (Tsopelas and Constantinou, 1994)

Modeling of the behavior of a high damping rubber bearing based on data from the testing specimens that had used at State University of New York, Buffalo. The test data on the scaled specimens obtained at pressure of 10 Mpa and frequency of 0.5 Hz are tangent shear modulus for shear strain $\gamma = 0.5$ to 1.0 G= 0.8 Mpa, equivalent damping ratio $\beta = 0.10$ at shear strain $\gamma = 1.0$, displacement limits D_1= 1.2T and D_2 =1.3T, yield displacement Y=0.07T, where T=total rubber thickness. Furthermore, the tangent stiffness beyond the displacement limit D_2 is $K_2=2K_1$.

2.3. Sliding Bearings

The second approach to increase a structure's flexibility to get a sliding or friction area between the base of the structure and the foundation. (Yang and Chang, 2003)

A purely sliding system is the earliest and simplest isolation system to be proposed. In the severe Indian earthquakes of Dhubai (1930) and Bilhar (1934) it was observed that small masonry buildings that slid on their foundations survived the earthquake, while similar buildings fixed at the base were destroyed. (Naeim, 1999)

In devastating 1976 Tangshan earthquake, it was observed that buildings that survived the earthquake had a horizontal crack at the bottom of the walls that the masonry superstructure from damage. (Kelly, 1999)

Most sliding systems have advantage that they are not affected by either natural frequency of isolated structure or the frequency content of the earthquake when sliding bearings are compared with elastomeric bearings (Yang and Chang, 2003). Nevertheless, most of the sliding systems are not able to return their initial position and residual displacements occur after major earthquakes. Coefficient of friction is the most important parameter for sliding systems because it determines whether sliding will occur or not at

certain levels of shear forces.

2.3.1. PTFE Sliding Bearings

PTFE (polyterafluorotethylene) is the most common sliding bearing type. PTFE bearings were used to provide low-friction supports for parts of bridge support structures from 1965. The coefficient of friction of a PTFE bridge bearing is typically of the order of 0.03, when operating at the very low rates arising from temperature cycling of the bridge superstructure. However, it is found that the coefficient of friction is very much higher and is dependent on pressure and sliding velocity, when operating velocity is typical of that which occurs in an isolator during a design level earthquake, and when the operating pressure is typical of that adopted for PTFE bridge bearings (Tyler, 1977). For operating conditions typical of seismic isolator actions during design level earthquakes, the frictional coefficients ranged from about 0.1 to 0.15 or more (Skinner, 1993)

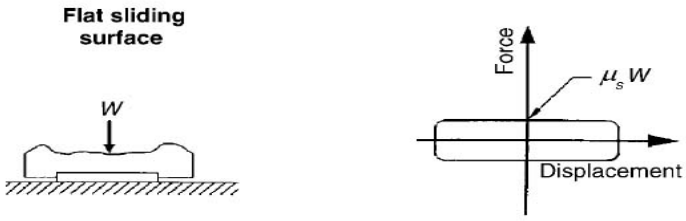

Figure 2.10. Idealized behavior of flat sliding bearings (FEMA 356, 2000)

2.3.2. Friction Pendulum System

The friction pendulum system (FPS) is a frictional isolation system that combines a sliding action and a restoring force by geometry. The FPS isolator has an articulated slider that moves on a stainless steel spherical surface. Friction between the articulated slider and

the spherical surface generates damping in the isolators. The effective stiffness of the isolator and the isolation period of the structure are controlled by the radius of curvature of the concave surface (Kelly, 1999).

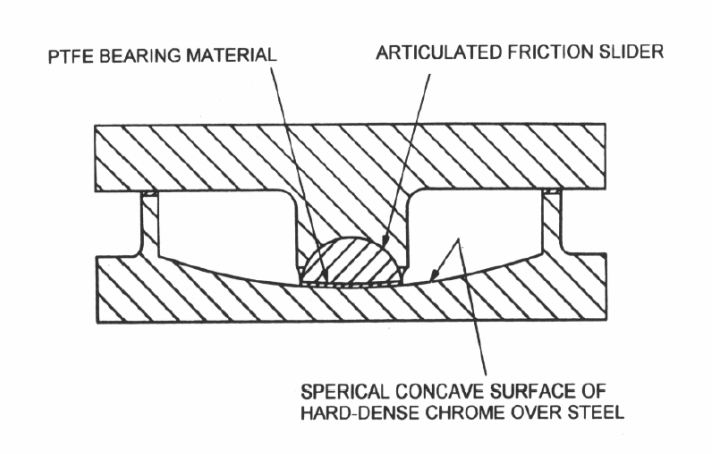

Figure 2.11. Parts of a FPS bearing

The friction pendulum isolators use the characteristics of pendulum to lengthen the natural period of the isolated structure so as to avoid the strongest earthquake forces.

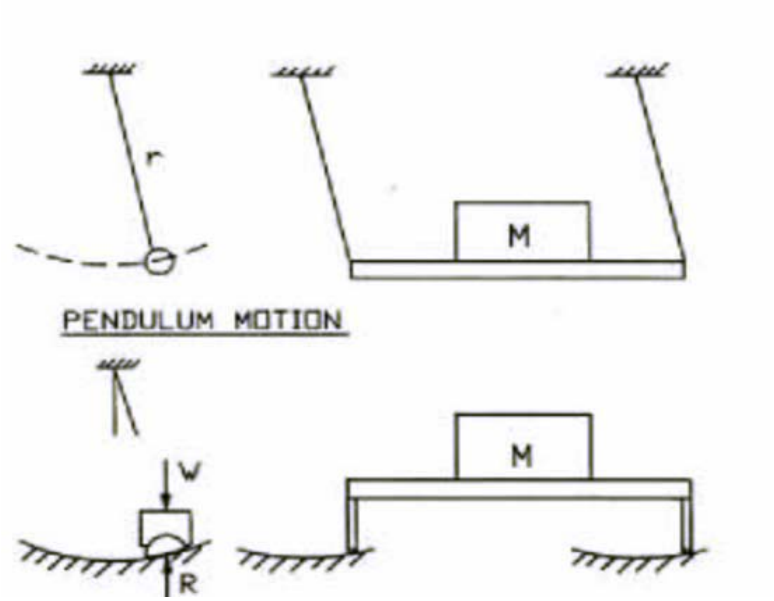

Figure 2.12. Characteristics of a pendulum motion

Figure 2.13. Prototype of FPS bearing (Uçkan, 2005)

Figure 2.14. Size of a FPS isolator that was used in Benecia Martinez Bridge

The friction pendulum bearing has the flexibility to achieve a wide range of properties. Changing the sliding period from 2 to 3 seconds and reduces the base shear and increases the displacement. When the earthquake forces are below the friction level, a friction pendulum supported structure responds like a conventionally supported structure, as its non-isolated period of vibration. Once the friction force level is exceeded, the structure responds as its isolated period, with the dynamic response and damping controlled by the bearing properties. (Cimilli, 2002)

It is known that friction pendulum bearing is independent of the mass of the supported structure is an important property which has in controlling the response of a structure.

2.3.3. Resilient Friction Base Isolator(R-FBI)

The Resilient-fraction seismic isolation (R-FBI) bearing is designed to overcome the high friction coefficient of Teflon on stainless steel at high velocities by using many sliding interfaces in a single bearing. Thus the velocity between the top and bottom of the bearing is divided by the number of layers so that the velocity at each face is small, maintaining a low friction of coefficient. (Naeim, 1999). In the center of the isolater a rubber core exists and it carries no service load. Nonetheless, the rubber core provides a restoring force. During the tests it was observed that the rubber core do not prevent the displacement from being concentrated in a single layer. Thus, to overcome this problem, a steel road is inserted in the rubber core. The steel in the core section improved the distribution of displacement at sliding layers.

2.4. Spring Type Systems

Elastomeric and sliding isolation systems lenghtening the period of an isolated system. These two isolation system only provide horizontal isolation. In contrast, for the three dimensional isolation system usually spring type of isolators are used.

2.4.1. Gerb System

The gerb system for seismic isolation was developed originally for the vibration isolation of power plant tribune generating equipment (Naeim, 1999). Large helical springs are used to provide flexibility in horizontal and vertical directions. Vertical frequency is approximately 3-5 times of horizontal frequency. In all three dimensional isolation system, there is very strong coupling between horizontal motion and rocking motion. Spring type of isolation system is practical for in cases such as center of gravity and center of stiffness are at the same level- in a reactor vessel in a nuclear power plant.

2.5. Dampers

Dampers are used as supplemental devices to the other isolation elements. The main goal of using dampers is to reduce the displacement that will occur at the isolation level during major earthquakes.

Hysteretic yielding dampers are generally steel, which may be configured to yield in bending, shear or axially, or lead which yields in pure shear. The configuration of dampers are in such places and deforms with interstory drifts.

Axially yielding dampers are generally steel, which may be configured as diagonal braces although they maybe although they may also be placed horizontally from the top of a partial height wall to an adjacent column. Shear or flexural yielding dampers can be configured to connect the top of a wall panel to the soffit of the girder of the floor above. The wall panel is a cantilever from the wall below, with a gap between the top of the wall and the floor above. As an alternative to a wall panel, the shear and flexural dampers can be mounted on a steel frame (Holmes Design Guideline for Dampers, 2001).

Lead is generally shows an elasto-plastic behavior which has no strain hardening. In contrast mild steel has a yield plateu followed by strain hardening behaviour to ultimate strength. Damping forces depend on strain levels and it can increase with displacement. Detailed description of different type of dampers are explained below

2.5.1. Steel Hysteretic Dampers

At the end of 1960s a number of damping mechanisms and devices have started to use for increasing the seismic resistance of a range of structures. Around that time, high capacity dampers were assumed to be developed in order to utilize the plastic deformation of steel beams. Since then, these steel-beam dampers have been used and improved to have hysteretic damping for seismic isolation in many countries. They are acting in shear, and also provide stiffness and damping.

These type of dampers are displacement dependent and so provide a maximum force at maximum displacement, which is additive to the force in isolation device.

2.5.2. Viscous Dampers

These devices provide damping but do not have service load resistance. They have no elastic stiffness and so add less force to the system than other devices. Most of the viscous dampers are fluid dampers which are similar to the shock absorbers in automobiles.

Viscous dampers are velocity dependent and provide a maximum force at zero displacement. Viscous damper devices have low resistance to loads which are applied slowly. In contrast, resistance capacity of increases as the speed at which the deformation is applied increases. General formula about viscous dampers is given as follows:

$$F_D = C|u|^{\alpha} \operatorname{sgn}(u) \tag{2.1}$$

F_D represents force of a damper, damper coefficient is denoted by C, u is the applied velocity and last α defines damper exponent which usually range s between 0.3 and 1.0. Some of the viscous dampers have a relief valve and beyond the limit value it provides constant damping force.

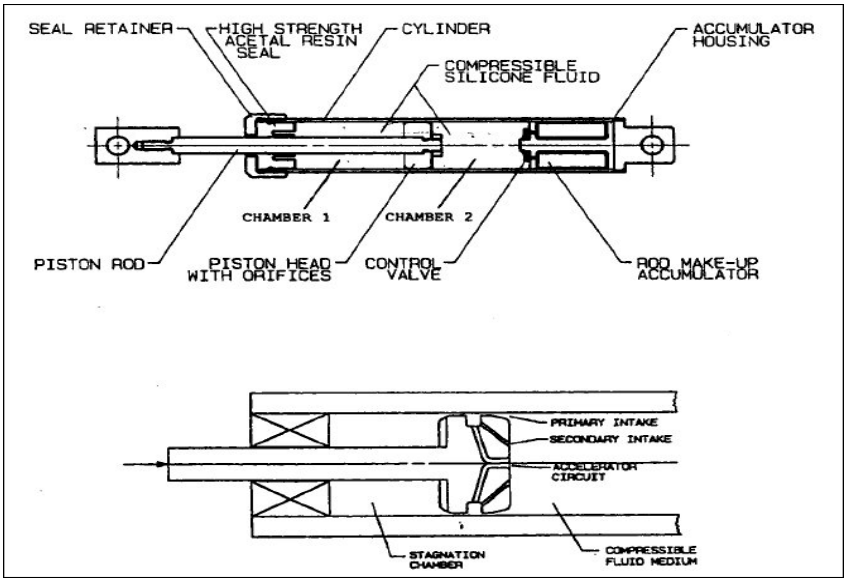

Figure 2.15. Section of a viscous damper

2.5.3. Friction Dampers

For in-structure damping the displacements are due to story drifts applied to the friction damper, which requires that the damper extends from floor to floor, connected by a structural element such as a brace or wall panel. This element has a finite stiffness and will act in a series with friction damper. This has the effect of providing a finite initial loading stiffness to the overall friction damping component.

Because all practical applications will have non-rigid elements to mount the damper, the actual hysteresis will resemble that of the yielding damper hysteresis rather than the rectangular hysteresis.

3. DESIGN CONSIDERATIONS OF ISOLATORS

3.1. General Definitions

In practice seismic isolation system should provide the requirements that have listed below.

1. Isolators need to have sufficient rigidity under service loads which is no different from a fixed supported system.
2. Sufficient energy dissipation capacity have to limit the displacements to a desired level.
3. Period shift of the isolated structure has to be achived by horizontal flexibility (except for very soft soils)

Most commonly used elastomeric isolators satisfy all the requirements. Laminated rubber bearings are usually used with additional damper devices such as viscous fluid dampers, steel dampers, lead dampers and friction damper with coned discs. Type of supplemental devices have shown in figure below

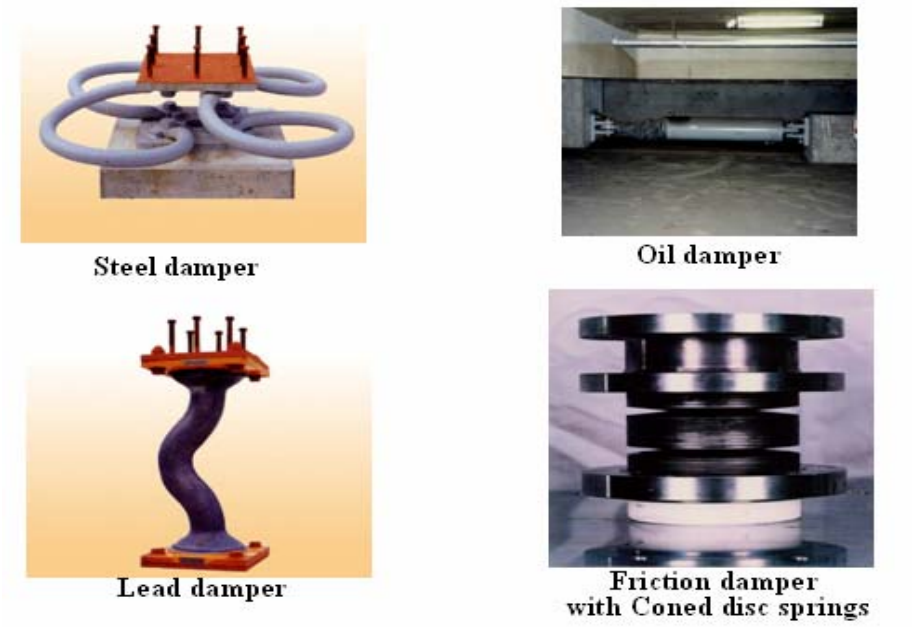

Figure 3.1. Different types of damper devices

Combination of elastomeric bearings with dampers have been widely used all over the world.If elastomeric bearing will be used as a combined system with dampers usually laminated natural rubber is preffered.

On the other hand, instead of using damper and isolation devices, HDR bearings and LRB bearings can be used or passive hybrid isolation systems which has two different type of isolation devices. Detailed description of HDR and LRB bearing were explained above.

3.2. Design Criteria for Isolators

Isolators should support the maximum gravity loads under gravity service loads during its life have to provide an adequate lengthening of period with low horizontal stiffness. In accordance with these design aims, the following design steps should be undertaken (Mayes and Naeim, 2001)

1) Determine the minimum plan size required and location of isolators under the maximum gravity loads.
2) Compute the dimensions of the isolators that will result in the desired period shift for reducing the earthquake forces
3) Determine the damping ratio of the isolator such that the displacement of the structure can be controlled within the design limit under wind loads
4) Check the performance of the isolators under gravity, wind, thermal, earthquake, and other possible load conditions

Design procedure for HDR,LRB and FPS which has a most common use are explained briefly under following titles

3.2.1. Design of High Damping Rubber Bearing

HDR bearing consist of rubber layers between the steeşl plates which has a special compound. Material that have used in the manufacturing process is highly nonlinear in terms of shear strains. HDR exhibits effective damping in the range of 0.1-0.2 as mentioned before. In practice, HDR is quite stable under several design earthquakes. Thus similar to what has been undertaken in most previous studies, for the preliminary design stage the HDR is assumed to be linear elastic and isotropic . The design procedure for HDR bearing can follow steps that have listed blow

1) Specifying the soil condition where the isolated structure will construct
2) Target design period, design shear strain $\gamma_{\max}$ and effective damping ratio ξ_{eff} for the bearing have to be selected
3) Maximum horizontal stiffness K_{eff} and maximum horizontal(design) displacement D of the bearing can be determined from code provisions or from static and dynamic analysis.

4) Manufacturer's test report is evaluated to select the Young Modulus E and Shear modulus G
5) Total Rubber thickness $\sum t$ is calculated from the design displacement D and design shear strain $\gamma_{\max}$

$$\sum t = \frac{D}{\gamma_{\max}} \tag{3.1}$$

6) Calculate the bonded rubber area A and the thickness of each individual layers

a. Select the shape factor S where no rocking exists. If first shape factor is greater than 10 ratio of vertical stiffness to horizontal stiffness at least have to be 400

$$\frac{K_v}{K_h} = \frac{\frac{E_c.A}{t_r}}{\frac{G.A}{t_r}} = \frac{E_c}{G} = \frac{E(1+2kS^2)}{G} \geq 400 \tag{3.2}$$

G, E and k values depend on the hardness of rubber. If values are not known the Table 3.1which is prepared by (Bridgestone,1990) can be used for the design.

b. If the vertical load P_{DL+LL} is calculated effective cross-sectional area can be calculated with the help of allowable stress σ_c. Formula is given below

$$\sigma_c = \frac{P_{DL+LL}}{Ao} \leq 80 kgf/cm^2 = 7.84 MPa \tag{3.3}$$

Table 3.1. Design values for rubber (Bridgestone, 1990)

Rubber Hardness IRHD+/-	Young's Modulus E (N/cm^2)	Shear Modulus G (N/cm^2)	Modified Factor k
30	92	30	0.93
35	118	37	0.89
40	150	45	0.85
45	180	54	0.8
50	220	64	0.73
55	325	81	0.64
60	445	106	0.57
65	585	137	0.54
70	735	173	0.53
75	940	222	0.52

c. Determination of effective cross-sectional area A_1 of isolator from the shear strain occurred under the vertical load P_{DL+LL}

$$\gamma_c\big|_{DL+LL} = \frac{6S.P_{DL+LL}}{E_c A_1} \le \frac{\varepsilon_b}{3} \tag{3.4}$$

where ε_b is the elongation of rubber at rupture, the limit of $\frac{\varepsilon_b}{3}$. This value is selected from ASSHTO guide specification

d.Minimum cross-sectional area A_{sf} is obtained for shear failure of isolator. Then A_{sf} is used to determine the dimensions of the bearing. Cross sectional area A_2 is computed as the reduced area A_{re} as shown below and figure shows the reduced area of HDR bearing

for rectangular HDR bearings

$$A_{re} = L(B - \Delta_s) \tag{3.5}$$

for a circular HDR bearings

$$A_{re} = \frac{d^2}{4}(\beta - \sin\beta) \tag{3.6}$$

$$\beta = 2\cos^{-1}(\frac{\Delta s}{d}) \tag{3.7}$$

Δs =horizontal displacement of the bearing

L,B= Plan dimensions of the bearing that perpendicular and parallel to the displacement

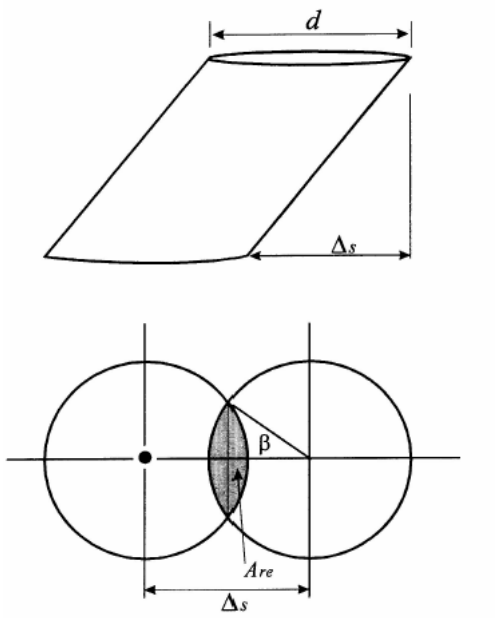

Figure 3.2. Reduced cross-sectional area

e. The design cross-sectional area A of the bearing is the maximum of the three values computed as A_0, A_1, A_2

f. Due to all calculation process that have done above dimensions of the rubber layer is selected regarding A design cross-sectional area

7. Single rubber layer thickness t and number of rubber layers N is determined

a. Rubber layer thickness depends on shape factor. Thus, shape factor have to be determined as shown below

shape factor for rectangular HDR bearings

$$S = \frac{L.B}{2(L+B).t} \tag{3.8}$$

Shape factor for circular bearings

$$S = \frac{\pi d^2 / 4}{\pi . d . t} = \frac{d}{4t} \qquad (3.9)$$

L, B=Plan dimensions of a rectangular bearing

d= diameter of a circular bearing

t= thickness of individual rubber layers

b. Required number of rubber layers will be $t_r = N \times t$

8. Calculation of steel plate thickness, t_s

$$t_s \geq \frac{2(t_i + t_{i+1}).(P_{DL+LL})}{A_{re}.F_S} \geq 2mm \qquad (3.10)$$

where

t_i, t_{i+1} : rubber layer thickness in top and bottom of the steel plate

F_s : $0.6F_y$

F_y : yield strength of the steel plates *(=274.4 MN/m^2)*

A_{re}: reduced cross-section area of the bearing under horizontal displacement

9. All above defined parameters should be checked against the shear strain and stability conditions. In case where these conditions are not satisfied an improved design should be investigated by repeating steps 2 to 8.

3.2.2. Shear Strain and Stability Conditions for HRD Bearings

1.The rubber layers selected should satisfy the shear strain requirement under the vertical load P_{DL+LL}

$$\gamma_{c,DL+LL} = 6S.\varepsilon_c = 6S\frac{P_{DL+LL}}{E_c A} \le \frac{\varepsilon_b}{3} \tag{3.11}$$

where the compression strain ε_c is defined as

$$\varepsilon_c = \frac{\Delta_c}{t_r} = \frac{P_{DL+LL}}{E_c A} \tag{3.12}$$

Δ_c : Compression displacement of the bearing

ε_b : Elongation of rubber at break

2. Stability condition: the average compressive stress σ_c of the bearing should be less than a tolerance to prevent the bearing from becoming unstable;

$$\sigma_c = \frac{P}{A} < \sigma_{cr} = \frac{GSL}{2.5t_r} \tag{3.13}$$

where L is the plan dimension of the rectangular bearing or the diameter d of the circular bearing.

3. Shear strain condition for the earthquake load

$$\gamma_{sc} + \gamma_{eq} + \gamma_{sr} \leq 0.75\varepsilon_b \tag{3.14}$$

with

$$\gamma_{sc} = 6S\frac{P_{DL+LL+EQ}}{E_c A_{re}}, \tag{3.15}$$

$$\gamma_{eq} = \frac{D}{t_r}, \tag{3.16}$$

$$\gamma_{sr} = \frac{B^2\theta}{2tt_r} \tag{3.17}$$

$$\theta = \frac{12De}{b^2 + d^2} \tag{3.18}$$

where,

γ_{sc} : shear strain under compression

$P_{DL+LL+EQ}$: combination of dead load, live load and earthquake load

γ_{eq} : shear strain under earthquake

γ_{sr} : shear strain under rotation

θ : rotation angle of the bearing induced by earthquake

e: actual eccentricity + 5% of accidental eccentricity

b, d : dimensions of the structure with rectangular plan

3.2.3. Design of Lead Rubber Bearings

Lead rubber bearings (LRB) are usually made of alternating layers of steel plates and natural rubber with a central hole into which the lead core is press-fitted. The lead core deforms almost in pure shear, when subjected to the lateral shear force. It has also a hysteretic deformation behavior over a number of cycles. Due to the recrystallization property of the lead core at normal temperature, no fatigue failure occurs under cyclic loadings. The design procedure for LRB is given as below.

3.2.4. Design Procedure for LRB

The main difference between HDR and LRB for the design procedure is that a special attention should be given to the design of the lead core.

1. Specifying the soil condition where the isolated structure will construct
2. Target design period, design shear strain $\gamma_{\max}$ and effective damping ratio ξ_{eff} for the bearing have to be selected
3. Maximum horizontal stiffness K_{eff} and maximum horizontal(design) displacement D of the bearing can be determined from code provisions or from static and dynamic analysis.
4. Manufacturer's test report is evaluated to select the Young Modulus E and Shear modulus G
5. Total Rubber thickness $\sum t$ is calculated from the design displacement D and design

shear strain $\gamma_{\max}$. Total rubber thickness can be found like a HDR bearing that was explained in equation 3.1

6. Lead core design: cross-sectional area, A_p, and diameter, d_p are determined based on the Q_d and f_{py}

$$A_p = \frac{Q_d}{f_{py}} \tag{3.19}$$

$$Qd = \frac{W_D}{4D} \tag{3.20}$$

$$W_D = 2\pi K_{eff} D^2 \xi_{eff} \tag{3.21}$$

f_{py} : yield strength of the lead plug in shear

Q_d : yield force of the lead plug

W_D: energy dissipated per cycle

D: design displacement of the bearing

7. Determine the thickness t and the area A and of individual rubber layers

a. shape factor S, under no rocking condition

$$\frac{K_v}{K_h} = \frac{\frac{E_c A}{t_r}}{\frac{GA}{t_r}} = \frac{E_c}{G} = \frac{E\left(1+2kS^2\right)}{G} \geq 400 \tag{3.22}$$

b. Effective cross-sectional area A_o of the bearing based on the allowable axial stress σ_c under vertical load P_{DL+LL}

$$\sigma_c = \frac{P_{DL+LL}}{A_o} \leq 80 kgf / cm^2$$

(3.23)

c. Effective cross-sectional area A_1 of the bearing from the shear strain due to the vertical load P_{DL+LL}

$$\gamma_c \Big|_{DL+LL} = 6S \frac{P_{DL+LL}}{E_c A_1} \leq \frac{\varepsilon_b}{3} \tag{3.24}$$

d. Elastic modulus K_r of the bearing

$$K_d = K_r \left(1 + 12 \frac{A_p}{A_o} \right) \tag{3.25}$$

e. where K_d is the post-yield stiffness of the LRB in horizontal direction.

$$K_d = K_{eff} - \frac{Q_d}{D} \tag{3.26}$$

f. Minimum cross-sectional area A_{sf} for shear failure of the bearing

$$A_{sf} = \frac{K_r t_r}{G} \tag{3.27}$$

g. use A_{sf} to determine the dimensions of the bearing. Then compute the effective cross-

sectional area A_2, the reduced area A_{re} is given below

for rectangular bearing,

$$A_{re} = L(B - \Delta_s) \tag{3.28}$$

for a circular bearing,

$$A_{re} = \frac{d^2}{4}(\beta - \sin\beta) \tag{3.29}$$

The design cross-sectional area A of the bearing is the maximum among the three values computed: A_o, A_1, and A_2

h. select proper dimensions for the rubber layer based on the design area A.

8. Thickness of individual rubber layer, t and the number of rubber layers, N:

a. The thickness of individual layer, t is determined from the shape factor S and dimensions of the rubber layer.

for rectangular bearing

$$S = \frac{L.B}{2(L + B).t} \tag{3.30}$$

for a circular bearing

$$S = \frac{d}{4t} \tag{3.31}$$

b. Required number of rubber layers, N is determined by $t_r = N \, x \, t$.

9. Steel plate thickness, t_s;

$$t_s \geq \frac{2(t_i + t_{i+1}).P_{DL+LL}}{A_{re}.F_s} \geq 2mm \tag{3.32}$$

10. Dimensions determined for the bearing should be checked against the shear strain and stability requirements. If these conditions are not satisfied, then repeat steps 2 to 9 for an improved design.

3.2.5. Shear strain and Stability Checks for LRB

1. When designing the rubber layers, shear stain condition for normal load case should be satisfied.

$$\gamma_{c,DL+LL} = 6S\varepsilon_c = 6S\frac{P_{DD+LL}}{E_c A} \leq \frac{\varepsilon_b}{3} \tag{3.33}$$

2. Stability condition: the average compression stress, σ_c of the bearing should fulfill the following condition

$$\sigma_c = \frac{P}{A} < \sigma_{cr} = \frac{G.S.L}{2.5t_r} \tag{3.34}$$

where L is the least dimension of a dimension of a rectangular bearing or the diameter d of a circular bearing.

3. Lead core provides initial stiffness and energy dissipation capability to the bearing. Lead core dimensions should satisfy the following condition.

$$1.25 \le \frac{H_p}{d_p} \le 5.0 \tag{3.35}$$

where H_p is the effective height of the lead core and d_p is the diameter of the lead core.

Load combination including the earthquake:

$$\gamma_{sc} + \gamma_{eq} + \gamma_{sr} \le 0.75\varepsilon_b \tag{3.36}$$

3.2.6. Design of Friction Pendulum Systems (FPS)

Rather than a flat sliding surface, the FPS allows the supported structure to return to

its original position through use of a spherical concave sliding surface. Isolated structure vibrate in a way similar to the pendulum by frictional pendulum. In the design of the frictional pendulum bearing, it is very important to make the natural period, T_D, long enough, therefore the forces transmitted from the ground to the superstructure can be reduced. The choice of the radius of curvature, R_{FPS} for the spherical sliding surface is related to the period T_D of the friction pendulum system isolated structure.

$$T_D = 2\pi\sqrt{\frac{R_{FPS}}{g}} \tag{3.37}$$

where g is the acceleration of gravity.

The period of FPS is independent of the mass of the supported structure, which is an advantage of the FPS in controlling the response of the isolated structure. Due to concave sliding surface of FPS, it has a recentering mechanism property which allows isolated structure to return its original position after earthquake. The effective stiffness of FPS is as follow;

$$K_{eff} = \frac{W}{R_{FPS}} + \frac{\mu W}{D} \tag{3.38}$$

where W is the vertical load carried by each FPS at the column base, μ is the frictional coefficient of the sliding surface and D is the design displacement. The effective damping ratio ξ_{eff} provided by the isolation system is a function of the design displacement.

$$\xi_{eff} \frac{2}{\pi} \frac{\mu}{\mu + D/R_{FPS}} \tag{3.39}$$

The vertical displacement δ_V of the structure caused by the curved surface of the isolator can be calculated as:

$$\delta_V \cong \frac{D^2}{2R_{FPS}} \tag{3.40}$$

where D is the horizontal displacement of the structure.

It should be ensured that the isolated structure will return its original position after earthquake. To satisfy this condition, horizontal displacement of the structure, D should meet the requirement that the restoring force F ($=WD/R_{FPS}$) is not less than the friction force μW .

$$\frac{D}{R_{FPS}} \geq \mu \tag{3.41}$$

4. LINEAR THEORY

Isolation system is basicly modeled as two-degree-of -freedom system. For preliminary design isolation system is assumed to behave like linear. The linear theory of base isolation is explained in detail by Kelly below . Generally theory is based on a two mass structural model. These two masses can be defined as structural mass and the mass of the base slab above the isolators. Structural stiffness and damping is denoted by k_s and c_s, and the stiffness and damping of the isolation is denoted by k_b and c_b.Absolute displacements of the structural mass and base slab masses are represented by u_s and u_b. But for the linear analysis instead of using absolute displacements relative displacements are prefered to use.

$$u_b = u_b - u_g \tag{4.1}$$

$$u_s = u_s - u_b \tag{4.2}$$

It is convinient to use relative displacements, because two of the important results are the displacement of isolation system which is denoted by u_b and the interstory drift represented by u_s. In terms of these terms, the basic equation of motion of two-degree-of-freedom model are

$$(m+m_b)\ddot{u}_b + m\ddot{u}_s + c_b u_b + k_b u_b = -(m+m_b)u_g \tag{4.3}$$

$$m\ddot{u}_b + m\ddot{u}_s + c_s\dot{u}_s + k_s u_b = -m\ddot{u}_g \tag{4.4}$$

which can be written in matrix notations as explained in 4.5

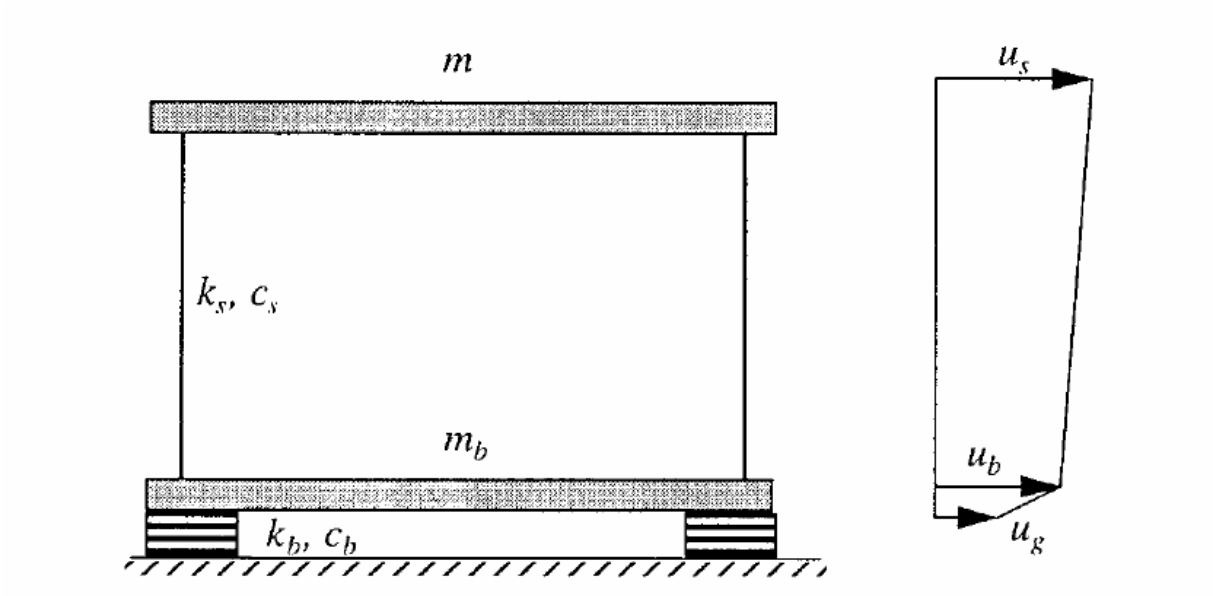

Figure 4.1. Two-Degree-of freedom system for isolated structures

$$\begin{bmatrix} \mathrm{M} & \mathrm{m} \\ \mathrm{m} & \mathrm{m} \end{bmatrix} \begin{Bmatrix} \ddot{u}_b \\ \ddot{u}_s \end{Bmatrix} + \begin{bmatrix} \mathrm{c_b} & 0 \\ 0 & \mathrm{cs} \end{bmatrix} \begin{Bmatrix} \dot{u}_b \\ \dot{u}_s \end{Bmatrix} + \begin{bmatrix} \mathrm{kb} & 0 \\ 0 & \mathrm{ks} \end{bmatrix} \begin{Bmatrix} u_b \\ u_s \end{Bmatrix} = \begin{bmatrix} \mathrm{M} & \mathrm{m} \\ \mathrm{m} & \mathrm{m} \end{bmatrix} \begin{Bmatrix} 1 \\ 0 \end{Bmatrix} \ddot{u}_g \tag{4.5}$$

where $M=m+m_b$ that is in matrix notation

$$M\ddot{v} + C\dot{v} + Kv = -Mr\ddot{u}_g \tag{4.6}$$

Mass ratio, γ is defined as

$$\gamma = \frac{m}{m+m_b} = \frac{m}{M} \tag{4.7}$$

and nominal frequencies ω_b and ω_s given by

$$\omega_b^{\,2} = \frac{k_b}{m + m_b} \tag{4.8}$$

$$\omega_s^{\,2} = \frac{k_s}{m} \tag{4.9}$$

and assume that $\omega_b^{\,2} / \omega_s^{\,2} = \in$ and $\in = 0(10^{-2})$

the damping factors β_b and β_s are given by

$$2\omega_b \beta_b = \frac{c_b}{m + m_b} \tag{4.10}$$

$$2\omega_s \beta_s = \frac{c_s}{m} \tag{4.11}$$

in terms of these quantities, the basis equation of motion become

$$\gamma u_s + u_b + 2\omega_b \beta_b u_b + \omega_b^{\,2} u_b = -\ddot{u}_g \tag{4.12}$$

$$\ddot{u}_s + \ddot{u}_b + 2\omega_s \beta_s \dot{u}_s + \omega_s{}^2 u_s = -\ddot{u}_g \tag{4.13}$$

The classical modes of the combined system will be denoted by ϕ^1 and ϕ^2 there

$\phi^{iT} = (\phi_b{}^i, \phi_s{}^i)$ i=1,2

with frequencies ω_1 and ω_2 . The characteristis equation for the frequencies is

$$(1-\gamma)\omega^4 - (\omega_s{}^2 + \omega_b{}^2)\omega^2 + \omega_b{}^2\omega_s{}^2 = 0 \tag{4.14}$$

the solutions of which are

$$\omega_1{}^2 = \frac{1}{2(1-\gamma)}\left\{\omega_b{}^2 + \omega_s{}^2 - \left[(\omega_b{}^2 - \omega_s{}^2)^2 + 4\gamma\omega_b{}^2\omega_s{}^2\right]^{1/2}\right\} \tag{4.15}$$

$$\omega_2{}^2 = \frac{1}{2(1-\gamma)}\left\{\omega_b{}^2 + \omega_s{}^2 + \left[(\omega_b{}^2 - \omega_s{}^2)^2 + 4\gamma\omega_b{}^2\omega_s{}^2\right]^{1/2}\right\} \tag{4.16}$$

And to first order in ε are given by

$$\omega_1 = \omega_b{}^2(1-\gamma \in) \tag{4.17}$$

$$\omega_2 = \frac{\omega_s{}^2}{1-\gamma}(1+\gamma \in) \tag{4.18}$$

and the mode shapes with ($(\phi_b^{\,i} = 1),\ \text{i=1, 2,}$ are

$$\phi^{1T} = (1, \in) \tag{4.19}$$

$$\phi^{2T} = \left\{1, -\frac{1}{\gamma}\left[1-(1-\gamma)\in\right]\right\} \tag{4.20}$$

To express the original displacements in modal coordinates, we write

$$u_b = q_1\phi_b^{\,1} + q_2\phi_b^{\,2} \tag{4.21}$$

$$us = q_1\phi_S^{\,1} + q_2\phi_s^{\,2} \tag{4.22}$$

where q1,q2 are time-dependent modal coefficients.

We note that modal quantities Mi,Li are given by

$$Mi = \phi^{iT} M \phi^i \tag{4.23}$$

$$MiLi = \phi^{iT} Mr \tag{4.24}$$

To first order in $\in$, those are

$$M_1 = M(1+2\gamma \in) \tag{4.25}$$

$$M_2 = M\,\frac{(1-\gamma)\left[1-2(1-\gamma)\in\right]}{\gamma} \tag{4.26}$$

$$L_1 = 1-\gamma \in \tag{4.27}$$

$$L_2 = \gamma \in \tag{4.28}$$

When (u_b, u_s) in Eqs.(2.1) and (2.2) are expressed in terms of ϕ^1 and ϕ^2, we have two equations in the modal coefficients (q1,q2) of the form

$$\ddot{q}_1 + 2\omega_1\beta_1\dot{q}_1 + \lambda_1\dot{q}_2 + \omega_1 q_1 = -L_1\ddot{u}_g \tag{4.29}$$

$$\ddot{q}_2 + \lambda_2\dot{q}_1 + 2\omega_2\beta_2 + \omega_2{}^2 q_2 = -L_2\ddot{u}_g \tag{4.30}$$

The terms $2\omega_1\beta_1$ and $2\omega_2\beta_2$ are calculated from

$$Mi2\omega_i\beta_i = \phi^{iT}\begin{bmatrix} cb & 0 \\ 0 & \text{cs} \end{bmatrix}\phi^i$$

(4.31)

From which we obtain

$$2\omega_1\beta_1 = 2\omega_b\beta_b(1-2\gamma\in) \tag{4.32}$$

$$2\omega_2\beta_2 = \frac{1}{1-\gamma}(2\omega_s\beta_s + 2\gamma\omega_b\beta_b) \tag{4.33}$$

leading to

$$\beta_1 = \beta_b(1-\frac{3}{2}\gamma\in) \tag{4.34}$$

$$\beta_2 = \frac{\beta_s + \gamma\beta_2\in^{1/2}}{(1-\gamma)^{1/2}}(1-\frac{\gamma\in}{2}) \tag{4.35}$$

The coupling coefficients λ_1 and λ_2 are computed from here

$$\lambda_1 M_1 = \phi^{iT}\begin{bmatrix} \text{cb} & 0 \\ 0 & \text{cs} \end{bmatrix}\phi^2 \tag{4.36}$$

$$\lambda_2 M_2 = \phi^{2T} \begin{bmatrix} c_b & 0 \\ 0 & c_s \end{bmatrix} \phi^1 = \lambda_1 M_1 \tag{4.37}$$

Thus,

$$\lambda_1 M_1 = (1, \in) \begin{bmatrix} c_b & 0 \\ 0 & c_s \end{bmatrix} \begin{pmatrix} 1 \\ -a \end{pmatrix} = c_b - \in a c_s \tag{4.38}$$

$$a = \frac{1}{\gamma}\left[1 - (1-\gamma) \in\right] \tag{4.39}$$

Using (M1,M2) , we have

$$\lambda_1 = \frac{2\omega_b \beta_b M - \in \left\{(1/\gamma)\left[1-(1-\gamma) \in\right]\right\} 2\omega_s \beta_s m}{M(1+2\gamma \in)} \tag{4.40}$$

$$\lambda_1 = 2\omega_b \beta_b (1 - 2\gamma \in) - \in 2\omega_s \beta_s (1 - 2\gamma \in) \tag{4.41}$$

$$\lambda_1 = 2\omega_b \left[\beta_b (1 - 2\gamma \in) - \in^{1/2} \beta_s \right] \tag{4.42}$$

And

$$\lambda_2 = \frac{2\omega_b \beta_b M - \in \left\{(1/\gamma)\left[1-(1-\gamma) \in\right]\right\} 2\omega_s \beta_s m}{\left[M(1-\gamma)/\gamma\right]\left[1 - 2(1-\gamma) \in\right]} \tag{4.43}$$

$$\lambda_2 = (2\omega_b\beta_b - \in 2\omega_s\beta_s)\left[1 + 2(1-\gamma)\in\right]\frac{\gamma}{1-\gamma} \tag{4.44}$$

$$\lambda_2 = 2\omega_b\left\{\beta_b\left[1 + 2(1-\gamma)\in\right] - \in^{1/2}\ \beta_s\right\}\frac{\gamma}{1-\gamma} \tag{4.45}$$

In structural application damping is mostly assumed very small.Thus the effect of the off-diagonal components are negligible and that the required solution can be obtained from the uncoupled modal equations of motions, namely.

$$\ddot{q}_1 + 2\omega_1\beta_1\dot{q}_1 + \omega_1^2 q_1 = -L_1\ddot{u}_g \tag{4.46}$$

$$\ddot{q}_2 + 2\omega_2\beta_2\dot{q}_2 + \omega_2^2 q_2 = -L_2\ddot{u}_g \tag{4.47}$$

If the input excitation is known, modal components $q_1(t)$,$q_2(t)$ can be computed from

$$q_1 = \frac{L_1}{\omega_1}\int_0^t \ddot{u}_g(t-\tau)e^{-\omega_1\beta_1\tau}\sin\omega_1\tau d\tau \tag{4.48}$$

$$q_2 = \frac{L_2}{\omega_2}\int_0^t \ddot{u}_g(t-\tau)e^{-\omega_2\beta_2\tau}\sin\omega_2\tau d\tau \tag{4.49}$$

and due to the estimation of maximum values of q_1 and q_2 is given

$$|q_1|_{\max} = L_1 S_D(\omega_1, \beta_1) \tag{4.50}$$

$$|q_2|_{\max} = L_2 S_D(\omega_2, \beta_2) \tag{4.51}$$

where $S_D(\omega, \beta)$ is the displacement response spectrum for the ground motion $\ddot{u}_g(t)$ at frequency ω and damping factor β.

In order to estimate various response quantities from the peak spectral values, it is necessary to use the SRSS method. The values of the maximum isolation system displacement and structural deformation are given by

$$|u_s|_{\max} = \left[(\phi_2^1 |q_1|_{\max})^2 + \left(\phi_2^2 |q_2| \max \right)^2 \right]^{1/2} \tag{4.52}$$

$$|u_s|_{\max} = \left[(\phi_1^1 |q_1|_{\max})^2 + \left(\phi_1^2 |q_2| \max \right)^2 \right]^{1/2} \tag{4.53}$$

Inserting the results obtained from Equations. 4.25, 4.26, 4.27,4.28 ,4.52) and (4.53), we get

$$|u_b|_{\max} = \left\{ \left[L_1 S_D(\omega_1, \beta_1) \right]^2 + \left[L_2 S_D(\omega_2, \beta_2) \right]^2 \right\}^{1/2}$$

(4.54)

$$|u_b|_{\max} = \left\{ (1-\gamma \in)^2 \left[S_D(\omega_1, \beta_1) \right]^2 + \gamma^2 \in^2 \left[S_D(\omega_2, \beta_2) \right]^2 \right\}^{1/2} \quad (4.55)$$

and

$$|u_s|_{\max} = \left\{ \in^2 (1-\gamma \in)^2 \left[S_D(\omega_1, \beta_1) \right]^2 + \gamma^2 \in^2 \frac{1}{\gamma^2} \left[1-(1-\gamma) \in \right]^2 \left[S_D(\omega_2, \beta_2) \right]^2 \right\}^{1/2} \quad (4.56)$$

$$|u_{s\max}| = \in \left\{ (1-2\gamma \in)^2 \left[S_D(\omega_1, \beta_1) \right]^2 + \left[1-2(1-\gamma) \in \right]^2 \left[S_D(\omega_2, \beta_2) \right]^2 \right\}^{1/2} \quad (4.57)$$

Generally, the term $\in S_D(\omega_1, \beta_2)$ can be neglected with earthquake spectra where the displacement at high frequencies(i.e, ω_2) is relatively smaller than at lower frequencies. This gives,

$$|u_b|_{\max} = (1-\gamma \in) S_D(\omega_1 \beta_1) \, (4.34) \quad (4.58)$$

If any terms greater than $\in^2$, then the estimate for the structural deformation or interstory drift, u_s, is given as

$$|u_s|_{\max} = \in \left[S_D(\omega_1 \beta_1)^2, S_D(\omega_2, \beta_2) \right]^{1/2} \tag{4.59}$$

Similar to the other quantities, the base shear coefficients Cs given by

$$C_s = \left| \frac{k_s u_s}{m} \right|_{\max} = \omega_s{}^2 \left| u_s \right|_{\max} \tag{4.60}$$

$$C_s = \left[\omega_b{}^4 S_D(\omega_1, \beta_1)^2 + \in^2 \omega_s{}^4 S_D(\omega_2, \beta_2)^2 \right]^{1/2} \tag{4.61}$$

$$C_s = \left[S_A(\omega_1, \beta_1)^2 + \in^2 S_A(\omega_2, \beta_2)^2 \right]^{1/2} \tag{4.62}$$

Becomes

$$Cs = \omega_s{}^2 \in \left[S_D(\omega_1, \beta_1)^2 + S_D(\omega_2, \beta_2)^2 \right]^{1/2} \tag{4.63}$$

Thus, if we retain only the first terms,we had found

$$|u_s|_{\max} = \frac{\in S_V}{\omega_b} = \in S_D(\omega_b, \beta_b) \tag{4.64}$$

$$|u_b|_{\max} = \frac{S_V}{\omega_b} = S_D(\omega_b, \beta_b) \tag{4.65}$$

and the design base shear coefficient Cs defined by

$$c_s = \frac{k_s u_s}{m} = \omega_s{}^2 u_s \tag{4.66}$$

Becomes

$$Cs = \omega_b S_V \left[1 + \in^{2} \frac{\omega_2{}^2}{\omega_1{}^2} \right] = S_A(\omega_b, \beta_b) \left(1 + \frac{\in}{1-\gamma} \right)^{1/2} \tag{4.67}$$

Linear theory can be extended for multi degree of freedom systems and detailed information is explained by Kelly in his book.

5. CODE PROVISIONS

5.1. SEISMIC HAZARD LEVEL

The seismic criteari that is adopted by current model codes involve a two level approach to seismic hazard, which are follows

Design Basis Earthquake (DBE) the level of ground shaking that has a probability of being exceeded in 50 years(475- year return period earthquake)

Maximum Capable Earthquake(MCE) The maximum level of ground shaking that may ever be expected at the building site. This may be taken as that level of ground motion that has a 10% probability of being exceeded in 100 years (1000 –year Return period earthquake)

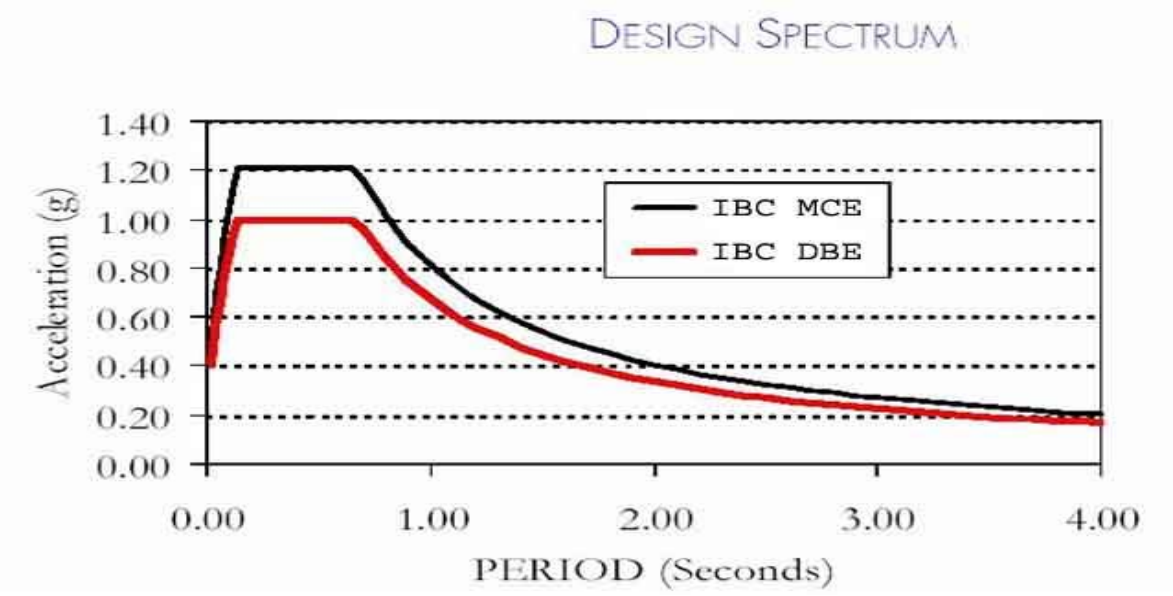

Figure 5.1. Design spectra in IBC 2000

5.2. Design Methods

Earlier versions of the UBC code emphasized a simple, statically equivalent method of design that took advantage of the fact for an isolated structure the displacements are concentrated at the isolation level and therefore, the superstructure moves almost as a rigid body(Kelly,1999) Design procedure was taken into consideration only the first mode of vibration and the design displacement is used to calculate the design forces for the superstructure. As a result design process was a very simple procedure. Then code has evolved and dynamic analysis has taken place in the specifications.

Furthermore, to perform static analysis is necessary for all seismic isolation designs. Minimum level for design displacements and forces is established by static analysis. For design review, static analysis helpful for the isolation system and the superstructure.in preliminary design when the dynamic analysis is required(Naeim, 1999).

Dynamic analysis may be carried out in the form of a response spectrum analysis or time history analysis. Site specific ground motions are required under the circumstances that explained below.

1. When the isolated structure is located on sa soft soil, soil type S3, S4
2. The isolated structure is within 10km of a known active fault
3. When the natural period of an isolated structure is more than 3 sec.

In IBC 2000, requirements for response spectrum analysis is stated below

1. The structure is located at a site S_1, as determined in previous sections, less than or equal to 0.6g
2. The structure is located on soil classified as A,B,C or D; or E (if $S1 \geq 0.6$ for BSE-2)

3. The structure above the isolation interface is not more than 4 stories or 65 feet(19.8m) in height
4. The effective period of the isolated structure at the design displacement, T_M, as determined in previous sections is less than or equal to 3 seconds.
5. The effective period of the isolated structure at the design displacement, T_D as determined in previous section is greater than three times the elastic, the fixed-base period of the structure above the isolation system as determined below
6. The structure above the isolation system is of regular configuration
7. The isolation system meets the following criteria

7.1. The effective stiffness of the isolation system at the design displacement is greater than one third of the effective stiffness at 20 percent of the design displacement.

7.2. The isolation system is capable of producing a restoring force as specified

7.3. The isolation system has a force-deflection properties that are independent of the rate of loading

7.4. The isolation system has a force-deflection properties that are independent of the vertical load and bilateral load

7.5. The isolation system does not limit maximum capable earthquake displacement to less than SM_1/SD_1 times the total design displacement, where SM_1 and SD_1 are determined

All the listed cases above is required for a response spectrum analysis.

Time history analysis may be used in lieu of response spectrum analysis, but if either the isolation system or the superstructure is highly nonlinear, a time history analysis is required(Kelly,1999)

5.3. Static Analysis

The static analysis formulas provide displacements and forces and are based on constant-velocity spectra over the period range 1.0-3.0 seconds. The constant-velocity

spectrum is derieved from the Applied Technology Council provision ATC-3-06 and for Z=0.4, a soil factor S=1, and 5% damping is 0.6m/s, leading to a displacement spectrum S_D given by

$$S_D = \frac{S_V}{\omega} = \frac{T}{2\pi}\frac{Z}{4}(0.6) = 0.25ZT \text{ m} \tag{5.1}$$

The spectrum that defined above is then modified for other seismic zones by applying soil factor and a damping factor which leads to the required design displacement D.There are three levels of displacement and they are briefly explained below.

- D, the design displacement, being the displacement at the center of rigidity of the isolation system at the Design Based Earthquake(DBE)
- $D_{T,}$ the total design displacement, being the displacement of a bearing at a corner of the building and including the component of the torsional displacement in the direction of D; and
- D_{TM}, the total maximum displacement, being the total design displacement evaluated at the Maximum Capable Earthquake (MCE)

The design displacement D is a reference point during all the design process, and it has to be calculated for all type of analysis. It assumes that the superstructure deformations are neglible. A large number of new terms added to IBC 2000 when it is compared with UBC 94. For instance the number of soil profiles extended and there are 4 seismic coefficients to be calculated in Zone 4. In addition to these parameters, Na and Nv have to be calculated which depend on Seismic Source type and seismic source distance.

Two basic displacement have to be calculated due to IBC 2000 are D_D and D_M at the center of rigidity of the isolation system. They are calculated as given below

$$D_D = \frac{gC_{VD}T_D}{B_D(4\pi^2)} \tag{5.2}$$

$$D_M = \frac{gC_{VM}T_M}{B_M(4\pi^2)} \tag{5.3}$$

where g is the gravitational acceleration, C_{VD} and C_{VM} are seismic coefficients, T_D and T_M are isolated periods, and B_D and B_M are damping coefficients which corresponds to DBE and MCE. The terms C_{VD} and C_{VM} are functions of the seismic zone factor Z, the site soil profile type and one of the near-source factors, $N_{v.}$ Definitions of the terms have to be used in computation are described in the following sections

5.3.1. Seismic Zone Factor Z

Four different seismic zone is presented in IBC 2000 and seismic zone factors vary from 0.075 for zone 1 to 0.40 for zone 4

5.3.2. Site Soil Profile Type

Site soil profiles are classified as S_A to S_E due to their average shear wave velocity in the top 30.5m of the soil layers. Shear wave velocity of soil profiles defined in IBC 2000 varies from 180 m/s for the soft soil(S_E) to over 1500 m/s for the rock hard rock profile (S_A). Another class of soil which is S_F requires site-specific evaluation and it does not take into consideration the shear wave velocity and very poor soil conditions exists in such sites. Moreover, S_F soil profiles are prone to liquefaction.

5.3.3. Seismic Source Types

Seismic faults are grouped into three categories based on the seriousness of the hazard they represent. Annual seismic slip rate, SR, of 5mm or more classified as type A sources.Faults capable of producing moderate-magnitude earthquakes(M<6.5) with a relatively low rate of seismic activity[$SR \leq 2mm$] are classified as type C sources. All the other sources are assumed as type B sources.

5.3.4. Near Source Factors :Na and Nv

Two factors are used to model the ground motion amplification due to near source effects. The first, Na, is intended for the short-period range corresponding to a constant – accleretaion segment of response spectra.Nv is corresponds to the midperiod range or constant –velocity segment of the response spectra , is the primary near source factor used in seismic isolation projects. Near-source factors are functions of closest distance to the seismic source and the seismic source type define the site-source distance as the closest distance between the site and the vertical projection need not include portions of the source at depths10 km or greater; therefore, a site sitting directly on the top of a fault deeper than 10km is not considered a near-source site (Kelly,1999).

5.3.5. MCE Response Coefficient M_M

MCE Response Coefficient M_M. ,The MCE response coefficient M_M is intended to

estimate the MCE response based on the DBE shaking characteristics.As such as, M_M is defined as a function of ZN_u and changes from 2.67 for ZN_u=0.075 to 1.20 for $ZN_u \geq 0.5$. The idea of assigning higher values of M_M for smaller DBE events stem from the fact that in regions will low seismicity the gap between the DBE and MCE events is generally much larger than those in zones which are in High Seismic zones and take values of M_M in IBC

Table 5.1. Response Coefficient due to IBC 2000

Design Bases Earthquake	MCE Response Coefficient
0.075	2.67
0.15	2
0.2	1.75
0.3	1.5
0.4	1.25
≥ 0.5	1.2

5.3.6. Spectral Seismic Coefficients: CVD,CVM and CAD, CAM

The specified coefficients are aimed to be used in design for to find minimum spectral ordinates. CVD and CAD represents the terms of constant velocity and constant acceleration regions for DBE spectrum, respectively; CVM and CAM have the same function for the MCE spectrum. CVD and CAD are the same as CV and CA defined for conventional structures by IBC 2000. The values of CVM and CAM, however are given in the seismic isolation Appendix of UBC IBC 2000

C_{VD} and C_{AD} are functions of seismic zone factor and site soil profile type. Values for Zone 4 must be multiplied by the appropriate near-source factor N_u or N_a

Similar information for $C_{VM,}$ C_{AM} are required and have to be muştiplied by factors explained in IBC 2000.

5.3.7. Damping Coefficients : BD and BM

The effective damping in the system at the DBE and MCE response level are reffered as β_D and β_M are computed as shown below,

$$\beta_D = \frac{1}{2\pi}\left(\frac{\text{total area of hysteresis loop}}{\mathrm{K}_{\mathrm{D,max}} D_D{}^2}\right) \tag{5.4}$$

$$\beta_M = \frac{1}{2\pi}\left(\frac{\text{total area of hysteresis loop}}{\mathrm{K}_{\mathrm{M,max}} D_M{}^2}\right) \tag{5.5}$$

$K_{D,\max}$, $K_{M,\max}$ are effective stiffnes terms for DBE and MCE. Damping reduction factot is defined in terms of β at Table 5.2., with linear interpolation to be used for intermediate values. A very close approximation to the table values is given by the formula shown in 5.6.

$$\frac{1}{B} = 0.25(1 - \ln \beta), \tag{5.6}$$

where β is given as the fraction of critical damping

Table 5.2. Damping Coefficient values in IBC 2000

Effective Damping BD or BM (Percentage of Critical)	BD or BM Factor
$\leq 2\%$	0.8
5%	1
10%	1.2
20%	1.5
30%	1.7
40%	1.9
$\geq 50\%$	2

5.3.8. Effective Vibration Periods: TD and TM

T_D and T_M are corresponds to the DBE and MCE, respectively and computed as shown in the formulas below.

$$T_D = 2\pi\sqrt{\frac{W}{\sum K_{D,\min} g}} \tag{5.7}$$

$$T_M = 2\pi\sqrt{\frac{W}{\sum K_{M,\min} g}} \tag{5.8}$$

Weight of the structure is denoted by W and g represents the gravity.

$$K_{D,eff} = \frac{\left(F_D^{+} - F_D^{-}\right)}{\left(D_D^{+} - D_D^{-}\right)} \tag{5.9}$$

$$K_{M,eff} = \frac{\left(F_D^{+} - F_D^{-}\right)}{\left(D_D^{+} - D_D^{-}\right)} \tag{5.10}$$

K_D, min= minimum value of $K_{D,eff}$ at D_D as determined by testing
K_D, max= maximum value of $K_{D,eff}$ at D_D as determined by testing
K_M, min= minimum value of $K_{D,eff}$ at D_M as determined by testing
K_M, max= minimum value of $K_{D,eff}$ at D_M as determined by testing

In the preliminary design stage the stiffness values determined by tests are not known and the design procedure have to start with an assumed value of K_{eff} which can be obtained from previous tests that have similar components or by using the material characteristics and schematic of proposed isolator. After the desired values for preliminary design stage, prototype of isolators can be ordered for the tests. Thus, K_D, min,K_D, max,K_M, min,K_M, max will be found from the results of the test. F_D^+, F_D^+, F_M^-, F_M^- and D_D^+, D_D^+, D_M^-, D_M^- maximum and minimum force and displacements on the prototype bearings, correponding to D_{BE}, M_{CE} response levels, used to determine the mechanical characteristics of the system (Naeim,1999). Preliminary design stage is refined with the test results and results establish bounds on the various quantities.

5.3.9. Total Design Displacements: DTD and DTM

The total design displacements DTD and DTM that takes into consideration of torsional responses are given in 5.11 and 5.12 respectively.

$$D_{TD} = D_D\left(1 + y\frac{12e}{b^2 + d^2}\right) \tag{5.11}$$

$$D_{TM} = D_M\left(1 + y\frac{12e}{b^2 + d^2}\right) \tag{5.12}.$$

where, e is the eccentricity plus 5% accidental eccentricity and y is the distance to a corner perpendicular to the direction of seismic loading. This formulation assumes that K_{effD} is applied through the center of mass, which is located at a distance e from the center

of stiffness. Assuming a rectangular plan, with dimensions b*d and a uniform distribution of isolators, the torsional stiffness of the isolation system is $K_{eff}(b^2+d^2)/12$ and the rotation θ is thus.

$$\theta = \frac{K_{eff} De}{K_{eff}\left[\left(b^2+d^2\right)/12\right]} = \frac{12De}{b^2+d^2} \tag{5.13}$$

The additional displacement due to rotation is

$$\frac{12De}{b^2+d^2} y \tag{5.14}$$

If the torsional stiffness of the system is computed and the additional displacement due to $K_{eff}D$ through e turns out to be less than the value given by 5.11or 5.12, then this value can be used, but it must be at least 1.1 times D_D and 1.1 times $D_{M,}$ respectively. The total maximum displacement DTM is required for verification of the stability of the isolation system(Kelly,1999).

5.3.10. Design Forces

Elements below the isolation system are calculated by using the formula shown below

$$V_b = K_{D,\max} D_D \tag{5.15}$$

The strength level for design of elements above the isolation system in terms of the minimum lateral seismic shear force is shown by the formula below

$$V_s = \frac{K_{D,\max} D_D}{R_I} \tag{5.16}$$

R_I is the design force reduction factor. In other words it means ductility factor ranging from 1.4 to 2.0

Table 5.3. Reduction factors for fixed-base and isolated structure

Construction	RI	R
Special moment-resisting frame	2	8.5
Shear wall	2	5.5
Ordinary braced frames	1.6	5.6
Eccentric braced frame	2	7

The reduction factors for fixed-base design are very much higher than those for isolated design for a number of reasons. One major element is period shift. As the structure yields, the period lengthens and force demand is reduced. Damping in the structure is increased because of hysteretic action due to yielding in the structural system. Moreover, redundancy and overstrength tend to spread the yielding to other elements. In case of an isolated structure, only overstrength and redundancy are applicable (Kelly, 1999).

5.3.11. Vertical Distribution of Force

In earlier version of IBC2000 (UBC94), the vertical distribution of the inertial forces on the structural system was based on the assumption that the participation of higher modes was negligible and that the accelerations were roughly the same at level of the structure. However, this might not be adequately conservative, and the vertical distribution was changed in subsequent editions of UBC. The lateral force in x direction is represented by Fx is determined from the base shear Vs by

$$F_x = V_s \frac{h_x w_x}{\sum_{i=1}^{N} w_i h_i} \tag{5.17}$$

h_x and h_i are the height of structure above the base slab level and w_x and $w_{i.}$. This formula assume that distribution of force is like a triangular while the basic theory would indicate that the distribution should be close to an uniform distribution. Computation of base shear coefficient Cs is shown below.

$$C_s = \frac{Vs}{W} = \frac{NZS}{B}\frac{1}{T}\frac{1}{R_I} \qquad (5.18)$$

5.3.12. Drift Limits

The maximum interstory limits for isolated structures are more conservative than the limits for fixed-based buildings and should not exceed $0.01/R_I$. This limit is less than half of 2.5% permitted for fixed-supported structure that has a natural periods less than 0.7sec and half of the 2% limit permitted for fixed-based buildings with no longer fundamental periods.

5.3.13. Dynamic Analysis

Site-specific spectra are required if

- $T_M \geq 3.0\,\text{sec}$ or
- The soil type is S_E, S_F or
- The structure is located within 10 km of an active fault.

In addition to those terms stated above, dynamic analysis is necessary if the effective period of the isolated structure T_D is greater than three times the elastic fixed-base period of the structure above the isolation system. If a site-specific spectrum is used code allows the spectrum to be used if it is higher than the codified spectrum but it is not allowed to be used if the site-specific spectrum is less than 80% of the codified spectrum.

5.3.14. Time History Analyis

Pairs of horizontal components from at at least three recorded events are necessary for a time history analysis. The selected records have to represent the site, soil, and source characteristics and have durations consistent with DBE and MCE. Time histories developed for a site within 15 km of a major active near-fault phenomena, although near-field phenomena are not defined.

5.3.15. Scaling

For each ground motion pair, the SRSS of the 5% damped spectra are computed. The motions are scaled so the average of the SRSS spectra does not fall below 1.3 times the target spectrum for the DBE or MCE by more than 10% over 0.5 T_D seconds to 1.25T_M seconds. When dynamic analysis is used, the design values are calculated in the following ways

- If three time histories are used, the design must be based on maximum response quantities.
- If seven time histories are used, the design can be based on average quantities.

When dynamic analysis is done, it is possible to have design displacements and design forces that are less than the calculated design displacements from the equivalent static formulas. Total design displacement D_{TD} for the isolation system can be reduced not less than 90% of that given by static formula, and the total maximum displacement D_{TM}

can be reduced to not less than 80% of the static formula result. The D_{TD} and D_{TM} are computed from D_D and D_M by the use of multipliers and the code permits a further reduction by placing D_D and D_M in the static formulas by D_D' and $D_{M'}$,where

$$D'_D = \frac{D_D}{\sqrt{1+(T/T_D)^2}} \tag{5.19}$$

$$D'_M = \frac{D_M}{\sqrt{1+(T/T_M)^2}} \tag{5.20}$$

T is the elastic fixed-base period of the superstructure computed by the emperical formula of the code. This further reduction allows the flexibility of the superstructure. Static formula assımes that superstructure is rigid.

5.3.16. Design and Testing Requirements for Isolaters

There are a lot of design requirement for the isolator units which are derieved from loads produced on the isolators due to overturning of the building as a result of horizontal accelerations(Kelly, 1999). The control of global overturning of the structure has to be done at the MCE with the full dead load being used in the calculations. When the check of this requirement is done uplift of isolators are allowed. The precise design requirement states that an isolator should be stable when displaced to the total maximum displacement D_{TM} under 1.2 DL+1.0 LL+Emax and 0.8DL –Emin at the MCE, where Emax is the maximum downward and Emin is the minimum vertical load on an isolator caused by overturning of the superstructure.

The requirement explained above also have to be provided for the test the test requirements. The code requires that at least two full sized specimens of each type of isolatorbe tested. The tests required are a specified sequence of horizontal cycles under DL+0.5LL for small horizontal displacements up to the total maximum displacement, with these primarily establishing the mechanical properties of the bearings for use in verifying the design. A sequence of extreme load tests are required where horizontal displacement cycles are combined with maximum and minimum downward loads. The maximum vertical load for these tests is defined as 1.5DL+0.5LL+Emaxand the minimum is 0.8DL-Emin

6. APPLICATIONS OF SEISMIC ISOLATION

Main concept about seismic isolation is to decouple the structure from the ground. The concept of seismic isolation is accidentally found by observations of structures which were accidentally built on soft soil layers and experienced limited damage during severe earthquakes and the structures were slipped on the soft soil layers as a rigid body. In contrast, adjacent structures that have fixed supports were experienced severe damages or most of them collapsed.

The first official reported seismic isolation was applied in the United States, in 1906. That was patented for an earthquake resistant structure attached on rollers. During the same time, ground resistance concept became so popular that another application was suggested in England (Kelly, 1986). Two years later, one more application was tried owing to those previous improvements in Italy. At a destructed region after an earthquake, using these rollers at the bases or isolating every foundation from its building by layering with sand.

Actually, some applications have been tried to adopt seismic isolation but especially for the last twenty-five years, the usage of this concept have been rapidly increasing throughout the world. At that time, elastomeric bearing devices have remarkably developed and one can easily reach these devices across the market. Apart from elastomeric bearings which are the most common seismic isolation devices, many other devices or generally methods have been developed.

In addition to this, public sensitivity is increased to assist to mitigate seismic hazards. Also, recognition to this concept is widely improved. Extreme destruction and losses of lives according to strong earthquakes are not desired any more. At least, decreasing or limiting methods to be considered such as the ones I have been explaining at this chapter.

Another fact is that, nowadays it is very easy to implement the seismic isolation devices to the structures. For instance, as I said the common type of this is the elastomeric bearings. It is too practical and easy to replace this with a damaged one of an existing bridge.

On the other hand, upgrading a structure's seismic resistance by seismic reinforcement increased the application field of seismic isolation, too. Now, here are some examples of diversive seismic isolation implementations at Turkey:

6.1. Seismic Isolation in the United States

In the Unites States, the seismically isolated bridges are much more than the seismically isolated buildings such as four times. The preferred applications for the seismically isolated buildings are critical, or expensive and valuable, contents such as hospitals and high technology centers.

The first use of seismic isolation in the United States appeared on 1979, when circuit breakers were attached to 7% damped elastomeric bearings. Since that time, the number of seismically isolated structures is steadily increasing

6.1.1. The Salt Lake City and County Building, Utah

The Salt Lake City and County Building is the first seismically isolated historic building with a massive five-storey; unreinforced brick, masonry and sandstone. The building is too vulnerable to earthquake damage, possibly coming from a close distance of 3 km by the Wasatch fault.

It was retrofitted with seismic isolation, using a combination of lead-rubber bearings and elastomeric bearings (Bailey and Allen, 1989). There are some difficulties at retrofitting process such as inaccurate detailing of the foundations on the original building plans, by variations at foundation level, and by the requirement that the structure be damaged as little as possible, so that impact tools could not be used for cutting through the stone (Skinner, 1993).

447 elastomeric bearings installed between the structure and its massive foundation system. Lead rubber bearings were located under the exterior walls to get high initial rigidity in order to resist for wind loads. Also, a reinforced retaining wall around the building earned about 30 cm gap to have enough space for the relative displacement at the isolation system level.

Figure 6.1. Salt Lake City Hall

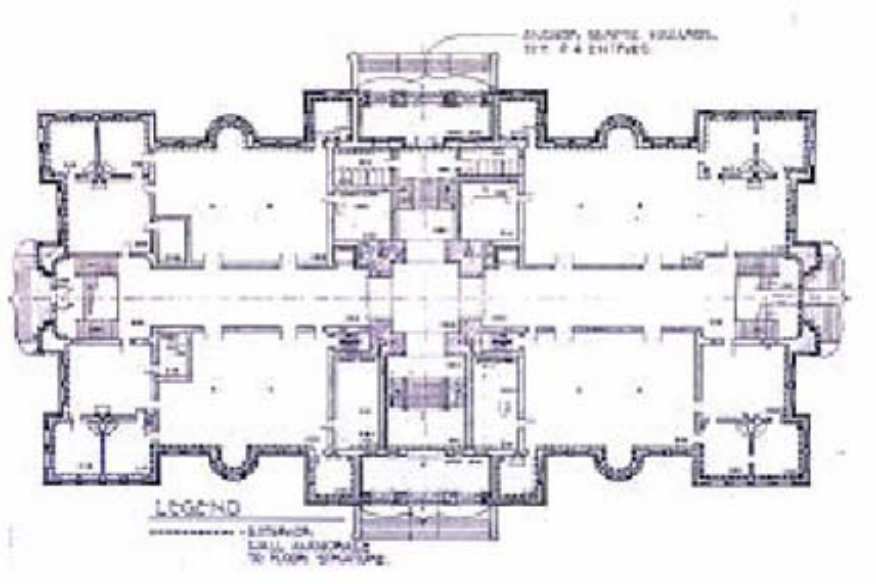

Figure 6.2. Plan view of Salt Lake City

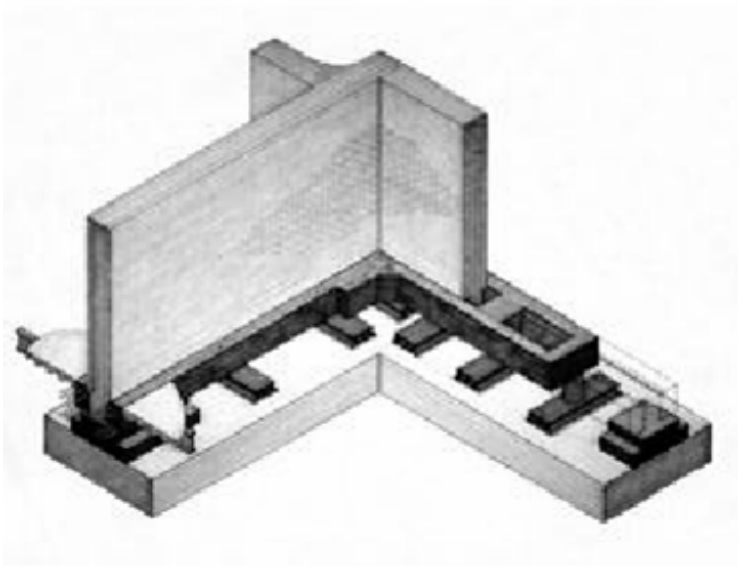

Figure 6.3. Wall connections of Salt Lake City Hall

6.1.2. The University Hospital of the University of Southern California

The University Hospital of the University of Southern California is the world's first seismically isolated hospital. It is also the first seismically isolated building in the United

States that wad faced to a strong earthquake excitation which was the Northridge earthquake in 1994.

It is an eight-storey, about 35 000m^2, steel-braced frame building with an asymmetric floor plan, scheduled for occupation in 1991 (Asher *et* al. 1990).

After assessment of its cost comparison among general and isolated alternatives, seismic isolation was decided to apply taking its potential benefits into consideration.

Seismic isolation solution was applied as a combination of lead-rubber bearings at the exterior braced-frame columns, and elastomeric bearings at the interior vertical load-bearing columns. A continuous 500 mm gap had also been provided, by construction a moat wall around the building, to make sure for enough room for large relative displacements at the isolation level. Also, all joints were produced and located to allow 75 mm larger seismic gap than the design displacement.

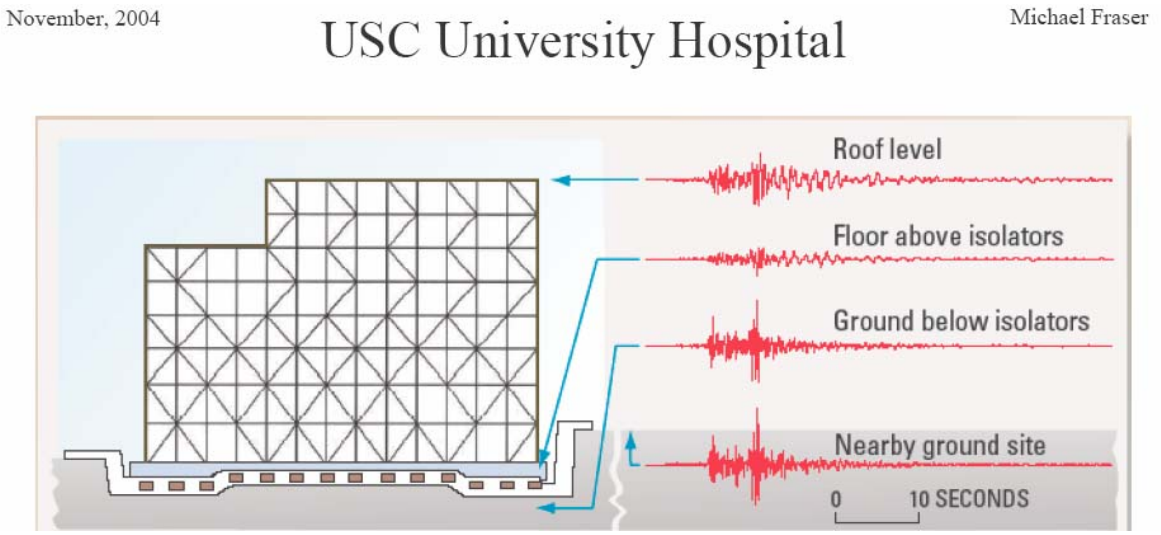

Figure 6.4. Acceleration records of USC University Hospital during 1994 Northridge earthquake

Figure 6.5. Test had done in for USC University and rolling effect of rubber

6.1.3. San Francisco City Hall

The San Francisco City Hall is one of the largest seismic retrofitting project in the world by the installation of 500 elastomeric isolators. The 90 year-old building was severely damaged at the 1989 Loma Prieta earthquake.

The purpose was increasing the building's seismic capacity without damaging its aesthetic view. At the exterior columns of the building lead-rubber bearings were applied, however, in the interior columns elastomeric bearings without lead plugs were used. The building designated to meet an 8.2 earthquake on the Richter scale.

Figure 6.6. View of San Francisco City Hall

6.1.4. Los Angeles City Hall

The Los Angeles City Hall is an historical building which was 32-storey high and constructed in 1926 without any earthquake resistance requirements.Even though many destructive earthquakes affected structures, it resisted all. Finally, during the 1994 Northridge earthquake, a significant damage was occurred at the structure.

The purpose was increasing the building's seismic capacity without damaging its unique aesthetic view. For deciding the retrofit method, inter-story drift and the floor accelerations are the main focuses. Among those different methods; it is recognized that while inter-story drift can be reduced by some of them, only seismic isolation reduces the floors' accelerations to acceptable levels.

Seismic isolation system was applied by using 416 high damping rubber bearings and 90 sliding bearings. In addition, to increase the energy dissipation capacity of the structure, 52 viscous dampers was added at the isolation level. Also, 12 dampers were

installed in the tower between the 24th and 25th floors to provide damping for higher modes. When it is completed, it was the tallest seismically isolated building in the world.

6.2. Seismic Isolation in Japan

The majority of seismically isolated structures in Japan are residential and office buildings. The first seismically isolated structure was a two-storey reinforced concrete dwelling in Japan. It was built on six laminated-rubber bearings located at the foundation level under its six columns.

The most popular city in terms of using seismic isolation systems at the structures is Tokyo. Furthermore, Japanese people have a tendency to pay extra initial cost for seismic isolation in order to reach higher levels of seismic protection.

It is widely preferred to use laminated-rubber isolation for the seismic isolation, with either steel or lead providing the damping.

Another thing is that most of the isolated structures are instrumented properly in oerder to record earthquake excitations. That's why, important data has been gathered for the seismically isolated systems. Also, the seismically isolated structure under an earthquake excitation can be compared to a closely located fixed-base one in order to confirm the benefits to use seismic isolation systems.

6.2.1. The High-Tech R&D Centre, Obayashi Corporation, Tokyo

The Obayashi Corporation building is a five-storey high, reinforced-concrete structure. The seismic isolation devices used in the building were 14 laminated-rubber bearings, with an axial dead load of 200 t, as well as 96 steel bar dampers of 32 mm diameter. For experimental purposes, friction dampers were also used as sub dampers.

Laminated rubber bearings lenghtened the natural period of the structure to 3 seconds. Seismic isolation has allowed a reduction of design strength and permits a large span structure with smaller columns and beams, which in turn provides open space (Skinner, 1993).

6.2.2. The C-1 Building, Tokyo

The C-1 Building which was the largest seismically isolated building in the world when completed in 1992 in Fuchi City, Tokyo.

The building is a seven-storey, composite reinforced concrete-steel structure. The protection of the building was the dominant design requirements because it would be used as a computer center. The superstructure is mounted on 68 circular lead-rubber bearings for seismic isolation. The bearings are between 1.1 and 1.5 m in diameter, with lead plugs from 180 to 200 mm in diameter (Nakagawa and Kawamura, 1991).

The natural period of the isolated building varies from 1.4 to 3 s depending on the intensity of the earthquake excitation. Also, the base shear at the isolators due to wind seems not more than 45% of the yield shear force, ensuring its safety against strong winds.

6.2.3. The Computer Center of the Tohoku Electric Power Company, Sendai

The computer center of the Tohoku Electric Power Company is constructed in Sendai, Miyako. Its content of electric power utility, the building was erected to house expensive. When the construction of the structure finished in 1990, it was largest seismically isolated building in Japan.

The structure was erected on 40 high-damping bearings. The bearings' diameters varies between 0.9 to 1.2 m. They have a capacity of 400 to 800 tons of vertical load. The seismic isolation system adoption was very simple and had an additional cost of just 5% on to its $20 million cost (Komodromos, 2000).

6.3. Seismic Isolation in New Zealand

As in the similar countries which were located in an area of high seismicity, New Zealand takes initiative for the seismic isolation concept in order to hold on against earthquakes. The activities on seismic isolation began in 1929, however, the practical applications were first carried out in 1973.

In New Zealand, seismic isolation intersects with energy dissipation in the isolation system to decrease the displacements or seismic loads. Also, the lead-rubber bearing system is the most preferred seismic isolation system.

6.3.1. New Zealand Parliament Buildings

The retrofit project of two historic buildings which are Parliament House and Parliament Library was the largest budget project at that time. These crucial buildings

wanted to be reinforced in order to resist destructive earthquakes.

The buildings are close to an active Wellington fault. As mentioned above, reinforcement of them is very important taking into their highly susceptibility to possible, great earthquakes. In order to keep their architectural value, their historical and architectural value provides them significant importance. Therefore, seismic isolation was chosen from many various options.

The main idea was locating these two buildings mostly on high-damping rubber bearings with lead cores. This was the first time that a hybrid isolation system had ever been used.

The installation of the isolators for the Parliament House was enabled by cutting some blocks out of the existing foundations. On the other hand, for the Parliament Library, a hybrid isolation system was used at its basement. At this basement level, bearings are installed in the foundation walls to provide enough flexibility.

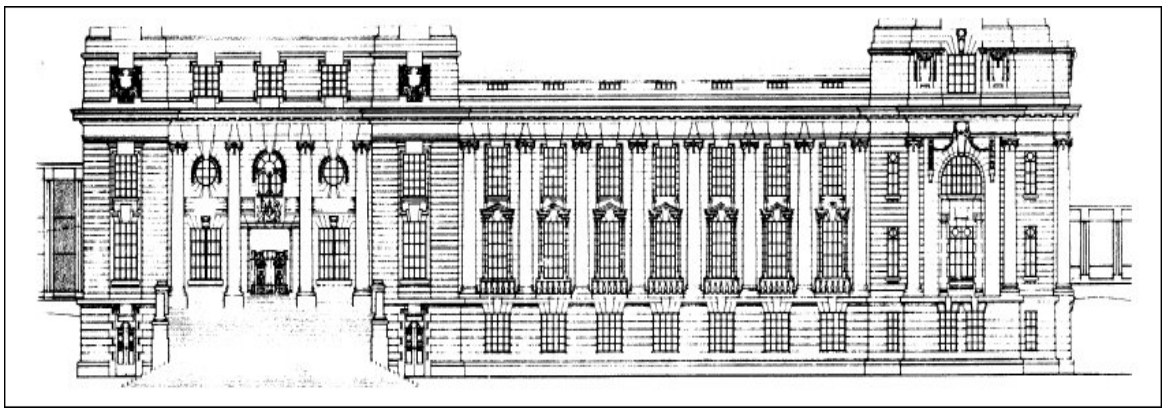

Figure 6.7. New Zealand Parliamant Building (Skinner,1993)

6.3.2. The William Clayton Building

The William Clayton Building was the first seismically isolated in New Zealand. It was also the first in the world to be seismically isolated on lead rubber bearings.

For the design concept of the building, 1.5 El Centro was selected as earthquake record by taking its close distance to the active Wellington fault.

The four-storey reinforced concrete frame building is mounted on 80 lead-rubber bearings. Those lead-rubber bearings which are consist of 600 mm by 600 mm by 207mm tall with a 105 mm diameter lead plug are placed under each of the columns. Every bearing has capacity of about 200 mm relative displacement in any horizontal direction.

6.3.3. Wellington Central Police Station

The Wellington Central Police Station which is a ten-storey, 38 m by 31 m reinforced-concrete building was seismically isolated in order to make sure that it will withstand in a major earthquake and it will remain operation to fulfill its functions in that kind of emergencies. The building was also supported by 15 m long piles. Also, it was too close –within a few hundred meters- to the active Wellington fault.

Upon those data, the building was designated to meet a 1.4 times stronger El Centro earthquake so that it could respond elastically under that excitation with a return period of 450 years.

As previous examples, among some alternatives, seismic isolation approach was adopted rather than the others. Thus, 10% of the structural cost saved and the resistance capacity to an earthquake was increased. Finally, it is highly expected that the possible repair costs after a great earthquake should be low.

6.4. Seismic Isolation in Italy

Among European countries, Italy has the significant tendency for applying seismic isolation, especially in bridges of the Italian highways with an emphasis on energy absorption. However, there are rare examples of buildings that are seismically isolated.

In order to support the applications, developments and researches on seismic isolation, a company called "National Working Group on Seismic Isolation (NWGSI)" was established in 1989. The NWGSI provides especially technical support to the entrepreneurs such as seismically isolated structures' designers.

The most commonly preferred seismic isolation system is high-damping rubber bearings according to the use in seismically isolated buildings and bridges in Italy. Also, for the buildings passive hybrid isolation systems are started to use in Italy.

6.4.1. The SIP Complex, Ancona

The SIP Complex is the administration center of the National Telephone Company in Ancona. It is seismically isolated with a seven-storey building.

The building is placed on 297 high-damping rubber bearings of diameters 0.5 to 0.6 m and height 0.19 m. The natural periods vary from 1.5 to 1.6 s. Also, a maximum displacement of 145 mm with a maximum response spectrum acceleration of 0.5g.

6.4.2. The Mortaiolo Bridge

The Mortaiolo Bridge was constructed in 1992. It is a major two-way bridge in the Livorno-Cecina section of the Livorno-Civitavecchia highway (Skinner, 1993).

Elasto-plastic devices on each pier with shock absorbers used in this 9.6 km long bridge which has 45 m long spans made of prestressed reinforced-concrete slab.

These devices which were utilized in the bridge manufactured by Italian companies such as FIP Industriale. Nowadays, FIP Industriale is one of the important firms in seismic isolation device manufacturing. Device has dissipating behaviors that is based on the steel hysteretic flexural deformations. By using this isolating system, additional cost was just 4.8% of the structural cost of the bridge.

6.5. Seismic Isolation in Turkey

Turkey is located in an active seismic zone and most of the major earthquakes occurred in Turkey have been generated by the North Anatolian Fault (NAF). Because of this reason, the studies that were conducted about mitigating the effects of earthquakes have a significant impact in Turkey. Kocaeli (17.08.1999) and the Duzce (12.11.1999) earthquakes occurred in highly populated regions in Turkey.

These two earthquakes not only caused modifications of seismic design but also made necessary to focus on evaluation and retrofit of existing structures in Turkey.
The use of seismic isolation systems for the structures become increasing parallel to the use over the world.

There are some crucial structures which have key role in Turkish regional points such as Kocaeli Hospital, Bolu Viaduct and Erzurum State Hospital. Some of the base isolation projects are presented below.

6.5.1. Kocaeli University Hospital

Kocaeli University Hospital was a new designated and constructed structure in Kocaeli. It is a seismically isolated building by using friction pendulum system (FPS) on the columns. The diameter of FPS is 0.79 m with a 6% coefficient of friction. The natural period of isolators is 3 s. Also, allowable displacement is 28 cm.

Figure 6.8. Kocaeli Hospital

Figure 6.9. Construction stages of Kocaeli Hospital

6.5.2. EGEGAZ, LNG Tanks

Egegaz LNG Tanks were new compounds. Seismic isolation system was applied to the structures such as lead-rubber bearings and natural rubber bearings. 112 and 241 of them were used, respectively. Damping ratios are 10% and 20%. Also, the displacement demands are 0.24 and 0.44 m.

Figure 6.10. Egegaz LNG storage tanks

Figure 6.11. Locations of isolation devices for LNG tanks

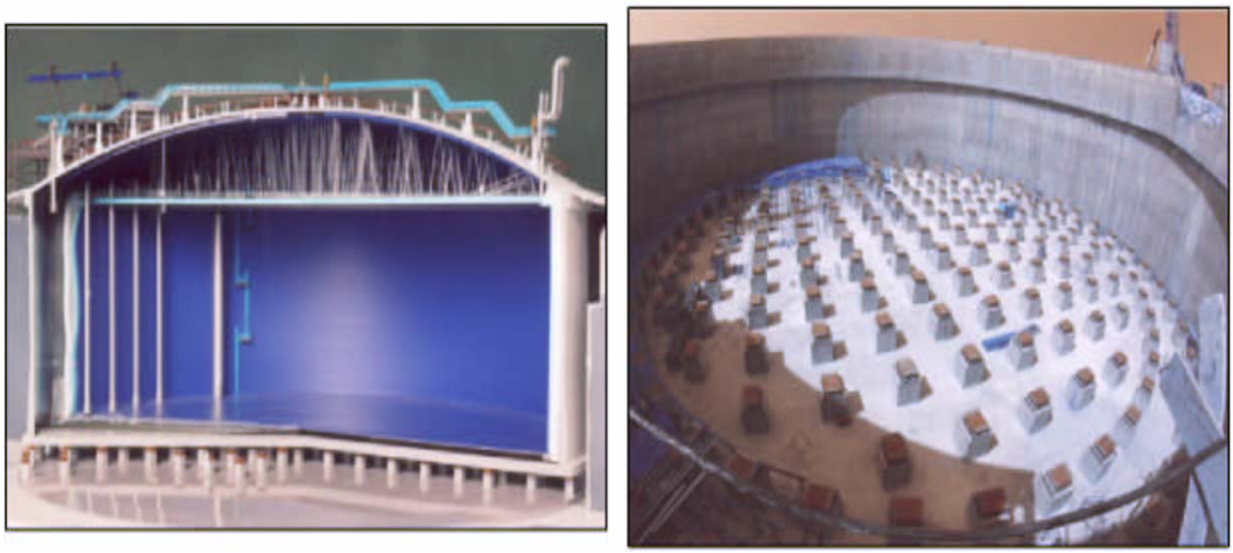

Figure 6.12. Cross-section of a LNG tank and location of isolators

6.5.3. Tarabya Hotel

The Tarabya Hotel is an old structure located at the seaside of Istanbul's European region. The hotel was retrofitted recently. It is a seismically isolated building by using friction pendulum system (FPS) at the piers. The diameter of FPS is 0.79 m with a 6% coefficient of friction. The natural period of isolators is 3 s. Also, allowable displacement is 28 cm.

Figure 6.13. Tarabya Hotel

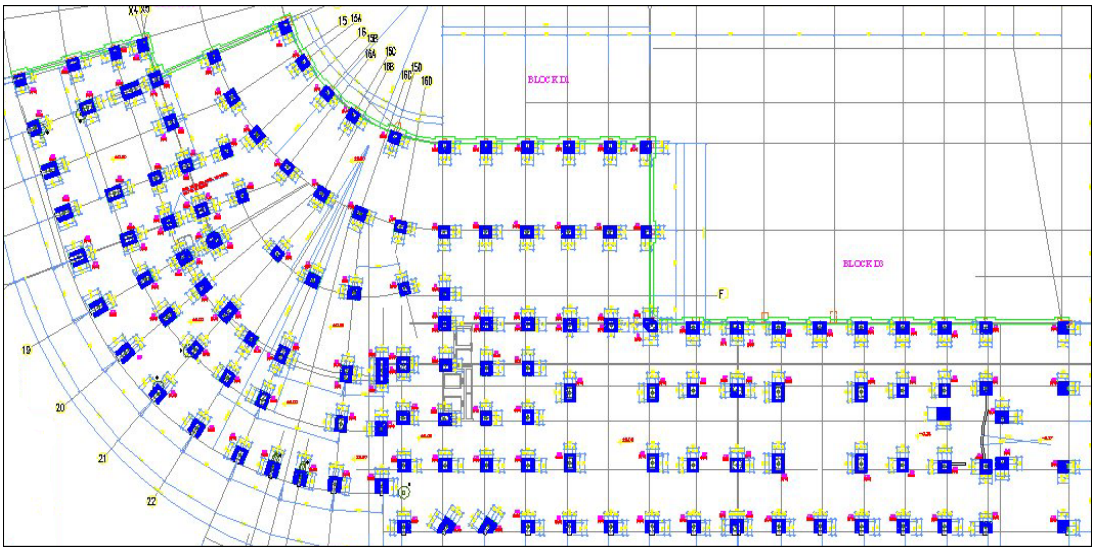

Figure 6.14. Locations of FPS bearings and plan view of Tarabya Hotel

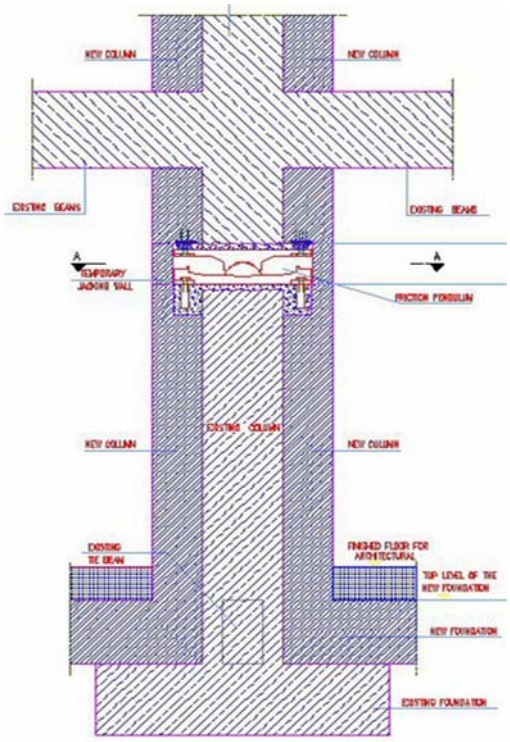

Figure 6.15. Cross-section of columns at Tarabya Hotel

Figure 6.16. Implemantation process of FPS

Figure 6.17. Implementation of FPS devices

Figure 6.18. Replacement of FPS isolators to colums for retrofit project

Figure.6.19. Mounted FPS isolator in Tarabya Hotel

6.5.4. TEB General Directorate Building

TEB General Directorate building is pending for construction stage. It will be carried out in Istanbul with seismic isolation system adoption. Seismic isolation system will be applied to the structure by using 87 natural rubber bearings and lead-rubber bearings. Three different types of isolators are planned to be used with diameters of 0.72, 0.97 and

1.12m. The natural period of the isolators is evaluated as 4.3 s. Also, the displacement demand is assessed as 0.40 m.

Figure 6.20. TEB Building

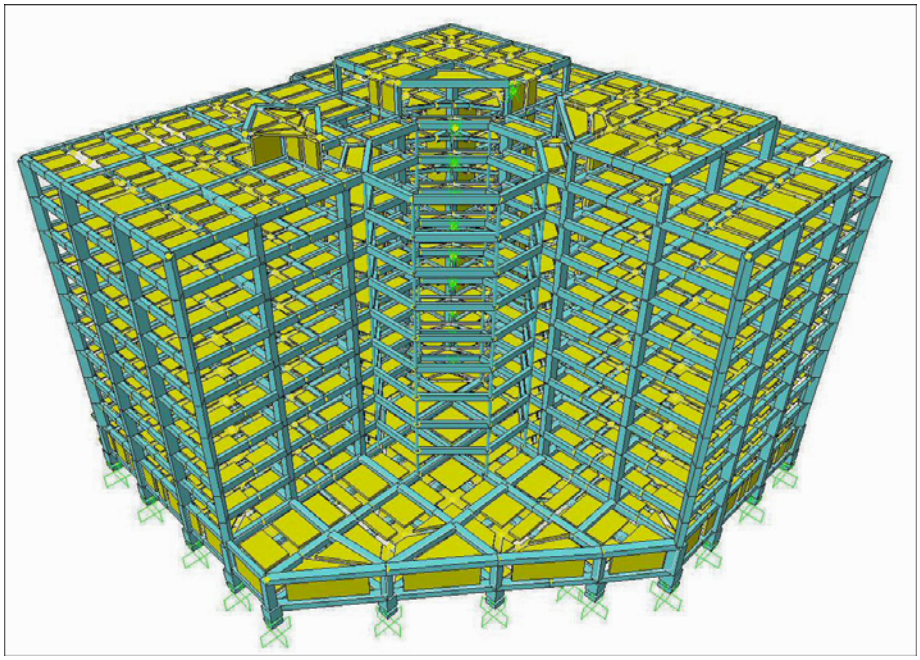

Figure 6.21. SAP2000 model of TEB building

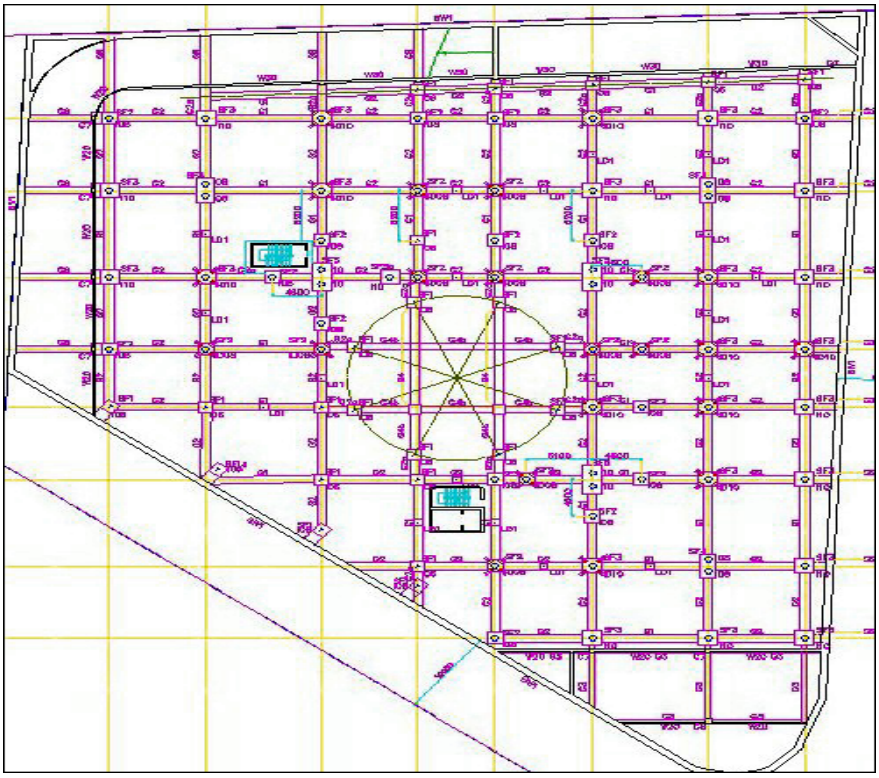

Figure 6.22. Plan view and isolator locations of TEB building

6.5.5. Atatürk Airport

The Atatürk Airport was constructed in Istanbul's European region. The airport was retrofitted recently. It is a seismically isolated building by using FPS at the piers. 100 of them were used at this seismic isolation. The coefficient of friction of FPS is 9%. The natural period of isolators is 3 s. Also, allowable displacement is 30 cm.

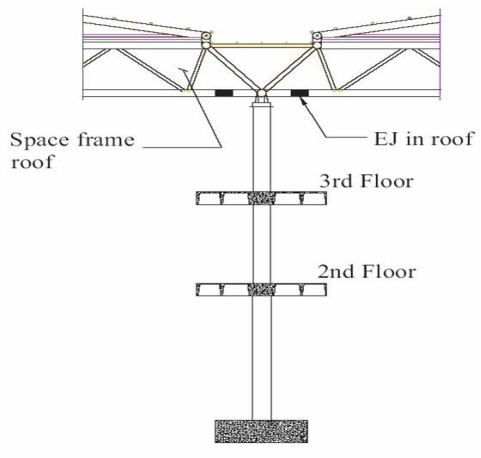

Figure 6.23. Location of FPS at airport

Figure 6.24. Locations of FPS isolators in Atatürk Airport

Figure 6.25. Location of a FPS isolator in Atatürk Airport

6.5.6. Bolu Viaducts

The Bolu Viaducts' construction was recently finished but it had been a headache for Turkey for many years. It took so long and so much money was spent for the project. They are seismically isolated structures by using two FPS isolators at the intermediate piers between the diaphragms and four at the expansion joints are inserted. The diameters of FPS units were 0.70 and 0.90 m (at fault crossing).

Figure 6.26. Bolu Viaducts

Figure 6.27. Locations of FPS isolators at bolu Viaducts

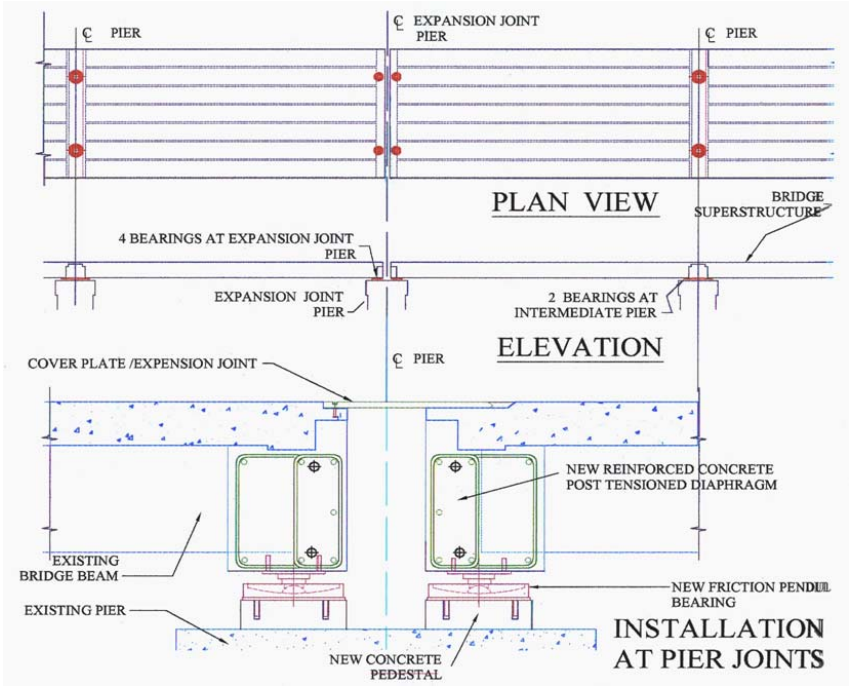

Figure 6.28. Plan view of Bolu Viaducts

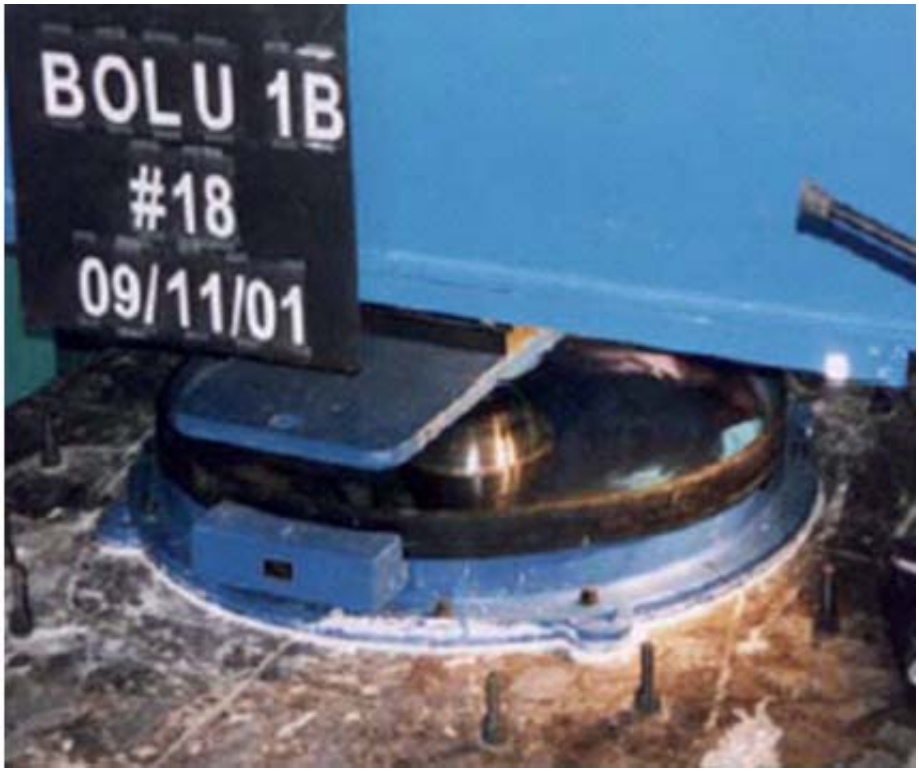

Figure 6.29. Mounted FPS isolator at Bolu Viaducts

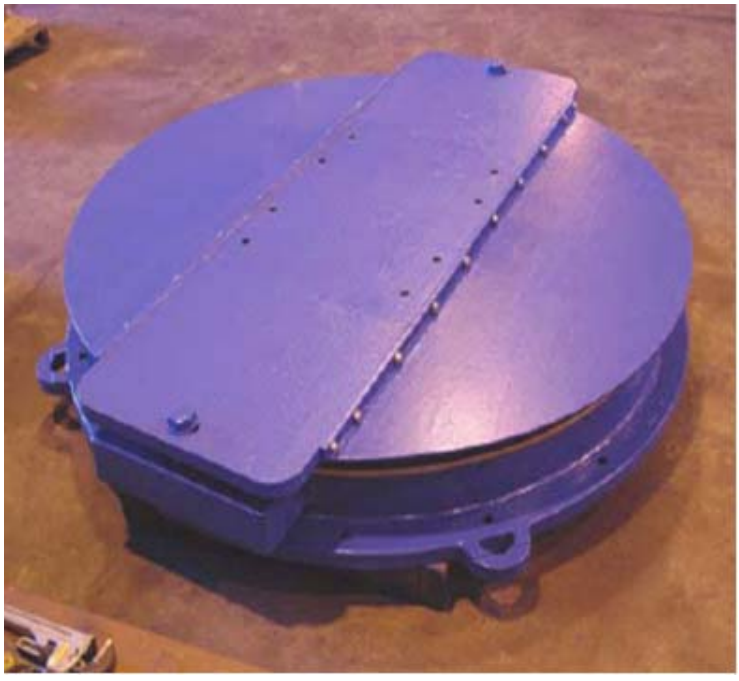

Figure 6.30. Size of FPS bearings that have used in Bolu Viaduct project

7. TEST SETUP AND INSTALLATION

7.1. Shake Table Test

Seismic isolation is not a new concept but it still develops with increasing interest. There are still some uncertainties about the isolation devices. To overcome this problem prototype tests have to be conducted at laboratories. To understand the behaviour of an isolation system, isolators need to undergo rigorous laboratory testing prior to their field installation. Manufacturers usually do some tests which define the mechanical characteristics of isolation devices. Also tests are carried out at some laboratories which are compatible with test specifications. Even though, shake table tests have to be conducted before the installation of isolation system for the important projects. The best way to evaluate the performance of isolator is testing the isolation system with a length scaled model which represents the application project that will be constructed. By this way undesirable response of the isolated structure can be observered during the tests.

Hybrid passive isolation system for a ¼ scaled three-story isolated steel structure is evaluated by shake table tests under sinusoidal harmonic motions and real earthquake data which had been time scaled. In addition, Pga value of the real-time earthquake data is adjusted to certain values to assess the effectiveness of an hybrid isolation systems. To understand the behaviour of an isolation system, isolators need to undergo rigorous laboratory testing prior to their field installation

7.2. Test Setup and Instrumentation

The test set-up consists of a 3-story steel structure and passive hybrid isolation system. The mock-up is placed on the uni-axial hydraulic shaking table of KOERI constructed by ANCO engineers, Inc. The ANCO R-148 is a uni-axial horizontal vibration shake table driven by a servo-hydraulic actuator. The table was designed by ANCO Engineers and it is capable of carrying a maximum 10-ton payload on the 3 m x 3 m table, and is capable of shaking a 10 -ton payload with 2 g acceleration (i.e. two times the acceleration of gravity in the horizontal direction). The shake table is ideally suited to seismic applications, because the hydraulic actuator can produce a stroke of +/- 12 cm (24 cm total stroke). The actuator has a 3-stage servo-valve controlled by an analog inner-loop control system (displacement based), and a digital outer-loop control system (acceleration feedback based). The structural model has a length scale of 4 and, time scale of 2, weighting 6.5 tons (isolated including base) and fundamental period of fixed supported system is 0.21 sec.

The story height is 0.9m and plan dimension is 2^{m}x1^{m}. Plan dimension of the structural system is shown in Figure 7.1.

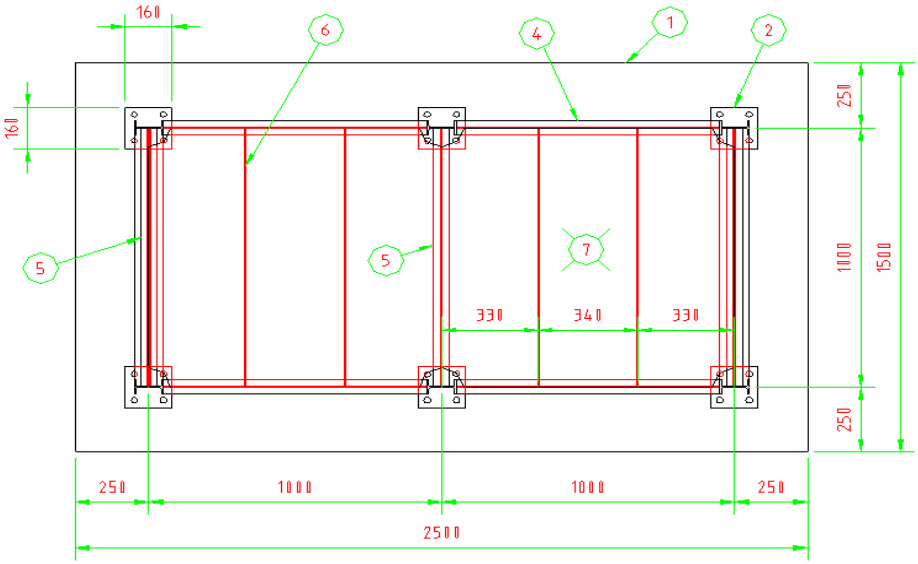

Figure 7.1. Plan view of the base slab and floor levels

Prototype of isolators are manufactured by FIP Industrial for shaking table tests in KOERI and mechanical properties of HDR bearings are determined in FIP laboratory.

Figure 7.2. Passive Hybrid Isolation System

7.3. The Isolation System

The isolation system is a combination of high damping rubber bearings and flat sliding bearings(PTFE). Hybrid isolation system consists of two rubber bearings and four sliding bearings. In addition, two different high damping rubber bearings were used to demonstrate the effect of shear modulus in elastomeric bearings. Moreover, sliding bearings are located below the corner columns and high damping rubber bearings mounted

below center columns. To overcome the disadvantage of flat sliding bearing, restoring force is provided by HDR bearings. Flat sliding bearings do not have a restoring force like friction pendulum systems. Contact surface of the sliding bearing is covered by special teflon material and the coefficient of friction depends on the relative velocity at the isolation interface. Coefficient of friction that has given by the manufacturer is verified with preliminary tests conducted in KOERI laboratory. Hybrid isolation system with SI-N 150/136 is named as isolation sytem1 and the other isolation system with SI-S 150/136 is named as isolation system2 for the evaluation of test and numerical results.

Table 7.1. Properties of 2 HDR bearings

Isolator Properties	SI-N 150/136	SI-S 150/136
kh	0.097kN/mm	0.048kN/mm
Vertical load capacity	27kN	15kN
Seismic displacement capacity	85mm	55mm
Shear Modulus	0.8MPa	0.4MPa
Total rubber thickness	136mm	136mm

Figure 7.3. Configuration of isolators

7.4. The Data Acquisition and Control System

Table motion and data acquisition are carried out by a Data Physics 550 WIN digital data control and acquisition system. Translational displacement response of the isolated structure is measured with the help of LVDTs that have been used at shake table, base slab and top floor levels,repsectively. Location of LVDTs are shown below.

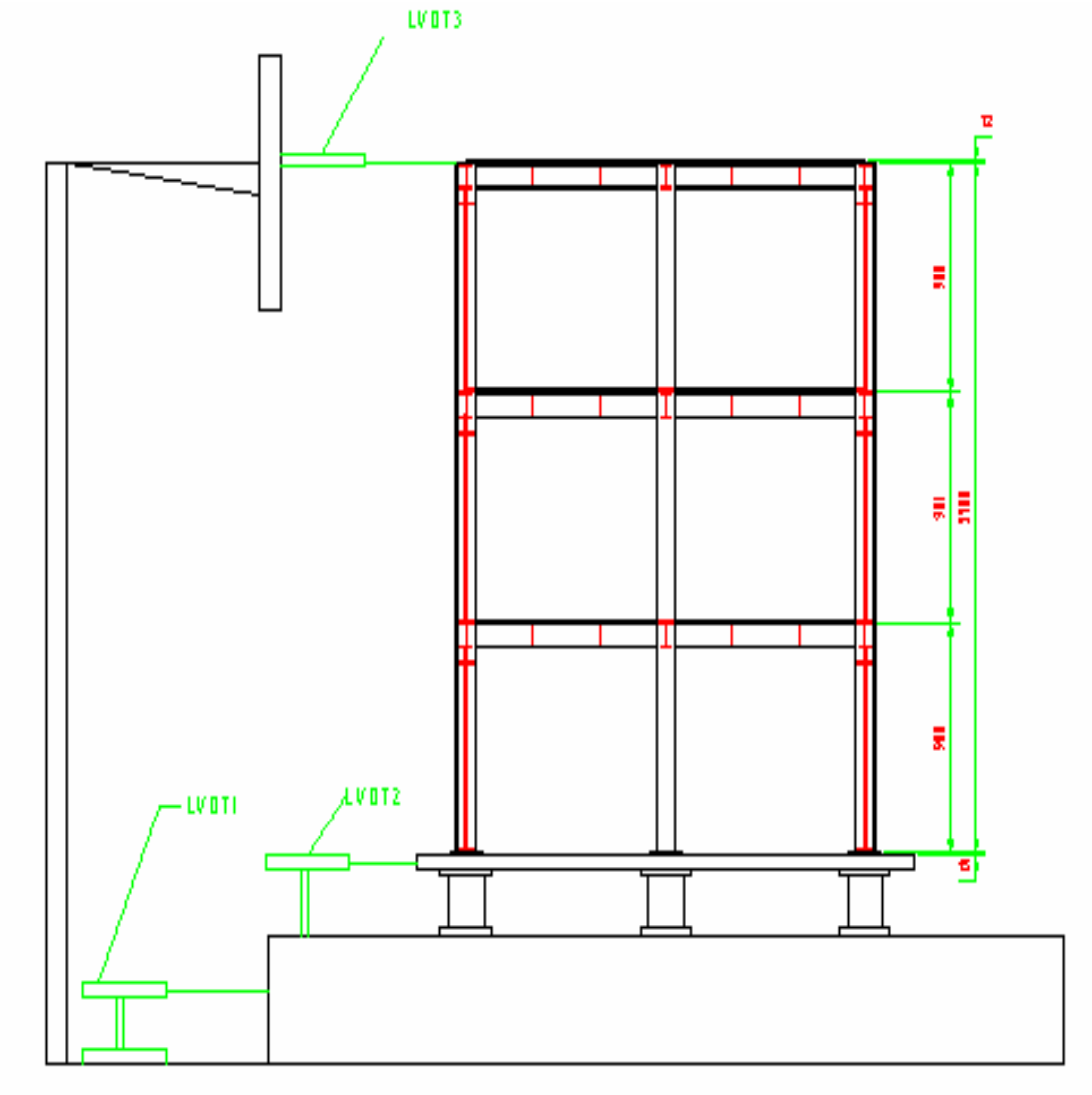

Figure 7.4. Locations of LVDTs to measure translational displacements

Accelerometers are attached to the shake table, base slab, first floor, second floor and top floor of the isolated structure. Also, another accelerometer is used in the transverse direction to measure the torsional response of the mass concentric system.

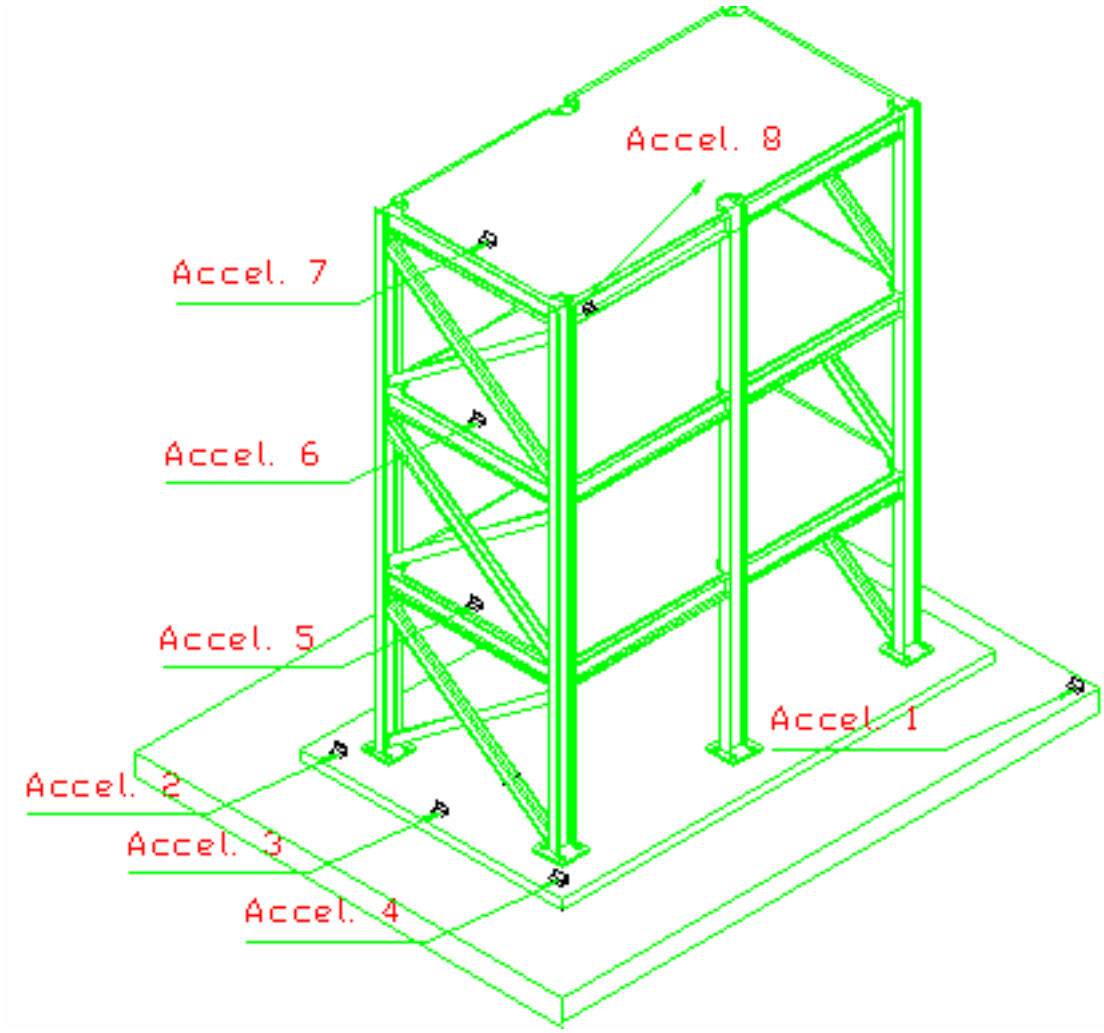

Figure 7.5. Locations of Accelerometers

7.5. Tests Conducted

Excitations performed in the longitudinal direction and series of tests are performed for onlymass concentric system. El Centro earthquake record is used for the test carried out in KOERI laboratory and peak ground acceleration values area scaled from 0.06g to 0.556g and in all cases earthquake records were time scaled by a factor of 0.5. Earthquake1 represents El Centro earthquake record which has a PGA value equal to 0.293g and Earthquake2 represents the same excitation that has scaled to 0.556g for the tests.

Furthermore, SI-N 150/136 are changed with SI-S 150-136 for the next test setup. The latter HDR bearing has a softer compound and its shear modulus value is 0.4 MPa and maximum seismic displacement capacity is smaller than the first HDR bearings. Because of this reason, second test setup is subjected to earthquake1 to avoid the concerns about the uncertainties after yield displacement.

8. TEST RESULTS

8.1. General Description

Shake table tests carried out under real time earthquake data and sinusoidal motions. Generally, real time earthquake data is gradually increased to see the effect of magnitude and two earthquake record is used to evaluate the effectiveness of the passive hybrid isolation system. In addition, for the second test setup new HDR bearings which have lower shear modulus value are installed below the center columns.

Furthermore, isolated period of two different system is investigated and transfer functions of the isolated structures are determined. Then, results of numerical analysis and tests are compared. Two type of high damping rubber bearings are used and the damping properties of these 2 HDR bearings are found from the baseshear-displacement loops. Same procedure to find out damping properties of the isolatedsystem is carried out for El Centro earthquake.

8.2. Input data for Shake Table Tests

Two different isolation system is excited by El Centro earthquake record. Time scale of earthquake data is 2 and time is multiplied by 0.5. Moreover PGA of the time scaled earthquake input is gradually increased from 0.07g to 0.556g to observe the effectiveness of the passive hybrid isolation system. In addition, harmonic motions are used to see damping properties of the HDR bearings under harmonic motions. Procedure to determine effective damping properties of HDR bearings are not only applied for harmonic motions

but also applied for real earthquake data at shake table tests. As mentioned above two different type of HDR bearing is used in the tests and properties of isolators has shown in Table 8.1 below

Table 8.1. Properties of HDR isolators

Isolator Properties	SI-N 150/136	SI-S 150/136
kh	0.097kN/mm	0.048kN/mm
Vertical load capacity	27kN	15kN
Seismic displacement capacity	85mm	55mm
Shear Modulus	0.8MPa	0.4MPa
Total rubber thickness	136mm	136mm

8.3. Tests of Normal Compound HDR Bearings at Different PGA Scaled Earthquakes (SI-N 150/136)

First isolation system that was used in shake table tests are consists of 4 flat sliding bearings below corner columns and two normal compound HDR (SI-N 150/136) bearings which were located below the center columns. Isolation system is excited by time scaled El Centro earthquake record which is also PGA scaled for tests. PGA values are in the range of 0.07-0.556g . Acceleration records, displacement records that has measured at different levels of isolated structure is shown in figures below. In addition to acceleration and displacement base shear of the isolated structure is calculated with the help of measured data.

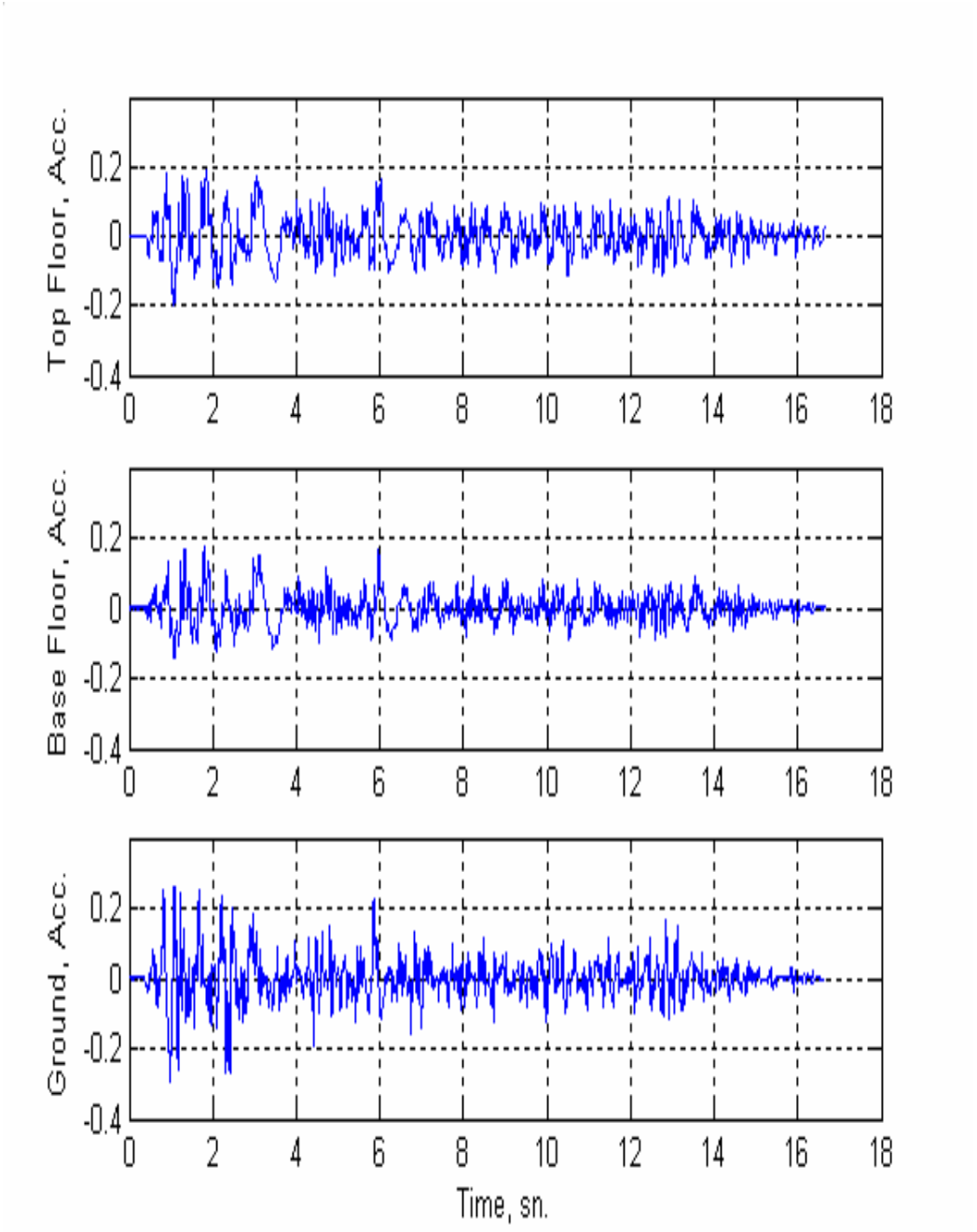

Figure 8.1. Acceleration records at three different levels of the isolated structure under

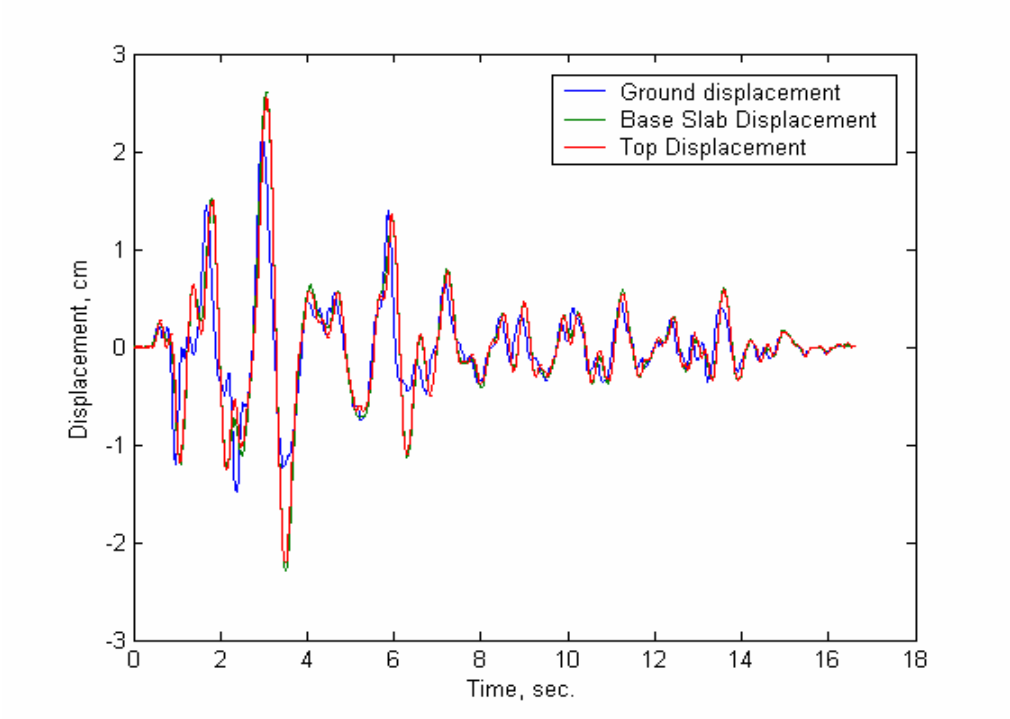

Figure 8.2. Displacement records from three different locations under El Centro Earthquake (Pga=0.293)

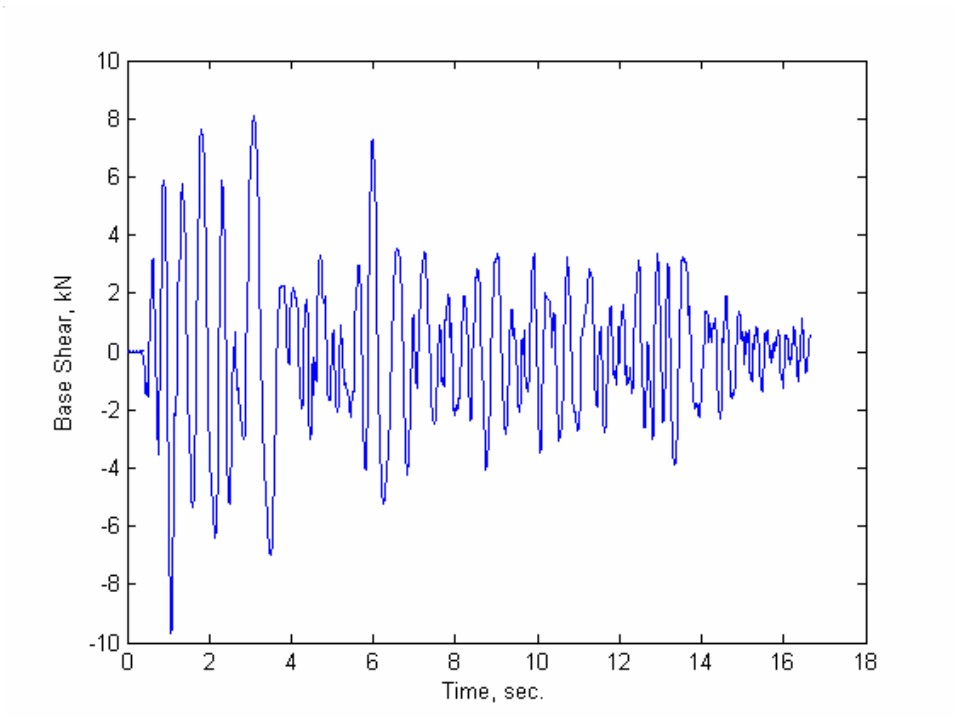

Figure 8.3. Base shear under El Centro Earthquake (Pga=0.293g)

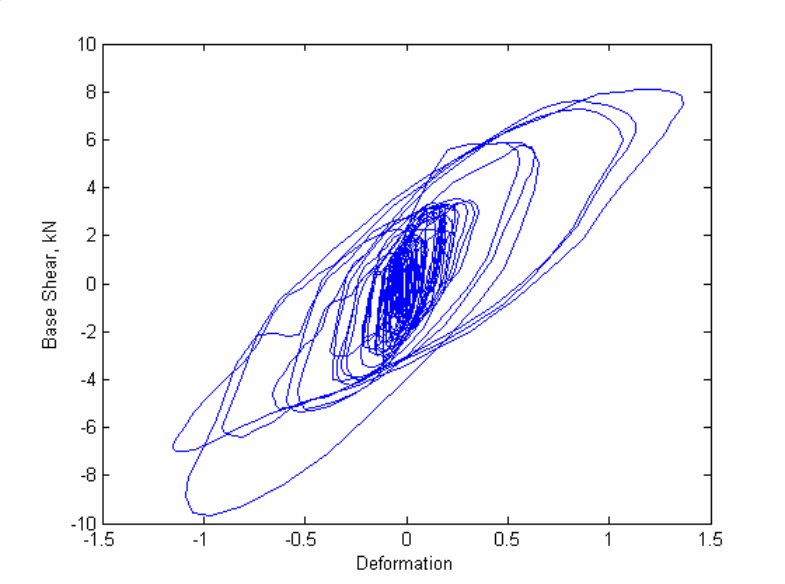

Figure 8.4. Base Shear-Displacement loops under El Centro earthquake (PGA=0.293g)

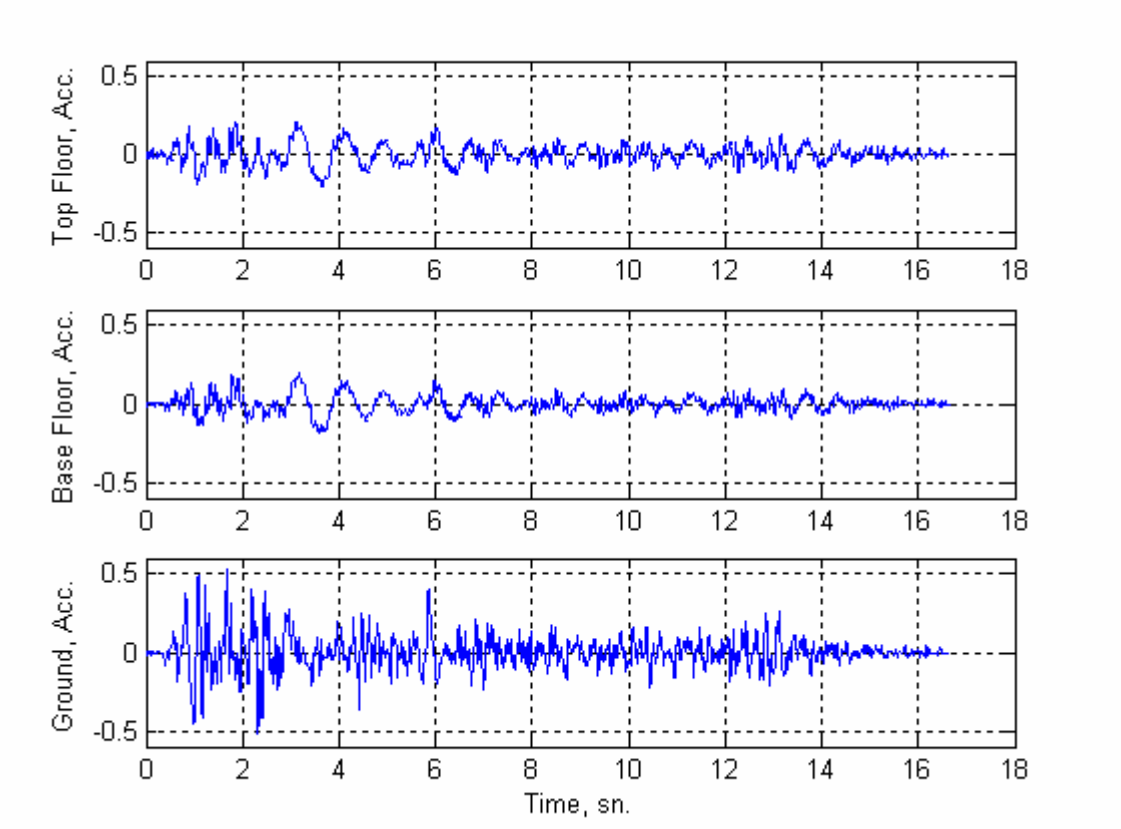

Figure 8.5. Acceleration records under scaled El Centro earthquake (PGA=0.556g)

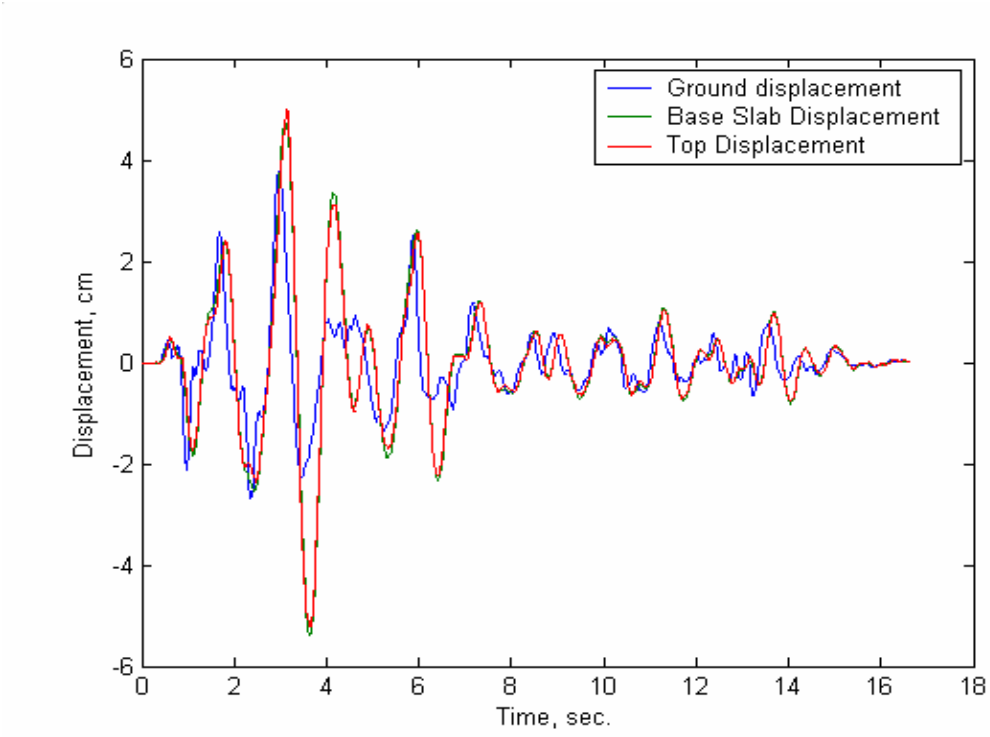

Figure 8.6. Displacement records under Scaled El Centro Earthquake (Pga=0.556g)

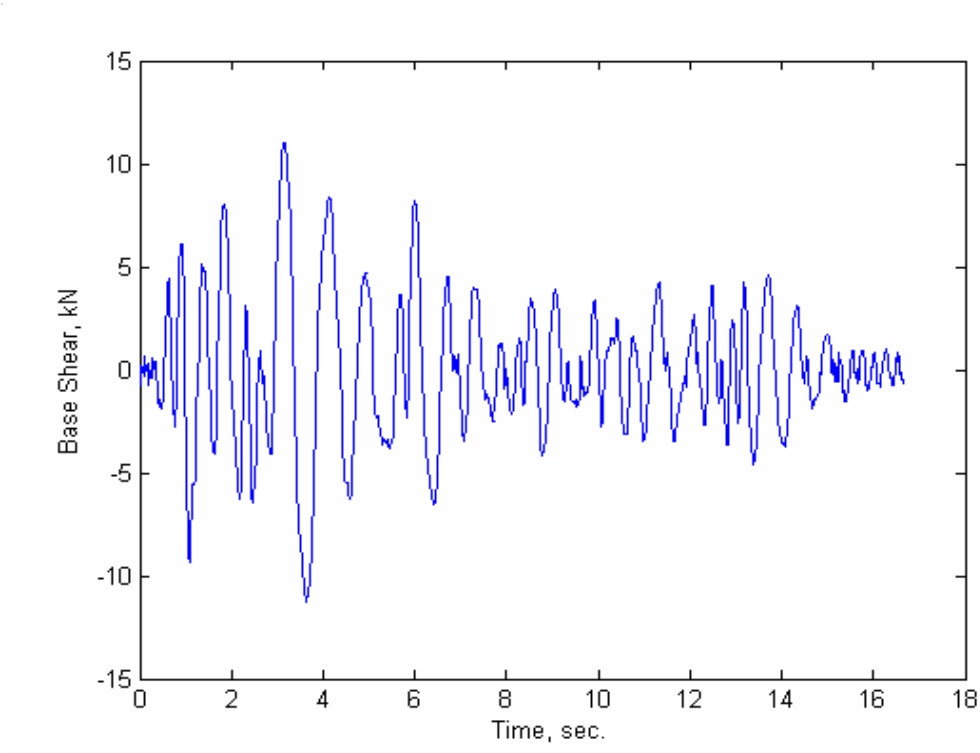

Figure 8.7. Base Shear at slab level under Scaled El Centro Earthquake(Pga=0.556g)

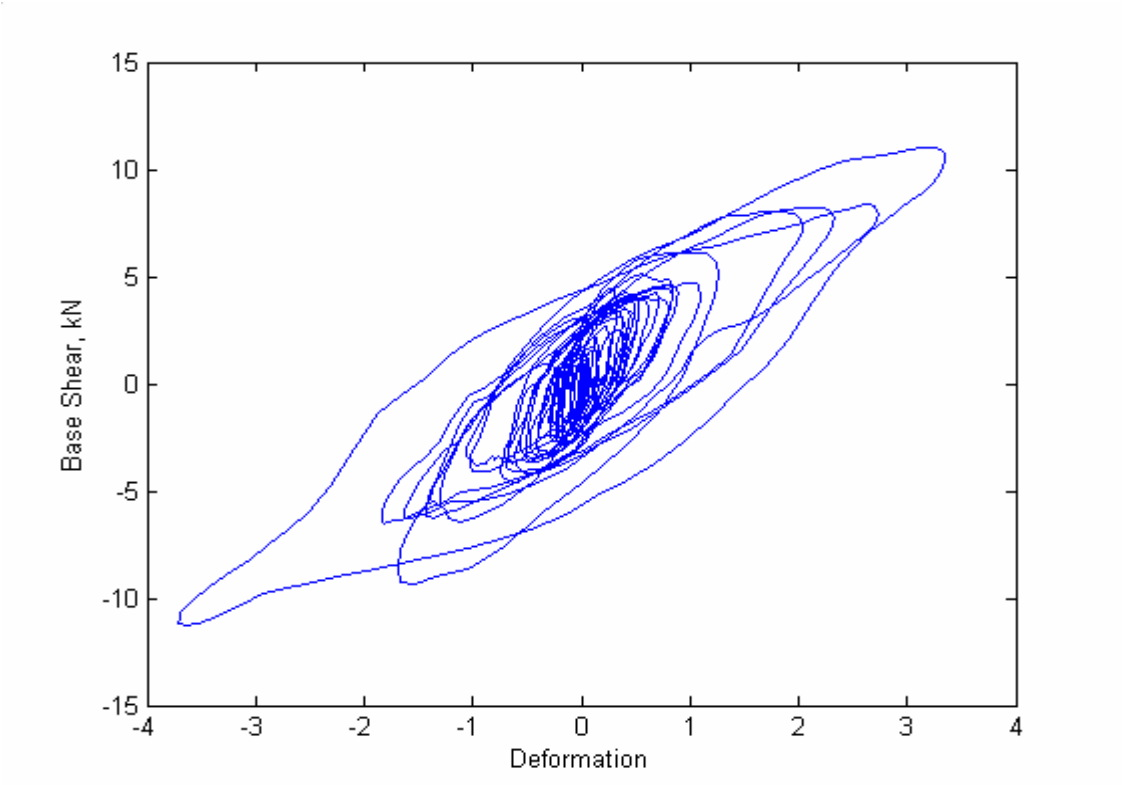

Figure 8.8. Base Shear-Displacement loops for PGA scaled El Centro (Pga=0.556g)

8.4. Tests of Soft Compound HDR Bearings at Different PGA Scaled Earthquakes (SI-N 150/136)

Second isolation system that was used in shake table tests are consists of 4 flat sliding bearings below corner columns and two soft compound HDR (SI-S 150/136) bearings which were located below the center columns. Isolation system is excited by time scaled El Centro earthquake record that was both time and PGA scaled for tests. PGA values are in the range of 0.07-0.293g . Acceleration records, displacement records that has measured at different levels of isolated structure is shown in figures below. In addition to acceleration and displacement base shear of the isolated structure is calculated with the help of measured data. Maximum input that was applied to second isolation system has Pga=0.293g because maximum seismic capacity of soft compound is 55 mm

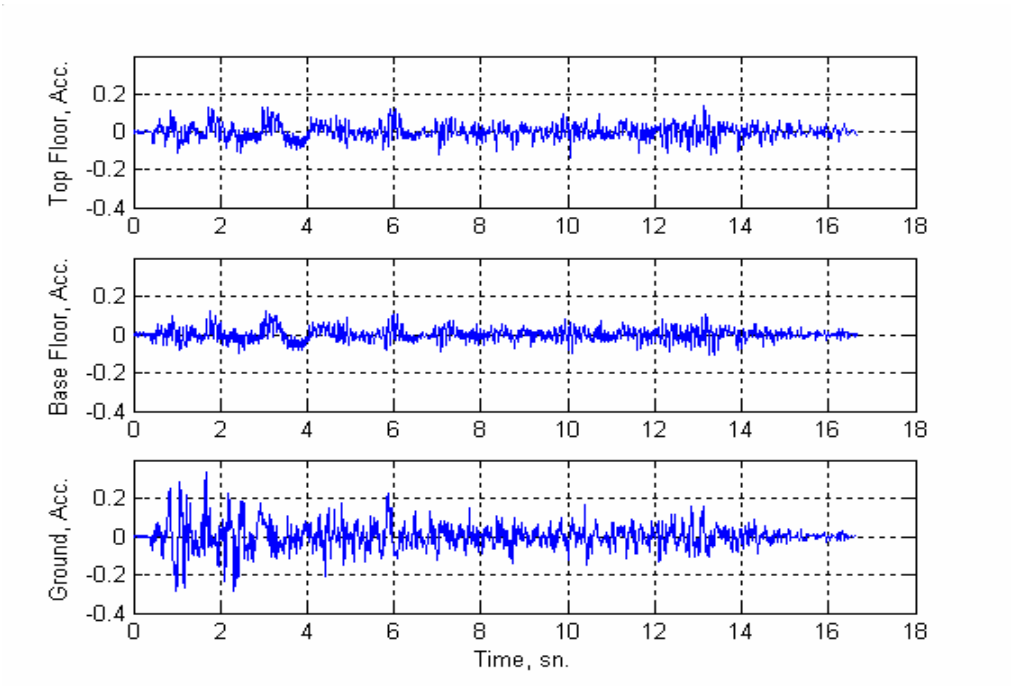

Figure 8.9. Acceleration records for the second isolation system under El Centro Earthquake(Pga=0.293)

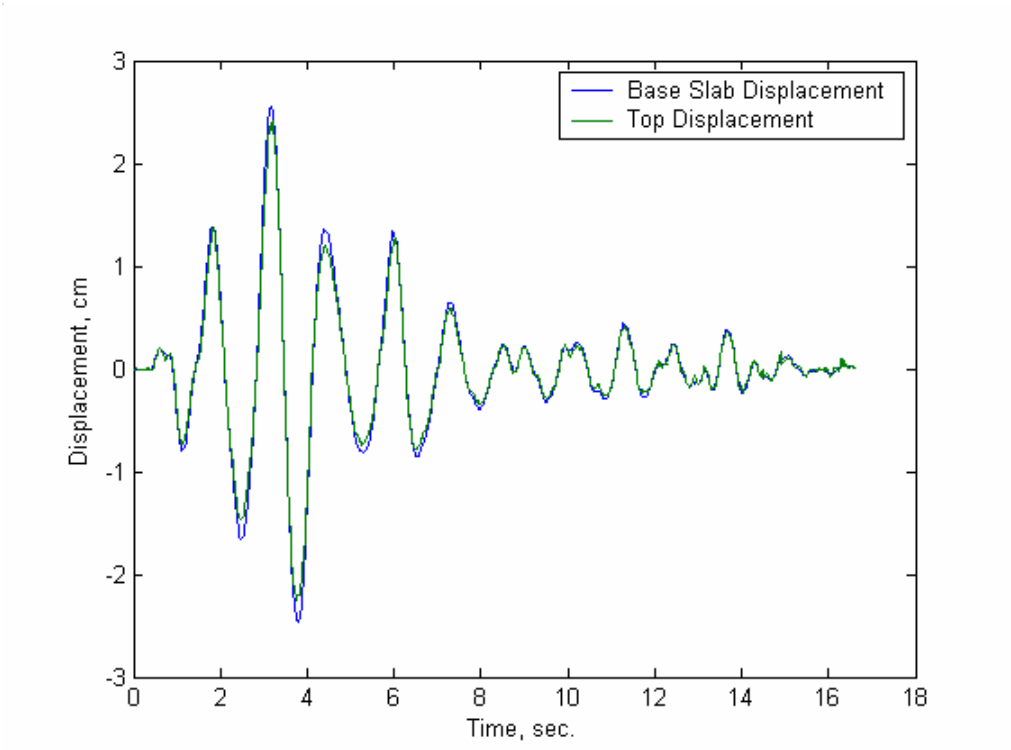

Figure 8.10. Displacement records for the second isolation system under El Centro earthquake (Pga=0.293g)

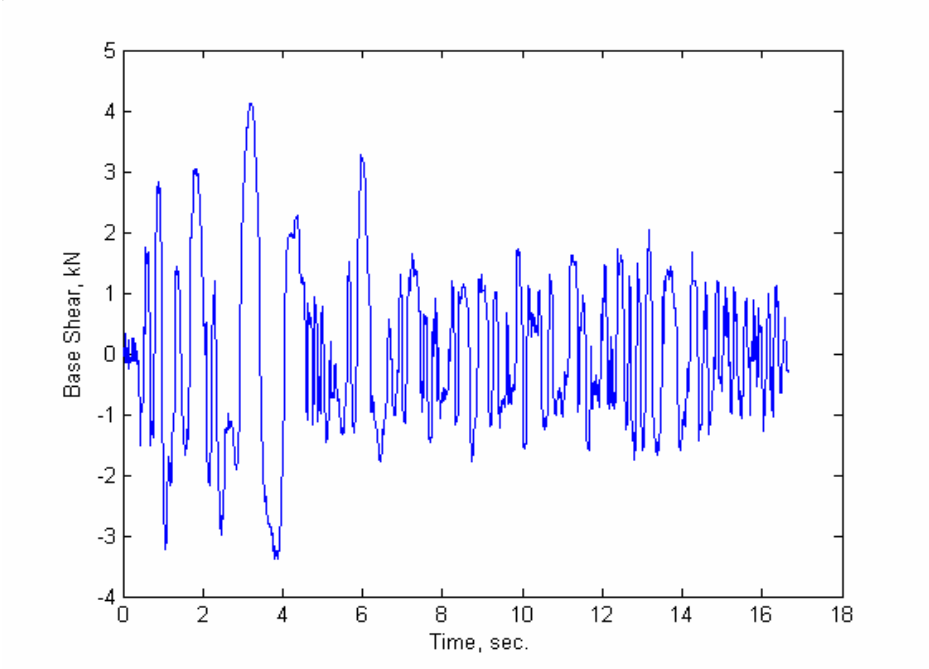

Figure 8.11. Base shear of second isolation system under El Centro earthquake (Pga=0.293g)

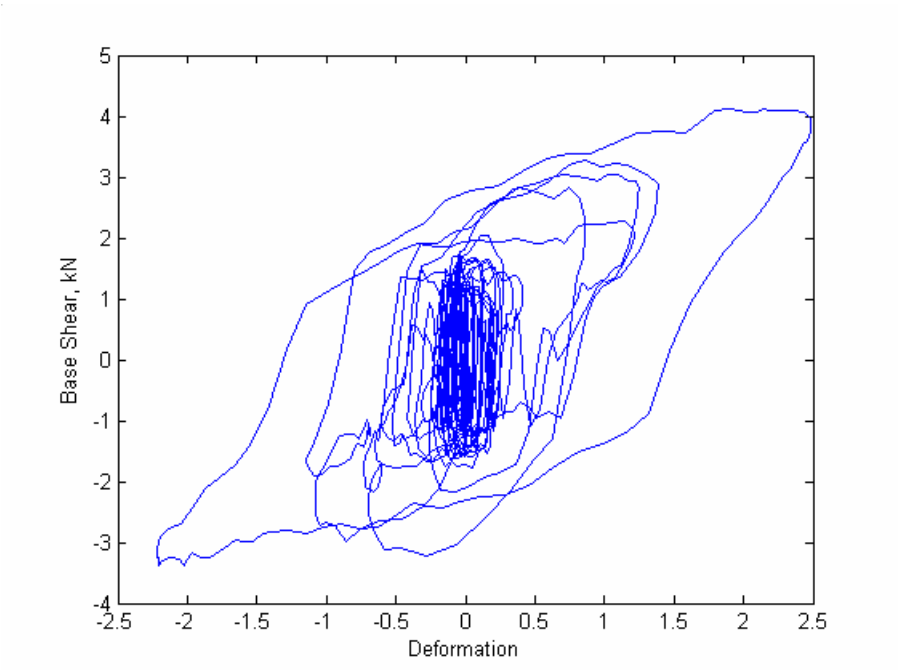

Figure 8.12. Base Shear Displacement loops for the second isolation system under El Centro earthquake (Pga=0.293g) Periods of hybrid isolation system

8.5. Sinusoidal Harmonic Tests

Harmonic excitations are applied to isolated systems and damping properties are determined from base shear-displacent loops of different harmonic motions. Properties of harmonic excitation is shown in Table 8.2. below and loops of harmonic motions to determine effective damping property is shown in figure 8.14. Effetive damping value for harmonic motion is decreased due to increasing displacement and effective damping values are presented in Table 8.2.

Table 8.2. Properties of harmonic motions that were applied during tests

	Sinusoidal 1	Sinusoidal 2	Sinusoidal 3
Duration	10	10	10
Amplitude	0.15	0.1	0.15
Frequency	1.85	1.5	1.5
Aloop	19.23	24.37	31.33
Maximum Displ.	1.77	2.41	3.14
Keff	3.71	3.56	3.14
Beff	27	19	16

In Figure 8.13 B represents the harmonic excitation, C represents the base slab acceleration and D represents the top floor acceleration . It is obvious that because of the isolated system harmonic excitation is reduced at base slab level. In addition to damping properties frequency and amplitude values of the excitation is increased gradually to check the resonance frequency of the isolated structure which was determined from numerical analysis. Resonance frequency of the isolated structure is observed as 1.7 Hertz.

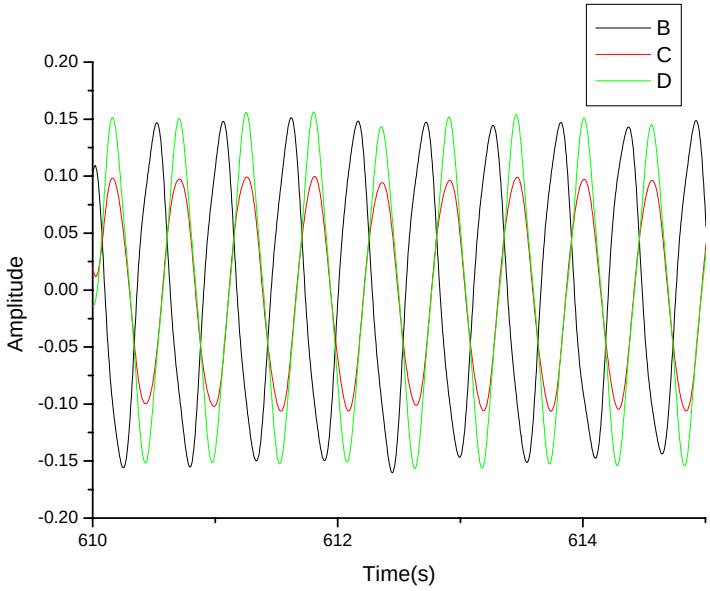

Figure 8.13. Acceleration records under Sinewave3

Figure 8.14. Comparison of harmonic excitations to determine the effective damping of SI-N 150/136

8.6. Comparison of Numerical and Experimental Results

Experimental and numerical results are compared with eachother to figure out the correctness of the numerical models of the isolated systems. Numerical analysis are carried out at SAP 2000 10.0.0 which has nonlinear link elements. Nonlinear link elements are used to model the isolators. Paramters that have been used in numerical analysis are determined from the test results of manufacturer. In addition to parameters that have defined by manufacturer code provisions are used as FEMA 356 and IBC 2000. Furthermore parameters that have used in numerical analysis are readjusted with respect to test results to get thebest results. It is important to readjust your parameters for the critical projects during the final design stage. Best way to determine the final parameters for the numerical modeling is to conduct laboratory tests for isolators. Comparison of numerical and measured results for SI-N 150/136 for El Centro earthquake record (Pga=0.293g) is shown below

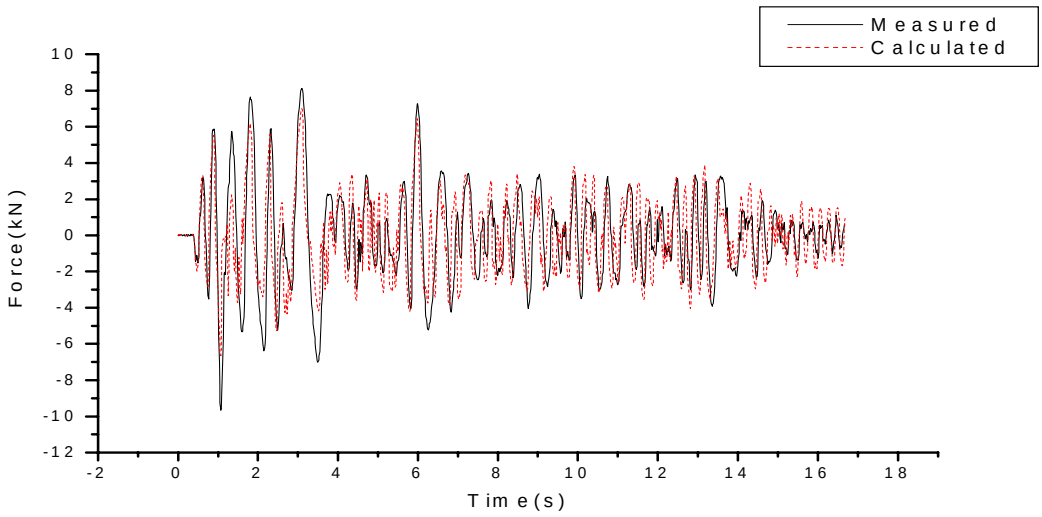

Figure 8.15. Comparison of Base Shear-time graphs

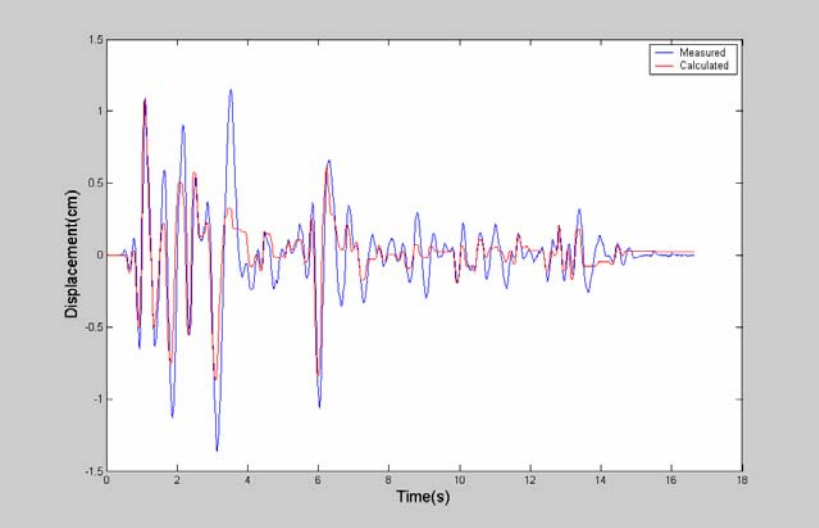

Figure 8.16. Comparison of numerical and measured relative displacements under El Centro Earthquake which has PGA value equal to 0.293g

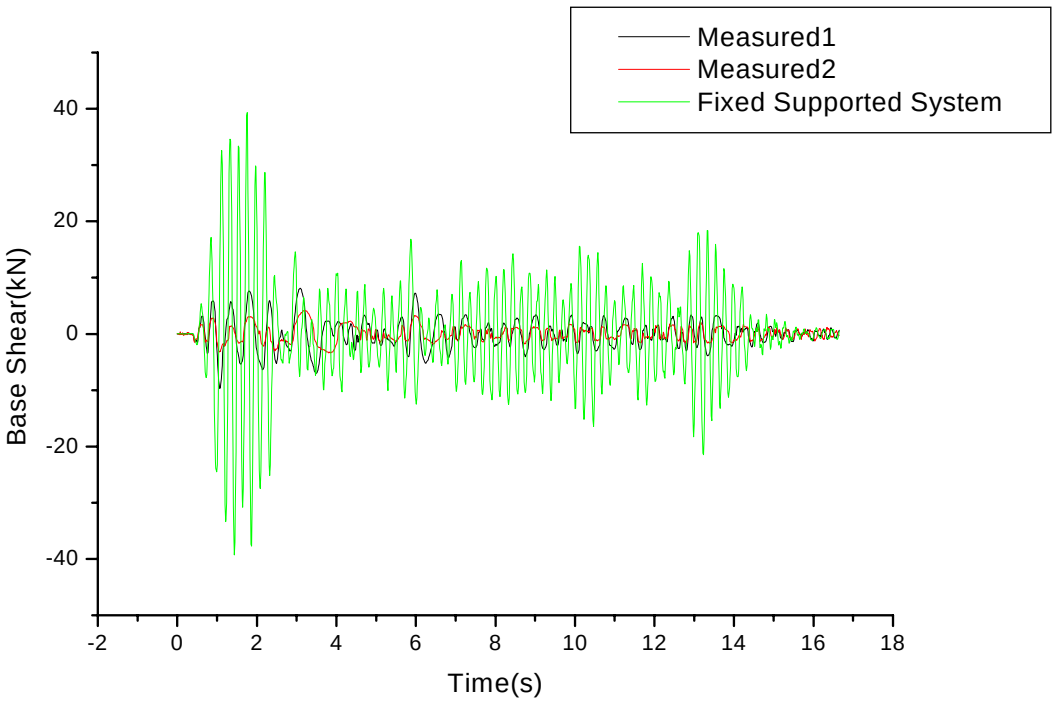

Figure 8.17. Comparison of base shear of fixed supported system with isolated system1 (SI-N 150/136) and isolated system2 (SI-S 150/136) under Pga=0.293g

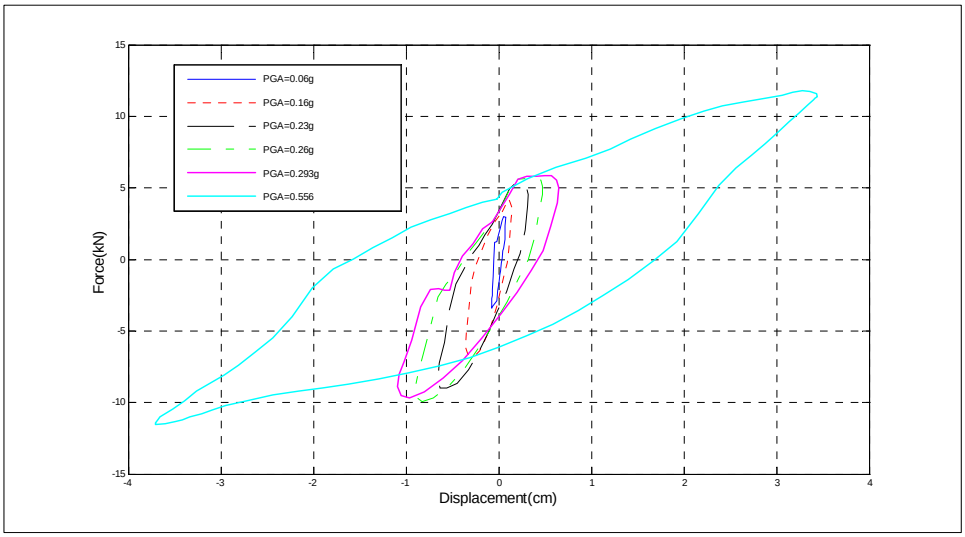

Figure 8.18. Comparison of effective damping of combined system under real earthquakes

8.7. Determination of Characteristic of Two Isolated Structure and Fixed Supported Structure

Modal characteristics of two different isolated structures with respect to type of HDR isolators that had used in shake table tests are determined with the help of transfer function. In addition to transfer functions of isolated structures modal characteristics of fixed supported structure is determined. Modal characteristics of isolated structure due to experimental results are in good agreement with numerical analysis that have been carried out in SAP 2000 version 10.0.0.1. Period of the first isolated system which has a normal compound HDR bearing is 0.59 seconds and the second isolated structure which has a soft compound is determined approximately 1.27 seconds. In numerical and experimental results for fixed supported system is found 0.21 seconds. Transfer functions of the isolated systems and fixed supported system is shown below.

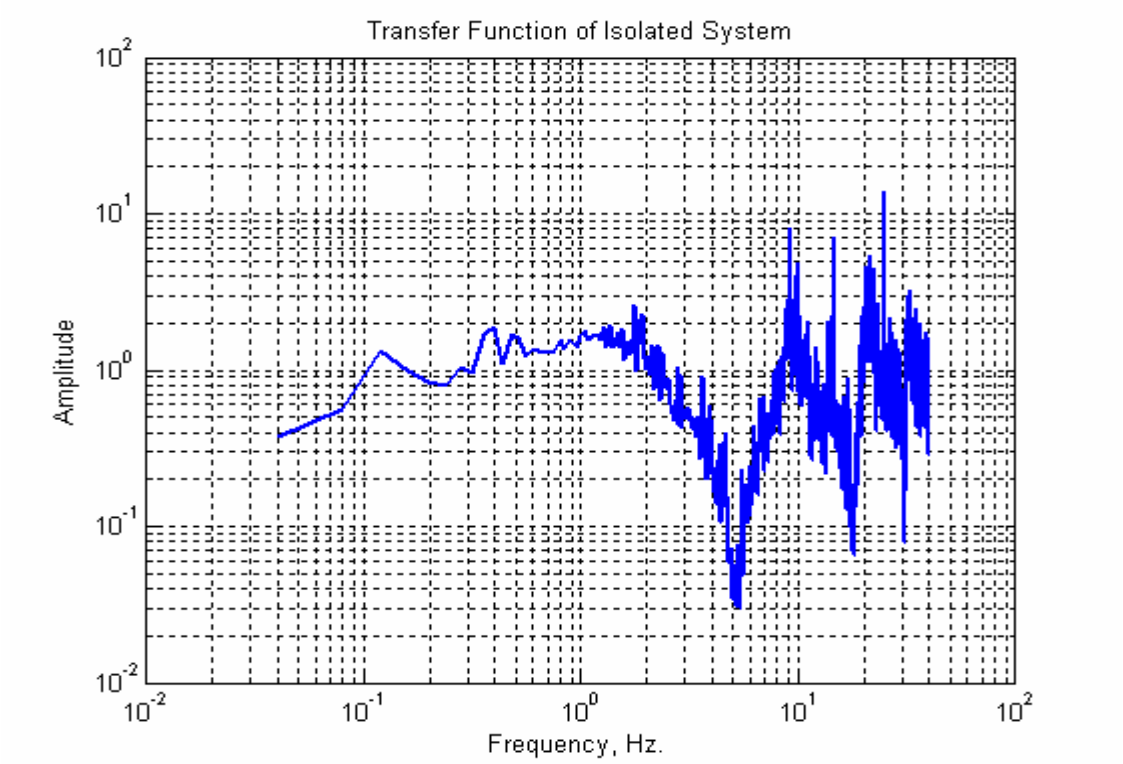

Figure 8.19. Transfer function of first isolated system that has normal compound high damping rubber

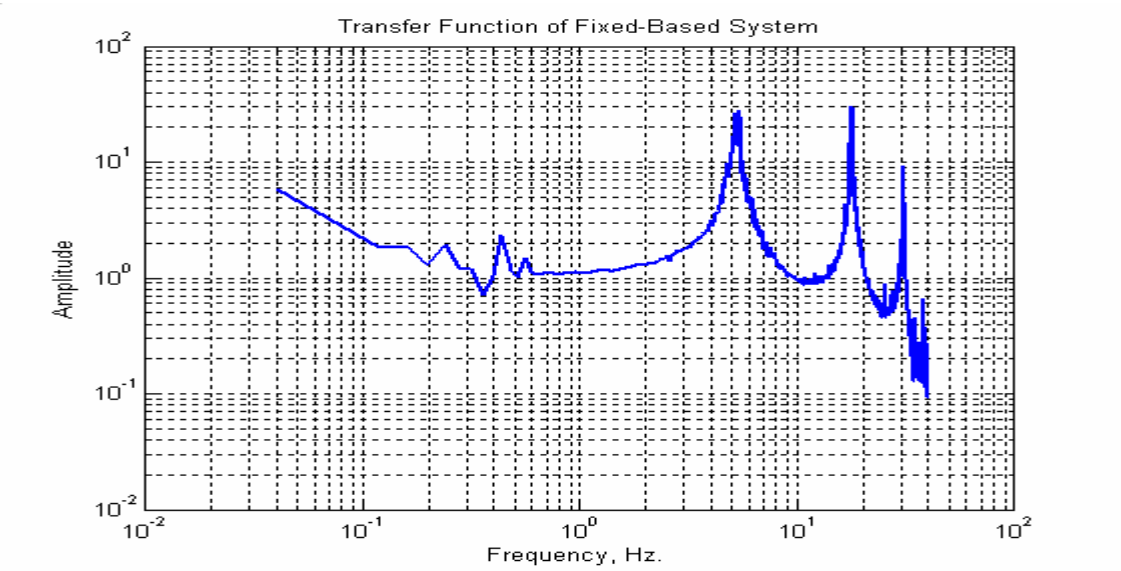

Figure 8.20.16 Evaluation of transfer function of fixed supported system for the first test setup

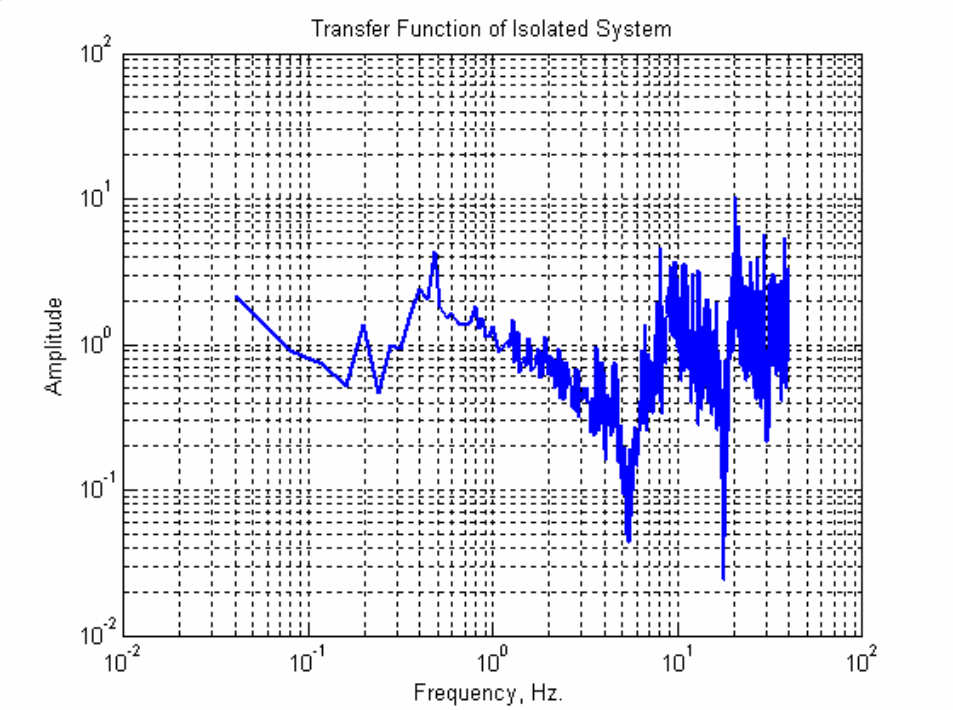

Figure 8.21. Transfer function of second isolated system which has soft compound high damping rubber

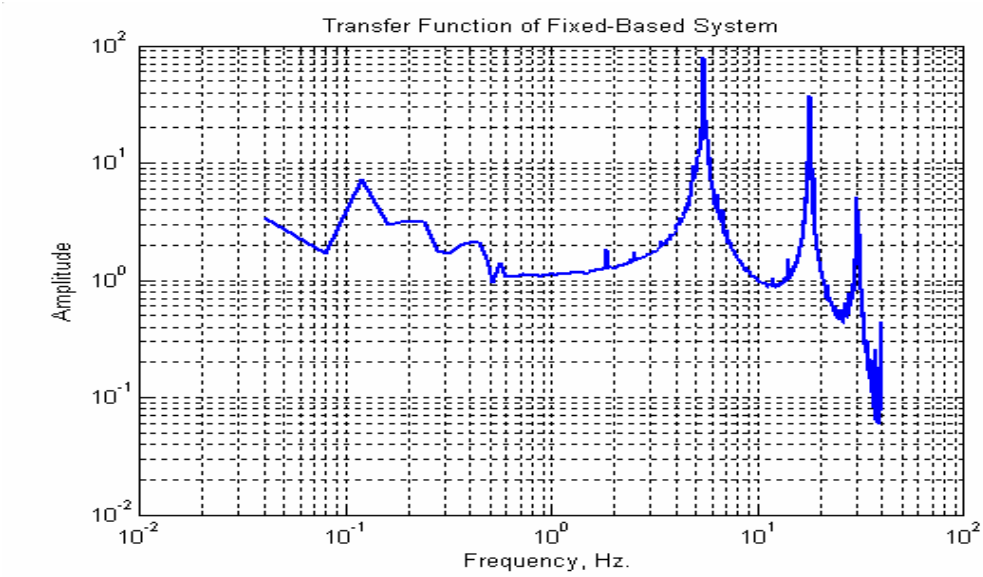

Figure 8.22. Transfer function of fixed supported system which had determined from second test setup

9. CONCLUSION

Shake table tests are conducted for a ¼ scaled 3 storey steel structure. which is a mass concentric and symmetric system and the test system is isolated with a passive hybrid isolation system. Isolation system is consisted of 6 isolators which are 4 flat sliding bearings and 2 high damping rubber bearings. Tests were carried out on the base of effectiveness of hybrid passive isolation system and evaluating the performance of the isolation system.

Tests have shown that base displacement are increased due to increased scale of peak ground accelerations. In addition, base shear of the fixed supported structure is significantly reduced as a result of hybrid isolation system. Second isolation system which has a low shear modulus is reduced the baseshear more than the first isolation system because of the low lateral stiffness that provided by soft compound that have been used in the manufacturing process.

Hybrid isolation systems are much more effective when peak ground acceleration value is relatively higher (Earthquake2(PGA=0.556g)>Earthquake1 (PGA=0.293g)) and effectiveness of the system is verified by shake table tests. Reduction of acceleration under higher values of PGA showed that this system protects the contents of the structure. No torsional responses had occured during the tests of a mass concentric symmetric system.

Numerical and experimental results are in good agreement. Relative displacements that had occured did not reach to upper bound shear strains and stiffening behavior is not observed at high damping rubber bearings.

As a result of experimental data and numerical analysis, passive hybrid isolation system that consists of HDR and flat bearings can be used as an alternative solution to structures which are concentric and symmetric systems. Moreover, this type of isolation system has some cost benefits because of the sliding bearings. In addition to those benefits, passive hybrid isolation systems can be used for the protection of sensitive equipments Nonetheless, configuration of isolation system should be selected carefully to overcome the disadvantages of this type of isolation system. For the further studies, torsional responses of the isolated system have to be tested with mass eccentric structures which are not symmetric and the change of axial loads on flat sliding bearings have to be measured by load cells to observe the change of axial load on sliding bearings.

APPENDIX A

Tests were carried out under real earthquake data which have been scaled at time domain. In addition, after that process Pga values are scaled to different values to understand the behavior of passive hybrid isolation systems. Results of two difeerent passive hybrid isolation systems (SI-N 150/136 and SI-S 150/136) are presented below. Main difference of two hybrid isolation systems is the compound of HDR that have been used during the manufacturing process.

Test1 Results under time and PGA scaled of earthquake record (PGA=0.07)

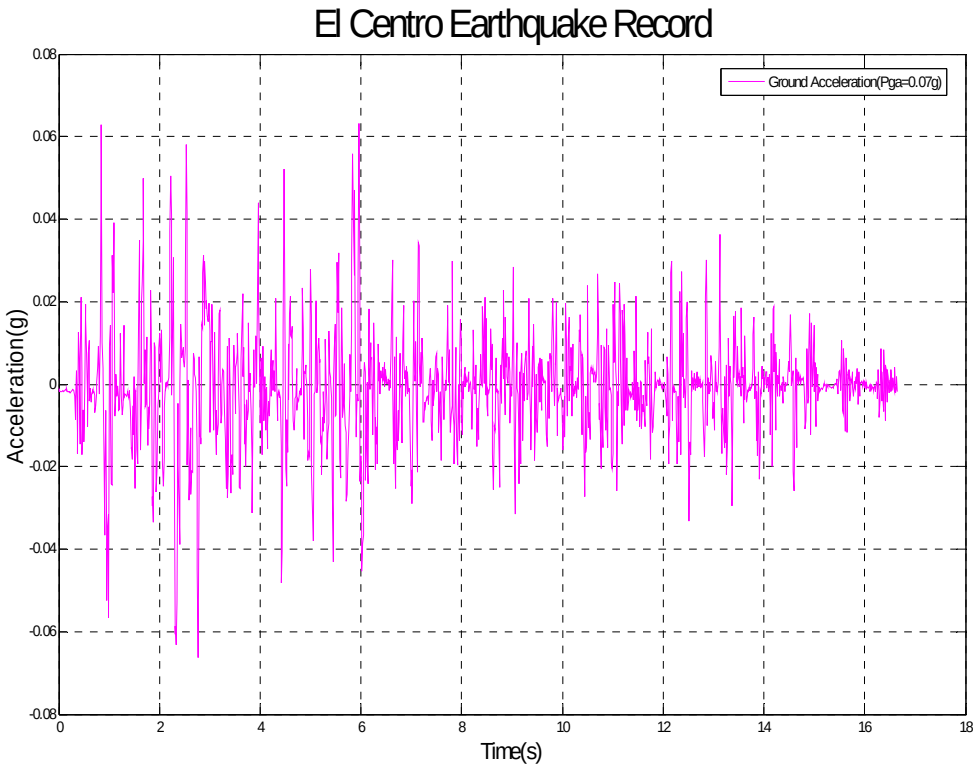

Figure A.1. Scaled El Centro record for test 1

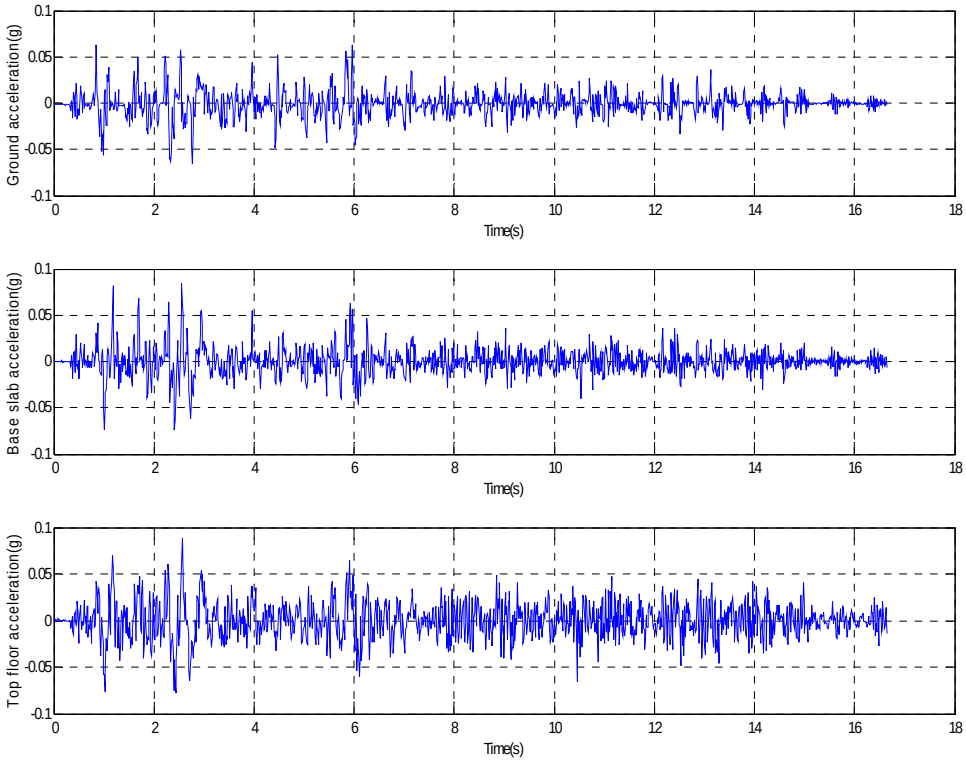

Figure A. 2. Acceleration records at different levels of isolated structure during test1

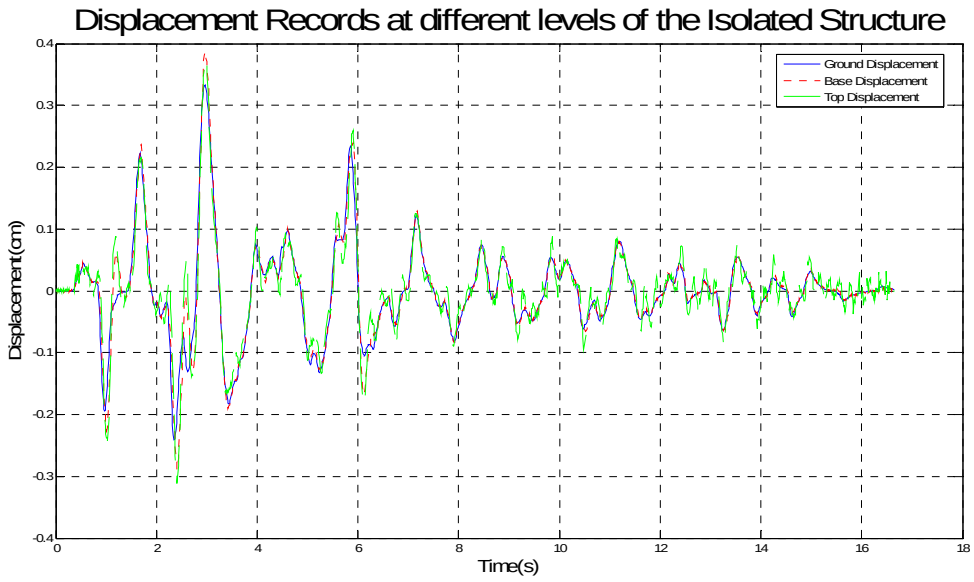

Figure A.3. Displacement records at different levels of the isolated structure during test1

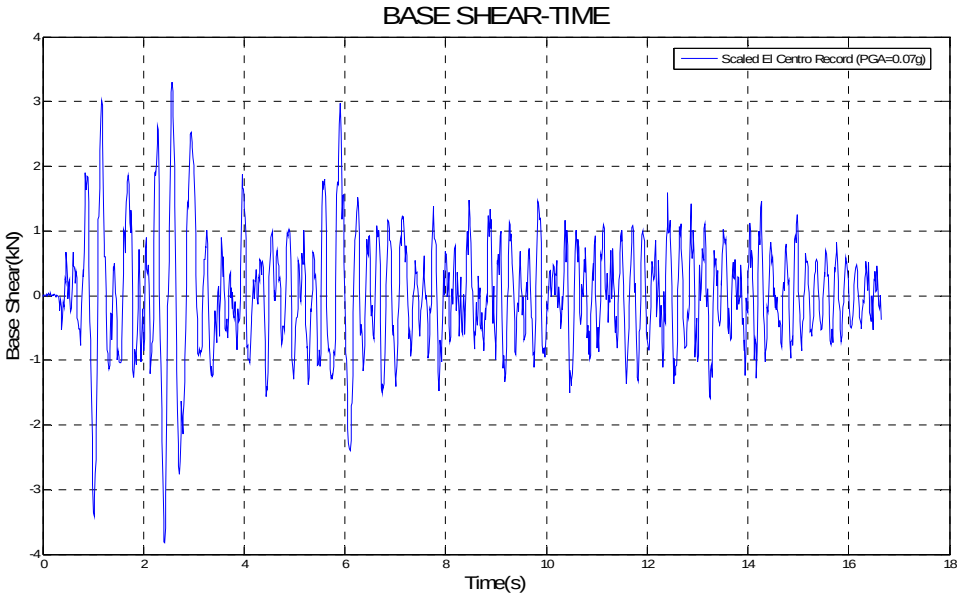

Figure A.4. Base Shear- Time graph of test1

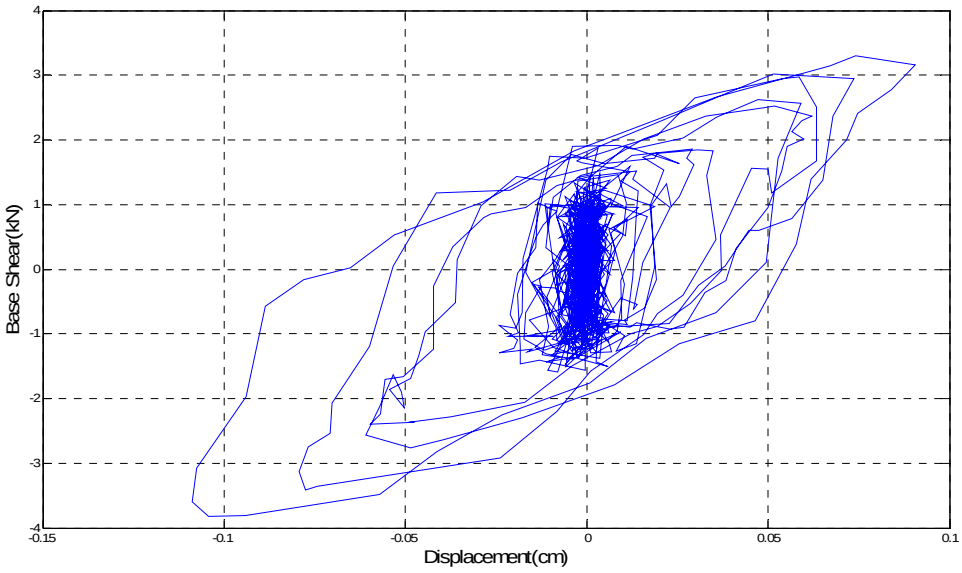

Figure A.5. Base Shear-Diplacement graph of the isolated structure during test1

Test 2 Results under time and PGA scaled of earthquake record (PGA=0.155g)

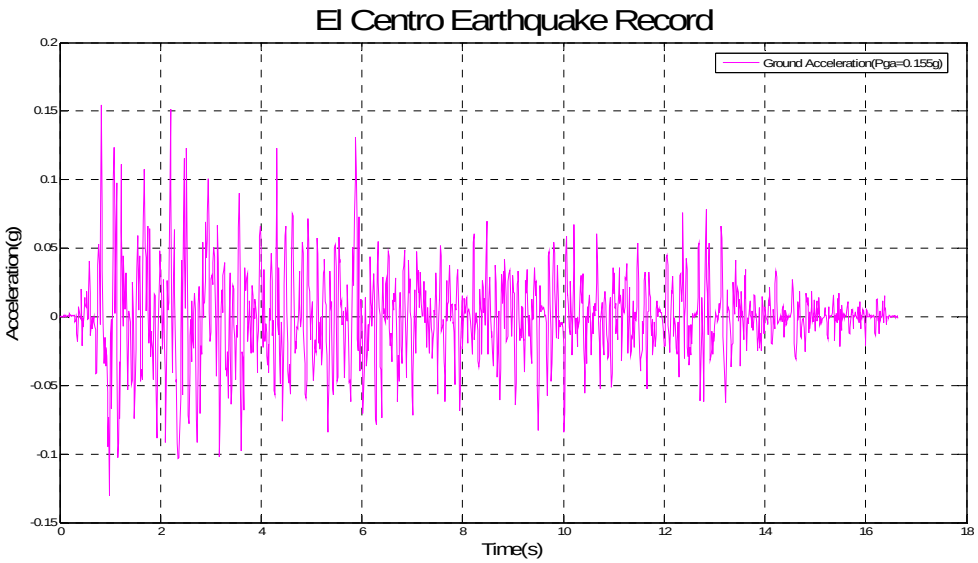

Figure A.6. Scaled El Centro record for test 2

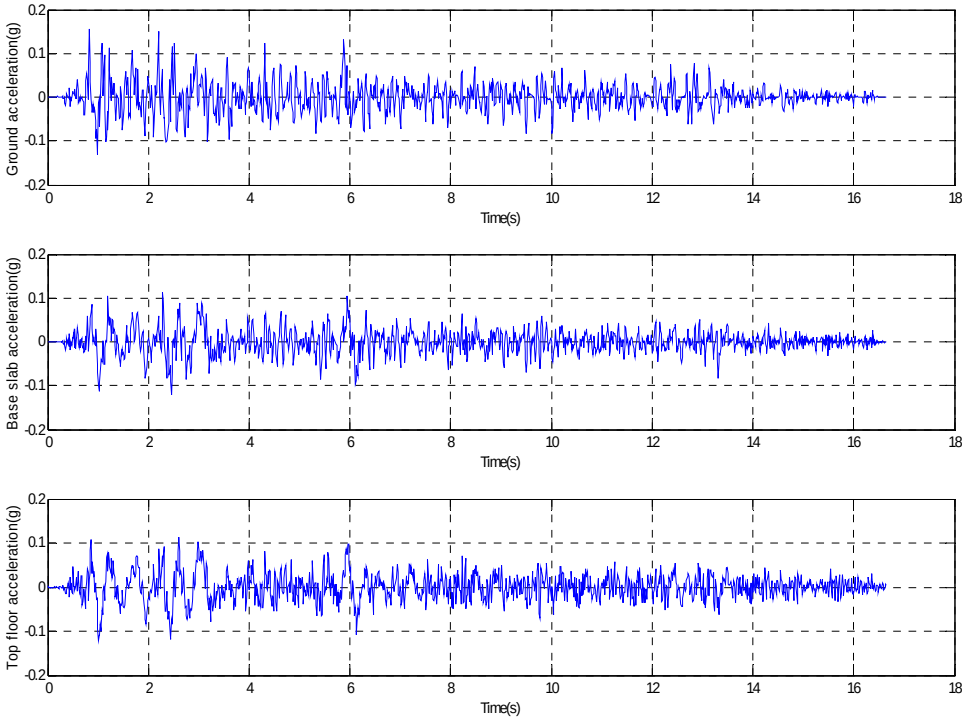

Figure A.7. Acceleration records at different levels of isolated structure during test2

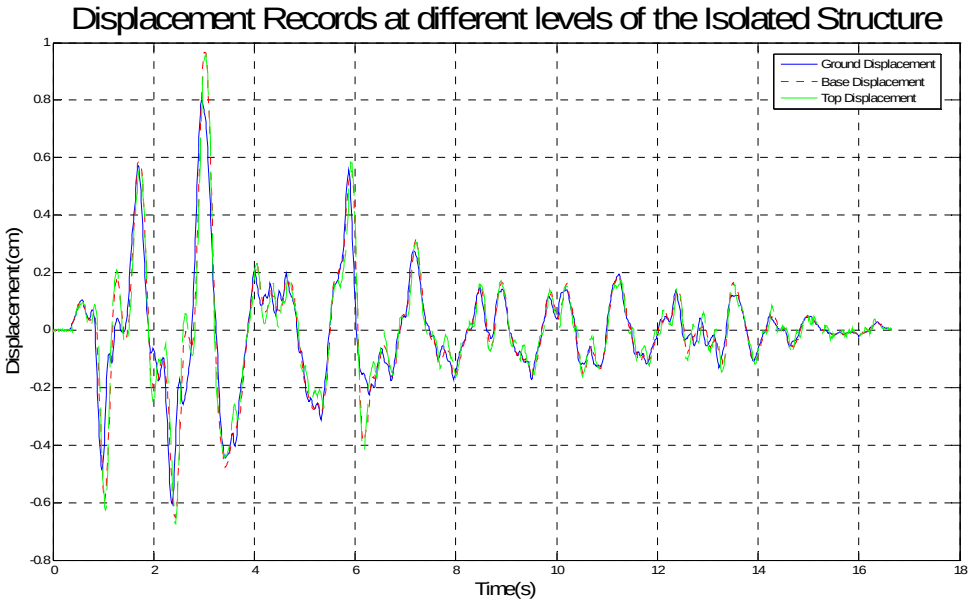

Figure A.8. Displacement records at different levels of the isolated structure during test2

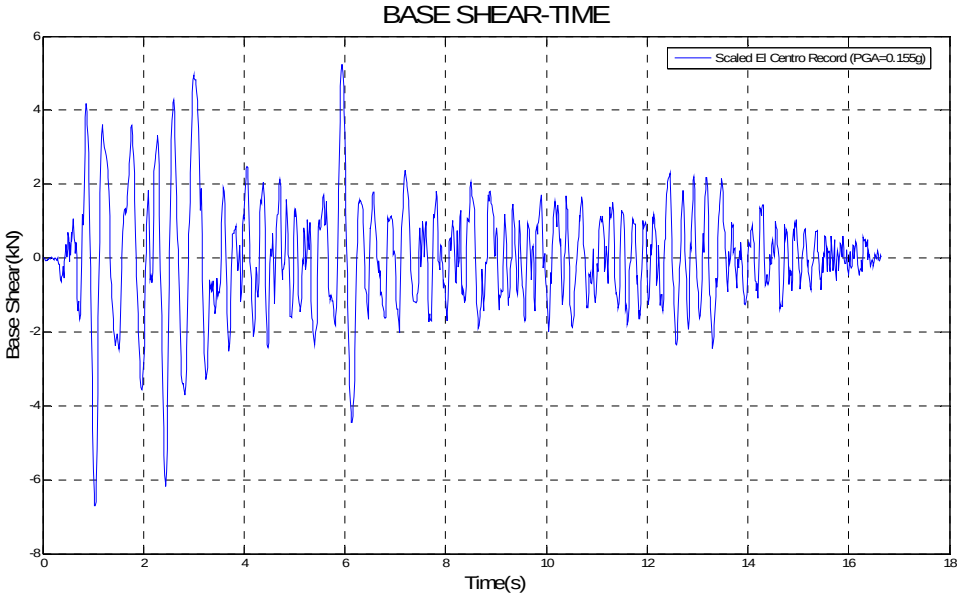

Figure A.9. Base Shear- Time graph of test2

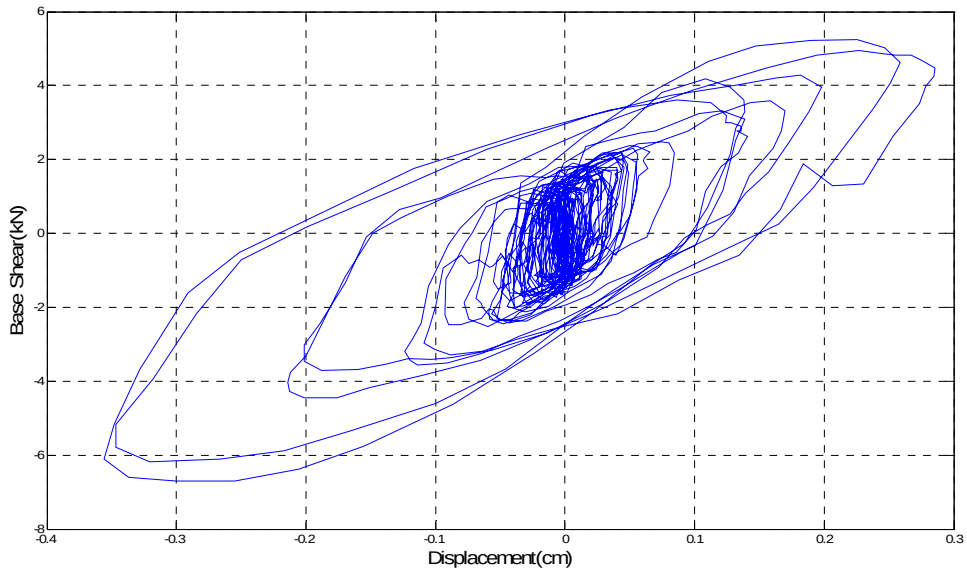

Figure A.10. Base Shear-Diplacement graph of the isolated structure during test2

Test 3 Results under time and PGA scaled of earthquake record PGA=0.234g)

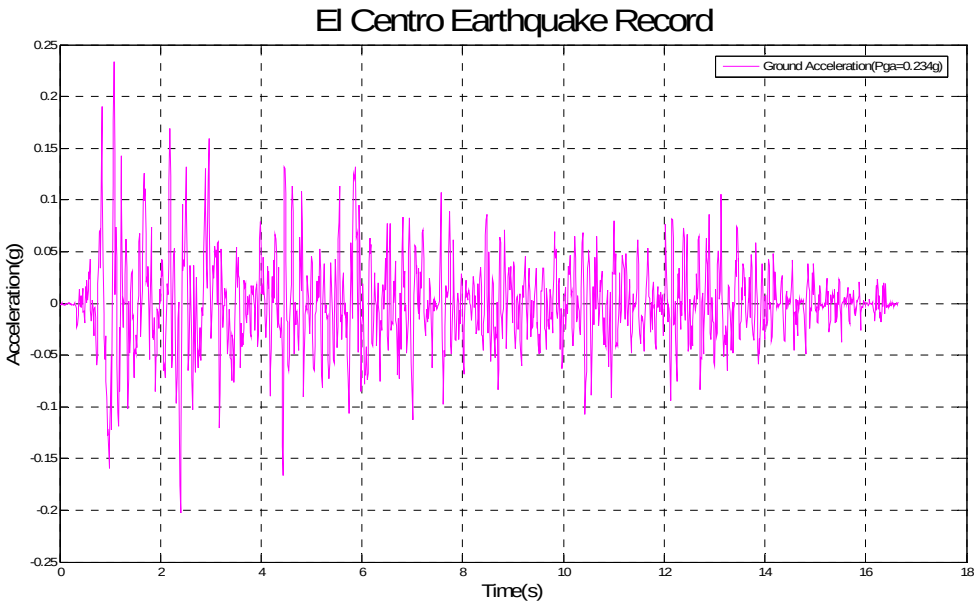

Figure A.11. Scaled El Centro record for test 3

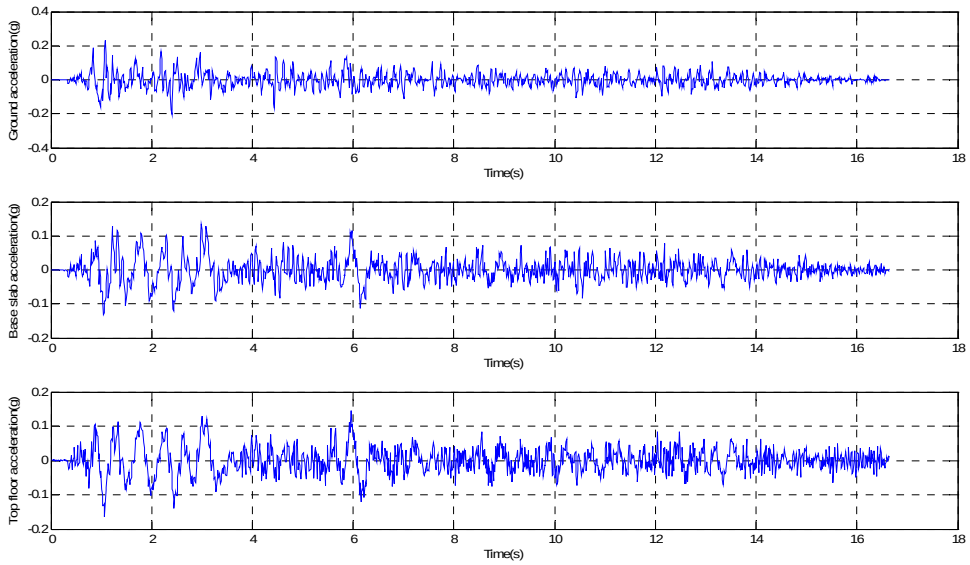

Figure A.12. Acceleration records at different levels of isolated structure during test3

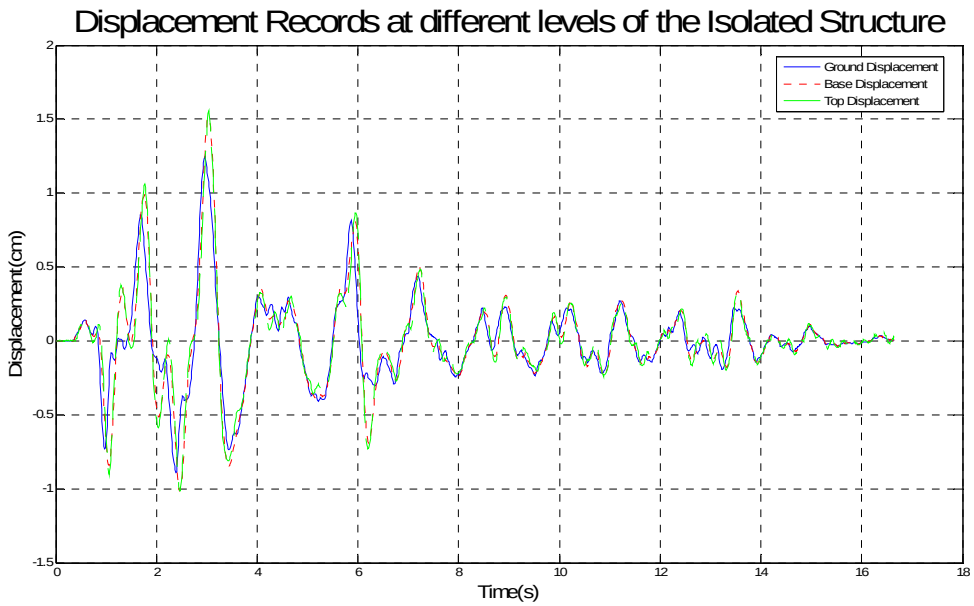

Figure A.13. Displacement records at different levels of the isolated structure during test3

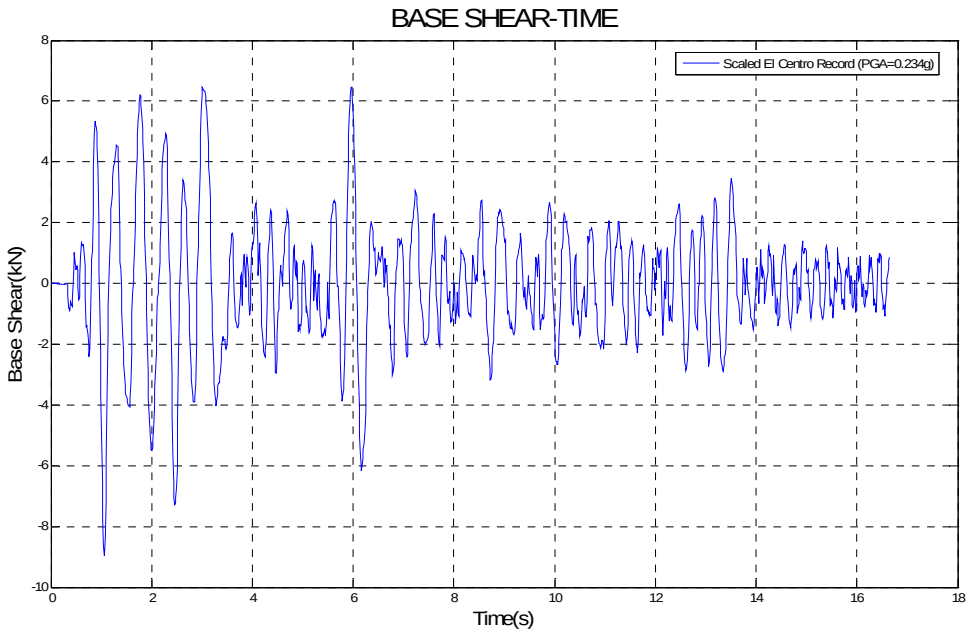

Figure A.14. Base Shear- Time graph of test3

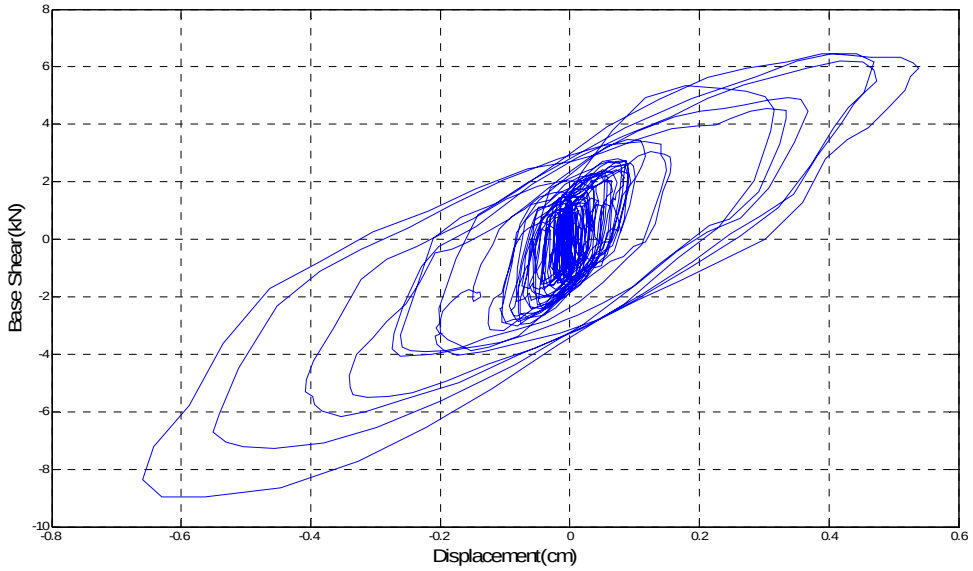

Figure A.15. Base Shear-Diplacement graph of the isolated structure during test3

Test 4 Results under time and PGA scaled of earthquake record PGA=0.263g)

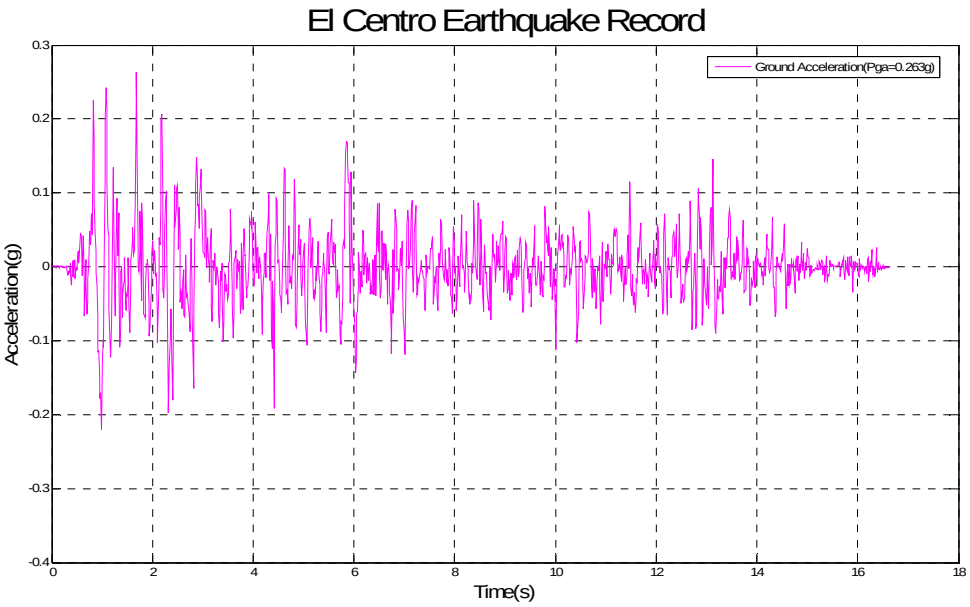

Figure A.16. Scaled El Centro record for test 4

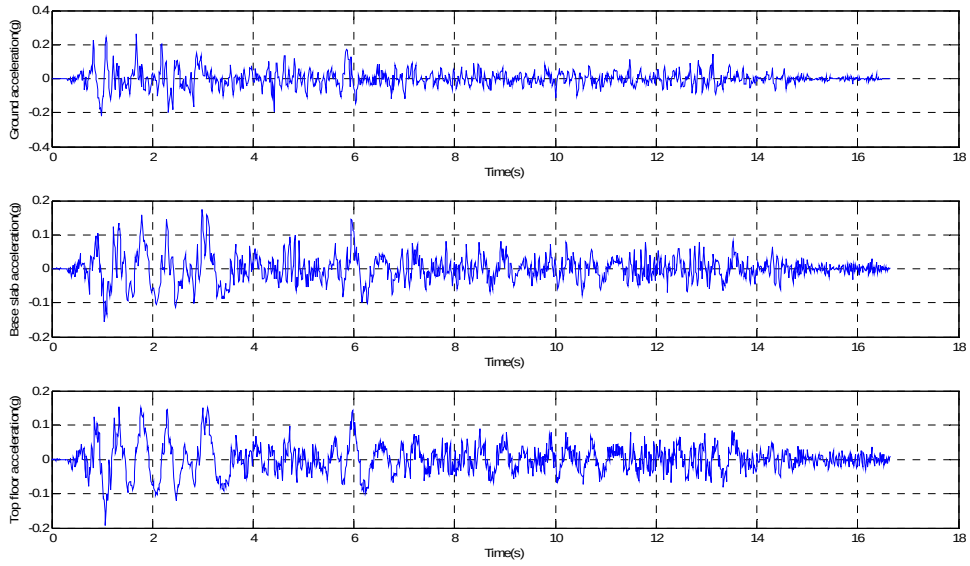

Figure A.17. Acceleration records at different levels of isolated structure during test4

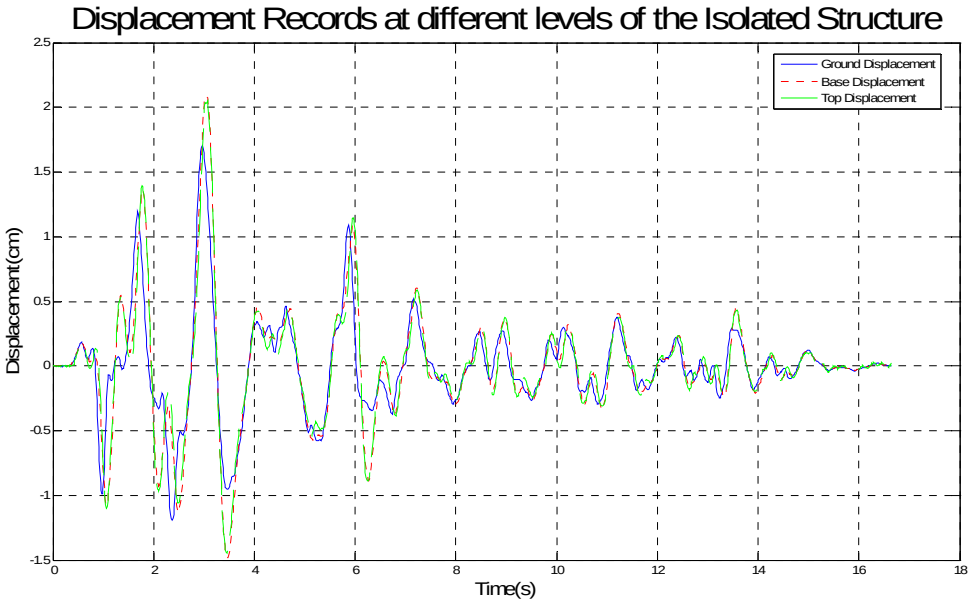

Figure A. 18. Displacement records at different levels of the isolated structure during test4

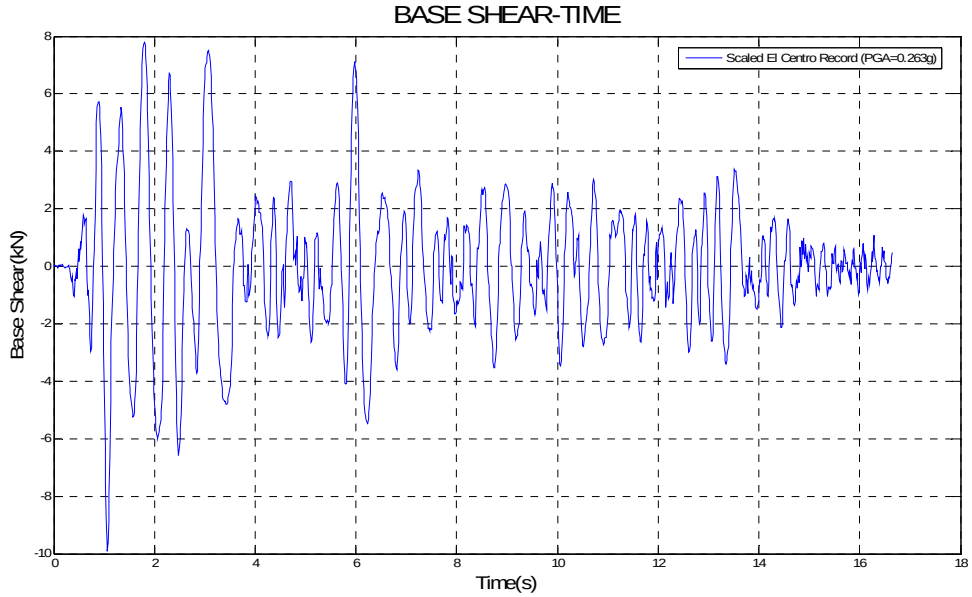

Figure A. 19. Base Shear- Time graph of test4

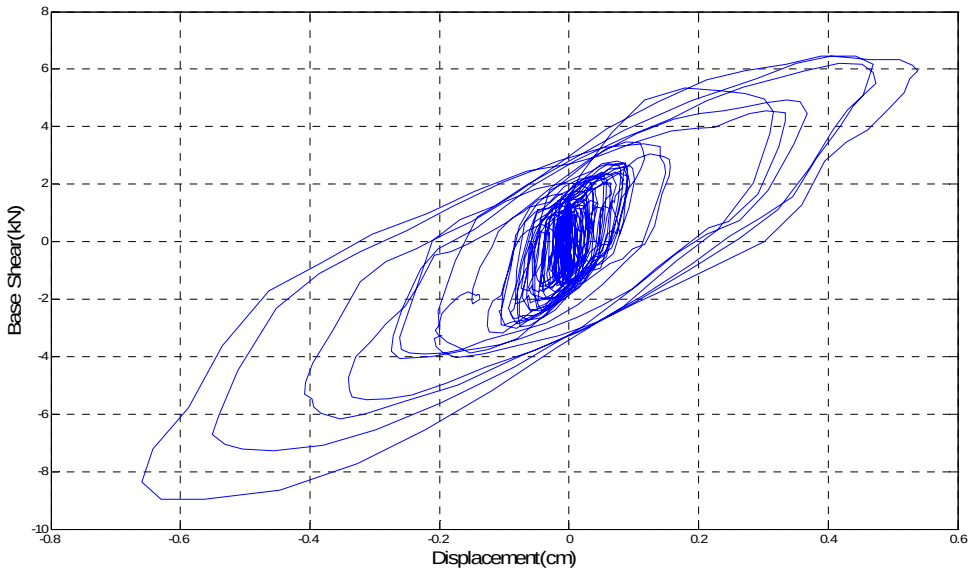

Figure A. 20. Base Shear-Diplacement graph of the isolated structure during test1

Numerical Model of Isolated Structure at Sap 2000 Version 10.0.0

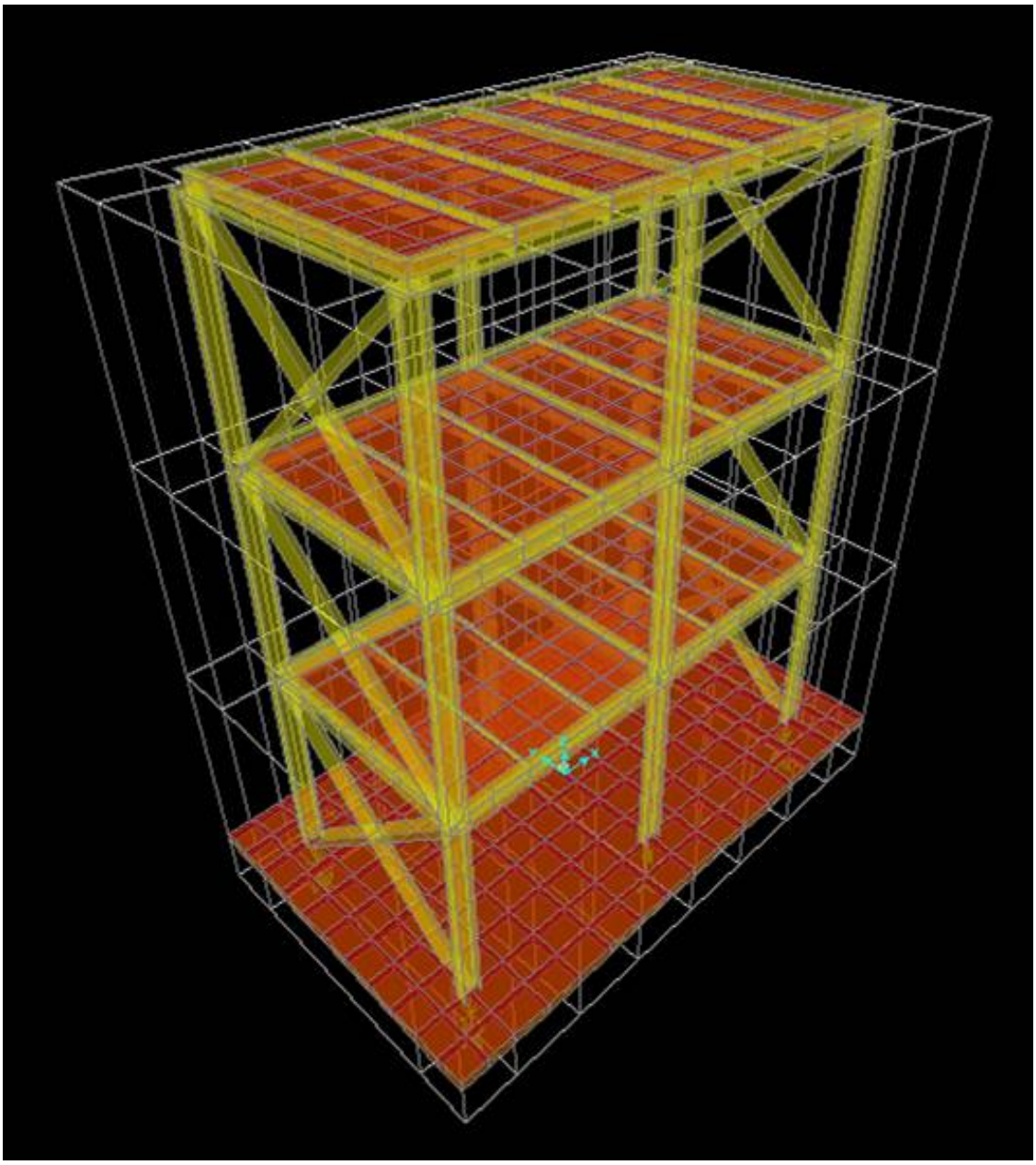

Figure A. 21. Sap2000 Model of the isolated building

Base Shear Displacement Loops of HDR bearing at SAP2000 under El Centro Earthquake Record (Pga=0.293g)

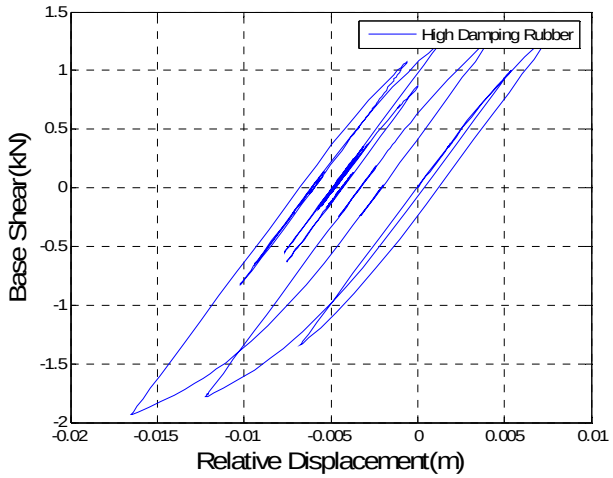

Figure A. 22. Base Shear–displacement loops of HDR bearings inSAP2000

Base shear displacement loops of flat sliding bearing at SAP2000 under El Centro Earthquake Record (Pga=0.293g)

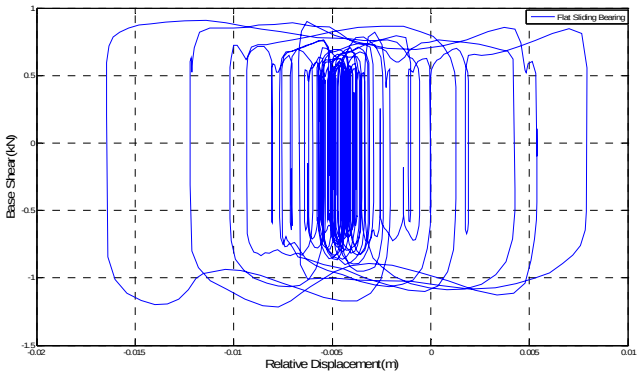

Figure A. 23. Base Shear–Displacement loops of flat sliding bearings

REFERENCES

Ahmadi, G., Fan F-G., Tadjbakhsh, G., "Base Isolation of a Multi-Story Building Under a Harmonic Ground Motion –A comparison of Performances of Various Systems", Technical Report No:88-0010, *National Center for Earthquake Engineering Research* , Buffalo ,NY, 1988

AASHTO, " Guide Specification For Seismic Isolation Design", *American Association of State Highway Officials*, 1991.

AASHTO, "Guide Specification For Seismic Isolation Design", American *Association of State Highway Officials*, 1998.

Applied Technology Council, Tentative Provisions for the Development of Seismic Regulations for Building , Including, Proposed Amendments, Report No ATC3-06, *Applied Technology Council*, Palo Alto, California, 1984.

Chopra, A.K., "*Dynamics of Structures :Theory and Applications to Earthquake Engineering",* Prentice-Hall, New Jersey, 1995.

Constantinou M. Caccese J. and Harris H. "Teflon Bearings in Base Isolation II: Modeling", *Journal of Structural Engineering*, Vol. 116, No2, February, 1990.

FEMA, NEHRP Guidelines for Seismic Rehabilitation of Buildings, *National Earthquake Hazards Reduction Program (NEHRP), FEMA*-274, 1998.

Kasalanati A., Constantinou C. M, "Experimental Study of Bridge Elastomeric and Other Isolation and Energy Disspation Systems with Emphasis on Uplift Prevention and HighVelocity Near Source SeismiC Excitattion", Technical Report No:99-0004 *Multidiciplinary Center for Earthquake Engineering Research* , Buffalo ,NY, 1993

Komodromos,P. ,"*Seismic Isolation for Earthquake-Resistant Strcutures*", WIT Press, Southampton, Boston, 2000

Naeim F. and Kelly J.M., "*Design of Seismic Isolated Structures*", John Wiley & Sons Inc., 1999.

Nagarajaiah S., Li, C., Reinhorn A.M., And Constantinou M.C., "3D-BASIS-TABS: Computer Program for Nonlinear Analysis of Three Dimensional Base Isolated Structures," Report No:NCEER-93-011, *Journal of Structural Engineering, ASCE*, Vol. 117, No. 7, pp. 2035-2068, September 1991.

Nagarajaiah S., Reinhorn A.M., And Constantinou M.C., "Nonlinear Dynamic Analysis of 3D base-isolated structures", *Journal of Structural Engineering, ASCE*, Vol. 117, No. 7, pp. 2035-2068, September 1991.

Nagarajaiah S., Reinhorn A.M., And Constantinou M.C., "Nonlinear Dynamic Analysis of Three Dimensional Base Isolated Structures(3D-BASIS ME)", *National Center for Earthquake Engineering Research* , Buffalo ,NY, 1993

SAP 2000 Structural Analysis Program, 1998, *Integrated Finite Element Analysis and Design of Structures*, *Analysis Reference*, Vol.1, Berkeley, California.

Skinner, I., Robinson H. W., McVerry G., "*An Introduction to Seismic Isolation*", John Wiley and Sons, 1993

Stadaucher, K., "Integral Earthquake Protection of Structures IV: Full Base Isolation and Seismic Mass Antology," *Eidgenossische Technische Hochschule (Zurich), Inst. für Baustatik und Konstrukton*, Bericht 134, Birkhauser Verlag, Basel Switzerland,1982

Taylor, A., Igusa Takeru, "*Primer on Seismic Isolation*", Special Publication of *ASCE*, 2004

Tezcan, S.,Cimilli S., "*Seismic Base Isolation", Higher Education Foundation*, June, 2002

Tezcan, S., Erkal A., "*Seismic Base Isolation and Energy Absorbing Devices*", *Higher Education Foundation*, July,2002

Tsopelas., Constantinou M.C ,Reinhorn A.M., And., "Nonlinear Dynamic Analysis of Three Dimensional Base Isolated Structures(3D-BASIS ME)" *National Center for Earthquake Engineering Research* , Buffalo ,NY, 1994

Tyler, R.G., 'Dynamic tests on PTFE sliding layers under earthquake conditions', *Bull. NZ Nat. Soc. Earth. Eng*., 10, no 3, 1977

Yang,Y. and Chang , L.," *Earthquake Engineering Handbook*", CRC Press LC, 2003